AXON PATTERNING IN THE MOUSE RETINOFUGAL PATHWAY

LEUNG Kin Mei

A Thesis Submitted in Partial Fulfillment
of the Requirements for the Degree of Master of
Philosophy
in
Anatomy

July 2002

ABSTRACT

AXON PATTERNING IN THE MOUSE RETINOFUGAL PATHWAY

Submitted by Leung Kin Mei
For the degree of Master of Philosophy
At The Chinese University of Hong Kong in July 2002

In the mouse, when retinal axons grow through the chiasm, they undergo several changes in fiber order. One of these is a repositioning of axons according to their ages, which takes place at the junction of the chiasm and the optic tract. Another is the sorting of dorsal from ventral retinal fibers in the optic tract, which takes place after axons have crossed the midline. The major questions asked in my study are the underlying molecular mechanisms that control the axon patterning in mouse retinofugal pathway. The first issue is to identify the role of a family of extracellular matrix molecules, chondroitin sulfate (CS) proteoglycans (PG), in controlling the growth cone position according to their ages in the optic tract of mouse embryos. Immunostaining of CSPGs was found to be restricted in the deep regions of the optic tract. Using brain slice preparations of the pathway from embryonic day (E) 14 C57 pigmented mice, the changes in age-related fiber arrangement in the chiasm and tract were examined after culturing the pathway in the presence of chondroitinase ABC that digests chondroitin sulfate glycosaminoglycans from the ventral diencephalon. It was found that removal of chondroitin sulfates disrupted normal growth cone distribution at the threshold of the optic tract. The restricted distribution of retinal growth cones at the superficial region of the tract was abolished after removal of chondroitin sulfates from the deep regions of the chiasm and the tract. Various subtypes of CSPGs were further characterized, including N-terminal neurocan, C-

terminal neurocan and phosphacan. Immunocytochemical staining has shown that the fiber order changes are related to a spatially restricted expression of these brain CSPGs. Besides CSPGs, another family of proteoglycans that are conjugated to heparan sulfate was also studied. The study demonstrated a complementary correlation of heparan sulfate proteoglycans and growth cone position in the optic chiasm and tract, suggesting a role of these proteoglycans in setting up the age-related fiber order.

The retinal axons grow along the surface of the diencephalon as fascicles and are bounded by adhesive molecules along their course in the pathway. One of these adhesive molecules is neural cell adhesion molecule (NCAM). NCAM is expressed in the developing mouse retinofugal pathway. Immunostaining for sialylated NCAM shows a regulated change at various regions of the chiasm. Using a monoclonal antibody 5A5 that recognizes specifically a highly sialylated form of NCAM, there is an obvious down-regulation of NCAM immunoreactivity when axons approach the midline of the chiasm and an up-regulation of this molecule when axons enter the optic tract. Moreover, while axons in the optic stalk are all immunopositive to the sialylated NCAM, only axons from the dorsal retina that are located in the posterior region of the optic tract are immunoreactive to this antibody. The functions of NCAM were shown to be modulated by the amount of polysialic acid on the molecule. These findings indicate that the changes in axon organization in the chiasm and the tract may be controlled by a regulated expression of NCAM or alternatively by a regulation of the amount of polysialic acid on the NCAM molecule. The present study investigates the functions of sialylated NCAM on the development of dorsal ventral fiber order in the optic tract of the mouse retinofugal pathway using a brain slice preparation with

perturbation of the NCAM functions with blocking antibodies to NCAM. Preliminary results show that appropriate axon growth to the dorsal region in the tract is affected after treatment. The characteristic expressions of different proteoglycans and NCAM in the retinofugal pathway were shown to take part in the establishment of different fiber orders.

摘要：

小鼠的視覺傳導通路中神經軸突分佈的型式

在小鼠中，當視網膜神經軸突生長至視交叉時，它們的排列順序就會發生一些變化。其中之一爲在視交叉和視束的結合處，神經軸突的順序按照它們年齡大小進行重排。另一個特點爲在神經軸突越過中線後，在視束中，背側視網膜神經纖維同腹側神經纖維分開。本論文旨在探討在小鼠視神經傳導通路中，控制視網膜神經軸突排位的機制。第一個實驗是研究硫酸軟骨素蛋白多糖，一族細胞外基質分子，在不同年齡小鼠胚胎的視束中，控制生長錐的位置所發揮的作用。利用免疫細胞化學方法觀察，發現硫酸軟骨素蛋白多糖局限於視束中深部區域。利用軟骨素酶 ABC 消化 14 天小鼠胚胎腦片中的硫酸軟骨素蛋白多糖，結果發現去除視束中硫酸軟骨素蛋白多糖就會破壞正常生長錐的分佈：在去除視交叉和視束深部的硫酸軟骨素蛋白多糖後，生長錐局限性的分佈在視束表層的型式就會消失。繼而研究硫酸軟骨素蛋白多糖各個亞型的特點，包括 N 末端 Neurocan，C 末端 Neurocan 和 Phosphacan。利用免疫細胞化學染色方法顯示，硫酸軟骨素蛋白多糖局限性的表達在一些區域與神經纖維順序的變化有關。此外，本論文還研究了另一族與 heparan sulfate 相結合的軟骨素蛋白多糖。結果顯示：在視交叉和視束中，heparan sulfate 軟骨素蛋白多糖的分佈與生長錐的分佈呈互補關係。說明這些軟骨素蛋白多糖在與年齡相關的神經纖維重排中有一定作用。

視網膜神經軸突呈束狀在間腦表面生長。在生長過程中，它們被黏連分子包裹，神經細胞黏連分子(NCAM)爲其中之一。本論文最後研究了神經細胞黏連分子在視覺傳導通道中的表達和作用。用免疫染色方法來觀察 NCAM 的表達。本論文用能特選性識別 NCAM 的單克隆抗體 5A5 觀察，結果發現：NCAM 在視網膜神經軸突接近中線時表達下調而在進入視束則表達上調；只有位於視束後部的視網膜神經軸突才對 5A5 有反應。用 NCAM 抗體封閉小鼠胚胎腦片中 NCAM 功能來觀察在小鼠視覺傳導通道中 NCAM 對在背側腹側視網膜神經纖維排列順序變化中所發揮的作用。結果發現，處理後的腦片中，視束背側區域中的正常神經軸突生長受到了影響。因爲分子表面的多唾液酸的數量影響 NCAM 的功能，所以以上結果表明 NCAM 或者表面的多唾液酸數量影響神經軸突在視交叉和視束排列的變化。

ACKNOWLEDGEMENT

I am so grateful to the many individuals who have supported me for the last two years. I would like to acknowledge them all, beginning with me supervisor.

I owe a special debt of gratitude to my supervisor, Dr Hector SO Chan, from whose insights and understanding I have benefited greatly. During the last three years under his patient guidance, I have learnt invaluable knowledge in scientific research. What's more important is that I have learnt to look into valuable questions, which is not only important to my academic path, but also precious to my life.

I am especially grateful to Anny Cheung and Alex Lin who have brought their expertise to bear on various technical supports; Ling Lin and Yan-Li Hao who have provided helpful suggestions at various stages and consistent encouragement. Thanks to my research fellows, Amy Chung, Barry, Claire and Dr Sheng-Xi Wu, who worked together in our laboratory.

I am deeply indebted to the many people at the department who have provided technical support and valuable information on my experiments, including Samuel Wong (for the spacious working place, too!), Jenny Chen, Jean Kung, Corinna Au and Simon Tong.

I would particularly like to thank Sau-Man Yeung and Billy Chan for your encouragement, support (especially during the hardest time) and great ideas (all kinds!). Thanks to Bo-Wah Leung, Vivian Chow, Wai-Chi Kwong, Shu-Yan Cheung, Simon Mok, David Ng, Richard Li, Terence Tam, Ki Lui, Raymond Tong, Thomas Wong and Stephen Sze. You all have made the last two years fun. Special thanks to Willow, Yiu, Liu and Lap-Yee, who helped me out when I really needed them.

Above all, I thank my family for their loving care.

LIST OF ABBREVIATIONS

The following abbreviations are commonly used in this thesis:

CS	chondroitin sulfate
DiI	1,1'-Dioctadecyl-3,3,3',3'-tetramethylindocarbocyanine perchlorate
DMEM/F12	Dulbecco's modified Eagle's medium
E	embryonic day
HS	heparan sulfate
NCAM	neural cell adhesion molecule
NGS	normal goat serum
ON	optic nerve head
OS	optic stalk
OT	optic tract
PB	phosphate buffer
PBS	phosphate buffered saline
PG	proteoglycan
PSA	polysialic acid
SSEA-1	stage specific antigen-1

TABLE OF CONTENTS

CHAPTER 1

GENERAL INTRODUCTION

Retinofugal pathway is the axon link between the retina and the central visual relays in the central nervous system. During embryonic development, retinal ganglion cells send out axons. After passing through the optic stalks, the axons from each eye meet at the midline to form an X-shaped pattern called optic chiasm. These fibers either cross the midline or turn back and remain uncrossed. After deciding their courses in the pathway at this decision point, the fibers separate, travel along the optic tract and project into their destined targets in the main visual nuclei in the brain (Guillery et al., 1995). Detailed structure and the fiber organization of the chiasm have long been an area of interest for researchers to study. Different arrangements of the axons throughout the course have been clarified. The understanding of the morphology and the developmental mechanisms of the retinofugal pathway set an excellent model for the studies of axon guidance in the central nervous system.

Pattern of fiber order in the retinofugal pathway

Topographic map in the optic stalk

After emerging from the eyes, axons are arranged in a way dependent upon the position of the ganglion cells from which they arise. This is called the retinotopic order (Reese and Baker, 1992; Guillery et al., 1995). In the developing mouse retinofugal pathway, axons from the ventral retina occupy the rostral and caudal extremes of the stalk in cross sections, whereas those from the dorsal retina are sandwiched in the central position (Chan and Chung, 1999). The optic fibers are

grouped within fascicles by glial cytoplasm from the optic nerve head throughout the extracranial part of the stalk (Guillery and Walsh, 1987; Colello and Coleman, 1997). However, this nicely organized pattern of the fibers gradually becomes defasciculated in regions adjacent to the chiasm (Jeffery, 1990; Harman and Jeffery, 1992). Together with this defasciculation, comes the gradual disappearance of retinotopic order as axons course through the optic stalk, which is eventually lost at the chiasm (Chan and Chung, 1999). Similar observations have been reported also in other animals, with different degree of the axon separation and the relative distance that the retinotopic order disappears (cats: Naito, 1986; hamsters: Baker and Jeffery, 1989; rats: Baker and Jeffery, 1989; Chan and Guillery, 1994; ferrets: Reese and Baker, 1993). The loss of fasciculation is associated with a change in glial organization (Guillery and Walsh, 1987), which in turn may be responsible for the change in retinotopic fiber order in the optic stalk. Yet, on top of the defasciculation of fibers and the loss of retinotopic order, another rearrangement of optic fibers is found in the chiasm.

Decussation pattern in the optic chiasm

In the retina, there is a naso-temporal division. When axons from both eyes enter the ventral diencephalon and meet each other in optic chiasm, they split into two groups. The optic chiasm is the decision point where retinal axons segregate to project into the optic tract on either the same side or the opposite side of the brain. Axons originating from the nasal retina cross the midline of the chiasm and project into the contralateral optic tract, whereas those originating from the temporal retina remain uncrossed and enter the tract on the same side (Godement et al., 1990; Taylor and Guillery, 1994; Guillery et al., 1995; Mason and Sretavan, 1997). This specific

segregation of crossed from uncrossed axons that takes place before axons reach the midline of the chiasm (Chan et al., 1998), sets up bilateral connections, which in turn establish an essential foundation for binocular vision. The relative proportion of cells that project contralaterally and ipsilaterally depends on the location of eyes in the head and the size of the binocular visual field (Cooper and Pettigrew, 1979; Drager and Olsen, 1980; Provis and Watson, 1981). Axons travel down the optic stalk in bundles wrapped by interfascicular glia. However, this fasciculation disappear when they reach the optic chiasm (Jeffery, 1990; Harman and Jeffery, 1992) where they segregate to form the partial decussation pattern. After passing through the chiasm, decussating axons mingle with the uncrossed axons from the other eye and head for the optic tract in the contralateral hemisphere (Baker and Reese, 1993; Chan and Guillery, 1994). Thus, the defasciculation of fiber in the prechiasmatic region may be an important step to make this segregation of axons possible.

Chronotopic order within the optic tract

Before leaving the chiasm, the defasciculated fibers regain a new order in the juxtachiasmatic optic tract. In the extracranial optic stalk, the axonal growth cones do not have a specific distribution through the cross sections (Guillery and Walsh, 1987; Colello and Guillery, 1992). However, advancing growth cones tend to accumulate near the subpial surface in the juxtachiasmatic stalk and in the tract (Colello and Coleman, 1997; Colello and Guillery, 1998). Thus, the advancing retinal growth cones tend to travel towards the superficial region as they pass through the optic chiasm and the tract. Resulting from this movement, axons are arranged in a deep to superficial order in the optic tract, which represents the sequence of axon arrivals,

with the fibers furthest from the pia being the oldest (ferrets: Walsh and Guillery, 1985; mice: Colello and Guillery, 1992). This change in the chronotopic order of fibers in the developing retinofugal pathway seems to be related to the change in the glial organization. The interfascicular glial structure is present in the optic stalk and changes into radial glia in the optic chiasm and optic tract (Guillery and Walsh, 1987; Colello and Guillery, 1992; Reese et al., 1994).

Retinotopic order in the optic tract

It has been reported that the crossed fibers from dorsal and ventral retina cross the midline at different locations. Fibers from the dorsal nasal retina cross the midline in the posterior part of the chiasm, whereas those from the ventral nasal retina cross in more anterior region of the chiasm (Naito, 1994). These different crossing positions of the fibers in the chiasm may establish a pre-ordering of the crossed fibers in the optic tract, which appears to extend to their appropriate termination in the lateral geniculate nucleus and superior colliculus (Dunlop et al., 2000). After passing the chiasm, the crossed axons mix with the uncrossed axons in the optic tract, i.e. axons originating from the nasal retina mingle with those originating from the temporal retina in the optic tract. In the contrary, axons from the dorsal and ventral regions of the retina segregate from each other to form a new order in the optic tract (cats: Torrealba et al., 1982; ferrets: Reese and Baker, 1993; rats: Chan and Guillery, 1994; mice: Chan and Chung, 1999). Axons from the ventral and dorsal retina occupy the anterior and posterior aspects of the optic tracts respectively (Chan and Chung, 1999). This segregation is established before the axons leave the chiasm (Chan and Guillery,

1994). This specific patterning of axon order in the optic tract contributes to the formation of retinotopic map in the visual targets.

Growth cones in the mouse optic pathway

To reach the destined target in the complicated retinofugal pathway, a growing axon must have a pioneer to explore the environment and decide its appropriate direction. The growing tip of an axon is called a growth cone.

Structure and role of growth cones

Growth cone is an irregular, spiky enlargement at the tip of each growing axon. It is an active growing structure of a neuron, which is specialized to identify an appropriate path for axon elongation (Alberts et al., 1994). The retinal axons are formed from molecules of tubulin, while the leading edge of the growth cone consists of lamellipodia and filopodia, which are formed from actin filaments (Forscher and Smith, 1988). Growth cone explores the surrounding environment with its filopodia and lamellipodia. When it contacts a favorable surface, it elongates. However, if the contact surface is unfavorable, it withdraws. In this way, neuronal growth cones guide the elongating axons to their appropriate targets (Alberts et al., 1994). Growth cones usually follow the paths that have traveled by other axons mediated by cell adhesion molecules on their surfaces (Rutishauser, 1993). The axons are then grouped together and travel down the pathway in tight bundles (Jeffery, 1990). One of the most important classes of these adhesion molecules is neural cell adhesion molecule (NCAM) (Edelman, 1983). In the retinofugal pathway, growth cones also encounter different components of the extracellular matrix, which give different guidance

signals along their way to target regions (Johnston and Wessells, 1980; Dodd and Jessell, 1988). We will discuss these surface and extracellular matrix molecules in more details later.

During pathfinding, growth cones respond to external guidance signals in the environment for neurite extension and directionality by making appropriate changes in morphology and behavior (Caudy and Bentley, 1986; Nordlander, 1987). As crossed axons navigate from the optic stalk to the postmidline chiasm (Chan et al., 1998; Chung et al., 2000b), and when uncrossed axons have turned back to the ipsilateral tract before hitting the midline, the complexity of retinal growth cone morphologies increases in mouse embryos (Godement et al., 1994). In decision regions where growth cones have to choose their paths, growth cones become larger, more lamellepodial and project more filopodia (Tosney and Landmesser, 1985; Bovolenta and Mason, 1987; Chan et al., 1988). Other than morphology, there are changes in behavior of growth cones at decision regions. A saltatory growth pattern of retinal axons has been reported in the chiasm of mouse embryos, which is usually followed by changes in growth direction of the axons (Godement et al., 1994; Chan et al., 1998). This growth pattern has been related to sampling guidance cues of the growth cones to go towards their targets.

Mechanism of axon guidance in retinofugal pathway

The retinofugal pathway is such a complicated route that all the axon orders involved must be delicately arranged by different kinds of mechanisms. The positional values of retinal ganglion cells in axon guidance have been demonstrated in

the orderly topographic map of the retinal projections in the retinofugal pathway (Metin et al., 1988). The origins of nasal and temporal retinal ganglion cells also contribute to the arrangement of retinal axon divergence (Colello and Guillery, 1990; Godement et al., 1990; Sretavan, 1990). While the retinal ganglion cells are evidently endowed with positional values, different guidance cues that exist in the retinofugal pathway is of equal importance in axon pathfinding. The only cellular substrates for these cues are the radial glial cells and neurons in the ventral diencephalon (Sretavan et al., 1994; Marcus and Mason, 1995; Chan et al., 1999). *In vitro* studies have demonstrated that neurite outgrowth of uncrossed axons is inhibited in the presence of chiasm cells or membrane fragments of these cells (Wizenmann et al., 1993; Sretavan et al., 1994; Wang et al., 1995), indicating a membrane mediated mechanism in the formation of axon divergence at the midline of the chiasm. Uncrossed axon routing is also mediated by an interaction between fibers from the two eyes. Eye removal before axons grow to the chiasm results in a loss of the uncrossed component from the remaining eye (Chan and Guillery, 1993; Taylor and Guillery, 1995; Chan et al., 1999). Whilst the cellular components of the chiasm have been described in detail, little is known for the molecules that are involved in axon guidance. In the present study, the underlined molecular mechanisms that control the axon patterning in mouse retinofugal pathway will be discussed, which include 1) proteoglycans, specifically chondroitin sulfate proteoglycans and heparan sulfate proteoglycans; and 2) neural cell adhesion molecule that are present in the developing mouse retinofugal pathway.

Proteoglycans

Proteoglycans (PGs) are proteins containing one or more covalently linked glycosaminoglycan (GAG) chains. They are first recognized in the extracellular matrix of cartilage and it is now clear that they are found in the matrices of all tissues. Proteoglycans vary greatly depending on the weights of their core proteins and the number and types of GAG chains (Alberts et al., 1994). In central nervous tissues, the dominant GAG chains on the proteoglycans are chondroitin sulfate (CS) and heparan sulfate (HS). These proteoglycans exist as either extracellular matrix or membrane associated molecules. There is increasing evidence that chondroitin sulfate proteoglycans and heparan sulfate proteoglycans are involved in axon guidance in the central nervous system (Bandtlow and Zimmermann, 2000).

Chondroitin sulfate proteoglycans

Chondroitin sulfate proteoglycans (CSPGs) have been implicated an inhibitory role for axon growth. During development, expressions of CSPGs have been found in regions that act as barriers to extending axons (Snow et al., 1991; Oakley and Tosney, 1991; Perris et al., 1991; Brittis et al., 1992; Landolt et al., 1995). *In vitro*, CSPGs have been shown to inhibit neurite outgrowth and elongation (Dou and Levine, 1994; Friedlander et al., 1994; Maeda and Noda, 1996; Niederost et al., 1999). Some studies have reported that the isolated core proteins of CSPGs (Dou and Levine, 1994; Maeda and Noda, 1996) cast the inhibitory effect, whereas some have demonstrated that the inhibitory effect is due to the presence of CS chains (Snow et al., 1990, 1991; Fichard et al., 1991; Chung et al., 2000b). Furthermore, the spatially restricted expression of CSPGs is correlated with chronotopic axon order in the developing optic tract of mice

(Chung et al., 2000a) and ferrets (Reese et al., 1997). CSPGs expressed in the deeper parts of the optic tract may repel newly arrived axons to the superficial regions. It is of interest to investigate the effect of CSPGs on setting up the chronologic fiber order in the mouse optic tract.

Contrary to the so many studies demonstrating the inhibitory effect of CSPGs, there are other arguments that support promoting functions of CSPGs to axon growth (Iijima et al., 1991; Lafont et al., 1992; Faissner et al., 1994; Fernaud-Espinosa et al., 1994). Two brain CSPGs, phosphacan and neurocan, serve good examples for the differential functions of the CSPGs. Phosphacan are diffusely distributed in the cortical anlage (Maeda et al., 1995), yet it does not seem to affect axonal extension (Maeda and Noda, 1996). Although neurocan has been shown to inhibit neurite outgrowth *in vitro* (Inatani et al., 2001), its spatiotemporal expression pattern in rat suggests that it plays some roles in forming the elongation pathway for early cortical afferent fibers in the somatosensory cortex (Oohira et al., 1994) as well as the delineation of efferent and afferent intracortical pathways during early development of the rat cortex (Miller et al., 1995).

Heparan sulfate proteoglycans

Heparan sulfate proteoglycans (HSPGs) belong to another family of proteoglycan molecules (Hardingham and Fosang, 1992). They have been shown to take part in many biological activities mediated largely by the HS chains, including cell adhesion (Cole et al., 1985; Schubert and LaCorbiere, 1985), cell growth and cell differentiation by binding to growth factors (Rapraeger et al., 1991; Yayon et al.,

1991). Moreover, they have been demonstrated to have a role in neurite extension (Hantaz-Ambroise et al., 1987). *In vivo* study of *Xenopus* shows that HSPGs are involved in regulating axon growth in the retinotectal projection (Walz et al., 1997). However, whether HSPGs are expressed in or how this expression would be related to the retinofugal pathway of mouse embryos is unknown.

Neural cell adhesion molecules

The neural cell adhesion molecule (NCAM) is a cell surface glycoprotein that occurs in several isoforms. This molecule has been shown abundantly on developing axons and the glial environment (Silver and Rutishauser, 1984; Brittis et al., 1995). It has been shown to mediate contact between optic nerve fibers in fascicular groups (Jessell, 1988). This fasciculation of axons into bundles is brought about by cell-cell and cell-substrate interactions (Acheson et al., 1991) through either homophilic binding mechanism (Rutishauser et al., 1982; Hoffman and Edelman, 1984) or heterophilic binding activity (Grumet et al., 1993). The modulation of these binding activities is related to the amount of polysialic acid (PSA) attached to the NCAM, which in turn affects neural growth and development (Acheson et al., 1991; Rutishauser and Landmesser, 1991; Tang et al., 1994; Yin et al., 1995). Distribution of NCAM is found in the retinofugal pathway in chicks and goldfish (Silver and Rutishauser, 1984; Bastmeyer et al., 1990). It has been shown to play a role in developing chick retinotectal system (Thanos et al., 1984). Thus, investigation of NCAM expression in the retinofugal pathway of mouse embryos is potentially interesting study in the light of the findings from chicks and goldfish.

Aim of study

This thesis examines the studies related to the molecular mechanisms that control the axon patterning in mouse retinofugal pathway. In the first study (Chapter 2), the possible role of CSPGs in the establishment of age-related fiber arrangement in the optic tract of mouse embryos is investigated by enzymatic digestion of the glycosaminoglycan CS chains using brain slice preparations. This is followed by characterization of two brain CSPGs, phosphacan and neurocan, (Chapter 3) during the major growth period of retinal axons at the chiasm. The next study (Chapter 4) investigates the possible role of HSPGs in axon guidance of the optic chiasm in mouse embryos by revealing their expression patterns at different developmental stages. The last study (Chapter 5) looks at the expression of sialylated NCAM in the developing mouse retinofugal pathway. Preliminary results on the possible function of NCAM in rearranging axon order in the optic tract are presented in this chapter as well.

CHAPTER 2

ENZYMATIC REMOVAL OF CHONDROITIN SULFATES ABOLISHES THE AGE-RELATED ORDER IN THE OPTIC TRACT OF MOUSE EMBRYOS

INTRODUCTION

During development, retinal ganglion cell axons segregate at the midline of the chiasm to form a partial decussation pattern (Godement et al., 1990; Chan et al., 1998). Before entering the optic tract, these axons undergo another rearrangement of position to generate a sequential lamination of axons within the optic tract in a deep to superficial order according to time of arrival in the pathway (Walsh and Guillery, 1985; Colello and Guillery, 1992; Reese et al., 1994). This obvious reorganization establishes an age-related order in the optic tract and suggests a mechanism exists at the chiasm which is responsible for the establishment of this deep to superficial chronotopic order (Torrealba et al., 1982; Colello and Guillery, 1992; Reese et al., 1994).

The chondroitin sulfate (CS) proteoglycans (PGs) are molecules that consist of a core protein with glycosaminoglycan chains attached to it. They are either extracellular matrix or cell surface molecules which have been shown to be important regulators of axon growth and patterning in the developing central nervous system (Margolis and Margolis, 1997). In the visual system, these molecules have been implicated in regulating the growth direction of axons in the developing retina (Snow et al., 1991; Brittis et al., 1992). The expression pattern of CS suggests a possible role of the molecules to guide the earliest axon growth (Chung et al., 2002a). Removal of

CS by chondroitinase ABC from intact retinas in culture induces changes in the pattern of retinal axon outgrowth (Brittis et al., 1992). Furthermore, CS removal results in disruptions of pathfinding of the early retinal axons in the chiasm and normal projection of axons to form the partial decussation pattern at the midline (Chung et al., 2000b). Immunoreactive CS restricted in the deep parts of the tract suggests an inhibitory role of the CS epitope to repel newly arrived axons, which gather mainly in the subpial regions, for the re-establishment of the age-related fiber order in the tract (Chung et al., 2000a). A similar distribution of CS in the initial segment of the post-chiasmatic optic tract in ferrets was also reported which correlates with development of chronotopic order of retinal axons in the optic tract of ferrets (Reese et al., 1997). Also, CSPGs are also found at the junction between the telencephalon and diencephalon in chick embryos and may serve to border the anterior course of optic axons in the tract (Ichijo and Kawabata, 2001). The expression of the CS epitope in the mouse optic tract may function similarly to confine the course of the optic axons to a superficial position in the diencephalon.

As CS epitope was shown to be an important regulator in axon guidance in different parts of the retinofugal pathway, in this study, we tried to find out if the chronotopic order of growth cones in the optic chiasm and optic tract was affected after an enzymatic removal of CS glycosaminoglycans from the pathway, using brain slice culture of the retinofugal pathway of mouse embryos.

MATERIALS AND METHODS

Preparation of brain slices

Time-mated C57 mice were obtained from the Animal House of the Chinese University of Hong Kong. The day that the vaginal plug is found is designated as embryonic day 0 (E0). Pregnant mice were killed by cervical dislocation and mouse embryos at E14 were removed by Caesarean section. The embryos were decapitated and kept in chilled Dulbecco's modified Eagle's medium (DMEM)/F12 medium containing penicillin (1000 U/ml) and streptomycin (1000 μg/ml). Brain slices were prepared by removing the dorsal and ventral parts of the head just above and below the eyeball with a razor blade, leaving the third ventricle and the floor of ventral diencephalon exposed. Brain slices of the retinofugal pathway that included the eyes, optic stalks, chiasm and proximal parts of the optic tracts were obtained. The brain slices were cultured in DMEM/F12 with 10% foetal bovine serum (Life Technologies, USA) at 37°C in a rolling incubator for 5 hours. Within the incubation period, the cultures were supplied with pure oxygen three times, as a jet of oxygen directed into the air space above the culture medium. In experimental brain slices, chondroitinase ABC (Seikagaku, Japan) in distilled water was added at the final concentration of 0.5 U/ml during the incubation. This enzyme catalyses the formation of unsaturated disaccharides from chondroitin 4- and 6-sulfate (Yamagata et al., 1968) and removes the glycosaminoglycan chains from the protein core of the PGs. This concentration of enzyme was able to remove most CS from the ventral diencephalon as shown by the immuno-staining using CS-56 antibody (Chung et al., 2000b), which was further confirmed in preparations of current study. The control cultures were maintained in the same medium for 5 hours but without the addition of enzyme. In another control preparation, 0.5 U/ml keratanase (Sigma, USA) was added to the brain slices during the incubation period. This enzyme cleaves specifically the keratan sulfate and does

not affect the CS moieties.

Rhodamine phalloidin staining of growth cones

The growth cones in the retinofugal pathway were stained with Rhodamine phalloidin (Molecular Probes, USA) that binds specifically to F-actin (Wulf et al., 1979; Colello and Guillery, 1992; Chung et al., 2001). After the incubation period, the brain slices were fixed in freshly prepared 4% paraformaldehyde in 0.1 M phosphate buffer at pH 7.4 overnight. The fixed tissues were embedded in a gelatine-albumin mixture. After making a cut on the block to mark the orientation, the blocks were sectioned using a vibratome. Serial frontal sections of the retinofugal pathway, at the thickness of 100 μm, from the eyes to the proximal parts of the optic tract were collected in phosphate buffered saline (PBS). The sections were washed three times with PBS, incubated in 0.1% Triton-X 100 in PBS for 30 minutes. After a brief wash, the sections were incubated in Rhodamine phalloidin (1:40 in PBS) at 4°C overnight, then washed again with PBS and cover slipped in 50% glycerol.

DiI injection in brain slices

In some preparations, all retinal axons and their growth cones in one eye were labelled with DiI (1,1'-dioctadecyl-3,3,3',3'-tetramethylindocarbocyanine perchlorate) (Molecular Probes, USA) (Godement et al., 1987). The dye was dissolved in dimethyl sulphoxide and injected into the vitreous using a picospritzer (General Valve Co., NJ, USA). In other preparations, a small number of axons from either dorsal nasal or ventral temporal retina were labelled by a DiI crystal. All injected slices were cultured for 5 hours in DMEM/F12 as described above and fixed

with 4% paraformaldehyde overnight at 4°C. For those with the whole retina labelled, dye-filled axons were examined in whole mount preparation of the chiasm. Brain slices with focal retinal label were sectioned frontally using a vibratome. Individual axons and growth cones at the junction of the chiasm and the tract were imaged using a confocal imaging system (MRC600, BioRad, UK). The sizes of all growth cones that were identified in these confocal micrographs were measured using the area measurement function in the MetaMorph software (Universal Imaging Co., USA) in order to determine whether the chondroitinase treatment produced any significant alterations to the growth cone morphology of retinal axons at the optic tract.

Immunocytochemistry

Some sections at the level of the optic stalk/tract junction were selected for double labelling for CSPGs and F-actin-rich growth cones. The sections were first incubated overnight in the antibody against the CS epitope (clone CS-56, Sigma, USA), then in a goat anti-mouse secondary antibody conjugated to Alexa Fluor 488 (Molecular Probes) for 3 hours (IgM, 1:200 in PBS, pH 7.4). The sections were then washed with PBS and incubated with Alexa Fluor 568-conjugated phalloidin (1:40 in PBS pH 7.4, Molecular Probes) overnight at 4°C. This combination of fluorophores gives a better separation of signals in our preparations than by using FITC-conjuugated secondary and Rhodamine phalloidin. The sections were cover-slipped in 50% glycerol in PBS and imaged by a confocal imaging system.

Retinal explant culture

Retinal explants from either the ventral temporal or dorsal nasal quadrant of

the retina were prepared from E14 embryos. The explants were plated on poly-L-lysine (0.5 mg/ml; Sigma, USA) and laminin (40 μg/ml; Sigma, USA) coated coverslips and cultured in DMEM/F-12 medium supplemented with 1% bovine serum albumen, 0.4% methycellulose, 0.5% insulin, 0.5% transferrin and 0.1% sodium selenite at 37°C. After 18 hours in culture, when extensive neurite outgrowth was observed in the retinal explants, chondroitinase ABC (in distilled water, final concentration is 0.5 U/ml) was added to the culture medium. We examined here whether the enzyme treatment triggered collapses and/or relocation of the actin filaments in the retinal growth cones. Control cultures received addition of equal volume of distilled water. After 5 hours, the retinal explants were fixed in 4% paraformaldehyde for 45 minutes. The retinal outgrowth in these cultures was captured using a Spot RT digital camera (Diagnostic Instruments, Inc., USA) connected to a Zeiss Axiovert 200 microscope (Germany). The numbers of all retinal neurites in each explant were counted in these phase images. The percentages of growth cones with a collapse versus normal morphology in control and enzyme treated explants were determined and compared. Some retinal explants were stained with Rhodamine phalloidin using the above procedures.

Confocal microscopy and image analyses

The images were captured with a confocal imaging system (Bio-Rad MRC 600, Hertford, England) connected to a Zeiss Axiophot photomicroscope (Oberkochen, Germany). A blue excitation filter set (BHS, 488nm excitation and 515nm emission long pass) was used to image the CS immunoreactivity. A green excitation filter set (GHS, 514 nm excitation and 550 nm long pass) was used to

reveal the DiI labelled optic axons and actin-rich growth cones in the retinal fiber layer of the retinofugal pathway and the retinal cultures. The digital images were processed using the Confocal Assistant software (BioRad, USA). The distribution of phalloidin labelled growth cones at the midline of the chiasm and at the initial segment of the optic tract was analysed in frontal sections of the brain slices using the intensity profile measurement of the MetaMorph software (Universal Imaging Corp., USA). A first order regression line was generated from each plot. Slopes of these regression lines in control and enzymes treated groups were tested for normal distribution, and compared using one-way ANOVA tests in the InStat software (GraphPad, USA).

RESULTS

Distribution of growth cones in the optic tract

Anterograde filling of the retinal axons with DiI in E14 brain slice preparations showed many axons at the optic chiasm and the optic tract (Fig. 1A). Rhodamine phalloidin was then used to reveal the distribution of growth cones in the chiasm and optic tract in frontal sections of E14 embryos. Frontal sections of the ventral diencephalon showed an accumulation of phalloidin positive growth cones at the sub-pial regions of the optic tract (Fig. 1B). In the same section, the distribution of chondroitin sulfate (CS) as revealed by the CS-56 antibody, showed a restricted distribution in the deep regions of the tract (Fig. 1C). These results demonstrate a complementary pattern of growth cone and CS distribution.

Chronotopic order at the tract was abolished after chondroitinase treatment

The functions of the CS epitope on the proteoglycan molecules on the age-related axon re-ordering were investigated by enzymatic digestion. In frontal sections of the caudal chiasm from the control preparations (n = 19), phalloidin staining of growth cones in the optic tract was restricted mostly to the superficial regions next to the subpial glia after 5 hours culture (Fig. 2A). Positively stained growth cone profiles were rarely seen in deep regions of the tract. These results indicate that the culture conditions do not produce any obvious alterations to the patterning of age-related order in the optic tract. After removal of CS with 0.5U/ml chondroitinase ABC, obvious changes in distribution of growth cones in the optic tract were observed. In the enzyme-treated embryos (n = 16), the distinct biased distribution of growth cones in the superficial region shown in control preparations was lost in most preparations (Fig. 2B). The actin rich region in growth cones stained by phalloidin in the optic tract dissappeared after enzymatic removal of CS. Complete removal of CS from the optic tract was confirmed by checking the presence of immunoreactive CS (Fig. 2D and E; n = 2 for the controls; n = 3 for the chondroitinase treated preparations). No influence on the age-related order in the optic tract was observed in brain slices treated with keratanase (Fig. 2C; n = 15). These results provide strong evidence for a specific effect of the CS moieties on the proteoglycan molecules in the formation of chronotopic axon arrangement in the optic tract.

The intensity (in pixel) of phalloidin staining along a line that extends from the superficial to deep parts of the optic tract was measured in all control, chondroitinase and keratanase treated brain slice preparations (from A to B in Fig. 2A-2C). In plots of the intensity profiles, there was a consistent decrease in phalloidin

staining from the superficial to deep region of the retinal fiber layer in control preparations (Fig. 3A). However, in preparations treated with chondroitinase, the reduction in staining intensity was not obvious (Fig. 3B). The plots in this experimental group showed a horizontal rather than inclining slope, indicating that the phalloidin positive growth cone profiles were distributed evenly in all depth of the tract. Regression lines were calculated from these plots using the InStat software (GraphPad, USA) (Fig. 4A). The slope of regression lines in chondroitinase treated preparations (means ± s.e.m.: -0.913 ± 0.263) is significantly different from that of the control preparations (-1.827 ± 0.187) or of the keratanase treated group (-1.956 ± 0.139; $n = 15$; $p < 0.05$, Kolmogorov and Smirnov Test followed by Dunnett Multiple Comparisons Test) (Fig. 4B). These results confirm the findings that removal of the CS carbohydrate side-chains from the proteoglycans abolishes the development of chronotopic axon order at the threshold of the optic tract in mouse embryos.

Axon order at the midline of the chiasm: The effect of chondroitinase treatment

It had been shown that CS was found in the deep part of the chiasm at the midline (Chung et al., 2000a). This raised a question of whether the arrangement of retinal growth cones at the midline is affected after enzymatic removal of CS glycosaminoglycans. To address this question, we examined the growth cone distribution at the midline of the chiasm in frontal sections of E14 brain slice preparations, about 100 μm rostral to the section that contains the optic tracts. In the control preparations ($n = 9$), without addition of enzyme, the phalloidin staining showed growth cone-like profiles largely at the superficial regions in the retinal fiber layer at the midline of the chiasm, but an obvious number of the profiles were also

found in deeper positions (Fig. 5A). This distribution pattern suggests that some retinal growth cones, unlike those at the tract, grow amongst the deeper optic axons at the midline (Colello and Guillery, 1998). In brain slices treated with chondroitinase (n = 10), the staining pattern of phalloidin positive growth cones showed a similar distribution (Fig. 5B). The growth cone profiles were found from the superficial to the deep region of the retinal fiber layer at the midline. It was noted in these sections that a bilateral patch of intense staining with Rhodamine phalloidin was found in the chiasm, suggesting that growth cones are accumulating lateral to the midline. This position corresponds to the lateral part of the midline glial raphe where uncrossed axons normally make their turn. Treatment of the brain slices with keratanase (n = 8) did not produce significant change to the growth cone distribution at the midline (Fig. 7A).

A plot of intensity profiles across the depth of the retinal fiber layer at the midline showed a gentle decrease in staining in most preparations from the superficial to the deep part at this region (Fig. 6A), which is significantly different from the dramatic reduction in staining intensity at the threshold of the optic tract ($U = 4$, $p < 0.0001$; Mann-Whitney nonparametric test) (compared 3A and 6A). This staining profile was shallower in preparations treated with chondroitinase (Fig. 6B). However, comparison of the mean slopes of the regression lines (-0.706 ± 0.135, -0.658 ± 0.090 and -0.975 ± 0.249 in control, chondroitinase and keratanase treated preparations, respectively) from these plots showed that there was no significant difference between the control, chondroitinase or keratanse (n = 8) treated preparations ($p > 0.05$, Kruskal-Wallis nonparametric ANOVA Test) (Fig. 7A).

The depth of retinal fiber layer at the chiasm and the tract is not restricted by expression of chondroitin sulfate

Another question that was addressed in this study was whether the depth of the retinal fiber layer at the chiasm and the tract is related to a restricted expression of CS previously reported in the chiasm and the tract (Chung et al., 2000a). The thickness of retinal fiber layer at the midline of the optic chiasm and at the threshold of the optic tract was measured in E14 mouse embryos using the MetaMorph software. A plot of the mean thickness of fiber layer at these two regions showed that there was no significant difference between the thickness of the fiber layer before and after chondroitinase treatment ($U = 39$, $p = 0.661$ for the midline; $U = 121.5$, $p = 0.448$ for the tract) (Fig. 7B). These results showed clearly that the depth of the retinal fiber layer at the chiasm and the tract is not defined by a spatially restricted expression of the CS glycosaminoglycans.

Chondroitinase treatment did not affect the phalloidin staining in retinal growth cones

Rhodamine phalloidin was used in this study to label growth cones in the retinofugal pathway, based on previous findings that growth cones are rich in F-actin whereas the axon shaft is relatively impoverished in F-actin (Wulf et al., 1979; Colello and Guillery, 1992; Chung et al., 2001). To test this assumption we examined the staining pattern of Rhodamine phalloidin in neurites from E14 mouse retinal explants collected from either ventral temporal or dorsal nasal retina, where clear imaging of the growth cone and axon shaft could be made. Furthermore, we asked

whether the chondroitinase treatment at a concentration that generated the redistribution of growth cones in the optic tract had any effect in producing growth cone collapses or causing a mobilization of actin filaments away from the growth cone. After culturing for 1 day on a laminin and polylysine subtrate, many retinal axons tipped with growth cones were observed (Fig. 8E). Rhodamine phalloidin staining was largely confined to the peripheral region of growth cones, particularly to the filopodial and lamellipodial extensions (Fig. 8A and 8B). The axons had the expected patchy staining and this was at a far lower intensity than in the growth cones, reflecting the distribution of F-actin.

Chondroitinase treatment (0.5 U/ml) did not produce obvious collapses in the retinal growth cones (Fig. 8F), nor did it generate any obvious redistribution of phalloidin positive actin filaments within the structure (Fig. 8C and 8D). Furthermore, in a growth cone collapse assay, the percentage of growth cones with a collapsed morphology in explants treated with chondroitinase was not significantly different from that in the controls (Fig. 8G) ($p > 0.05$, Mann-Whitney Test), indicating that this enzyme did not produce significant increase in collapse of retinal growth cones that might otherwise complicate interpretation of the current results obtained in the brain slice culture study.

Dye filled growth cones in the optic tract failed to accumulate at the subpial region after removal of chondroitin sulfate

We further investigated the effects of chondroitinase treatment on the age-related ordering of retinal axons in the optic tract using a focal label of ganglion cells

and their axons with DiI in brain slice preparations of the E14 mouse retinofugal pathway. In control preparations, dye-filled retinal axons tipped with growth cones were found largely in the superficial half of the optic tract contralateral to the injected eye (Fig. 9A and 9C). In the deep half of the tract, only a few growth cones were occasionally seen. In contrast to these observations, growth cones were found in all thicknesses of the fiber layer after the enzymatic removal of CS (Fig. 9B and 9D). Retinal growth cones in these preparations often grew and apposed the deep margin of the tract (Fig. 9D), which was rarely observed in the control preparations (Fig. 9C). Similar results were found in preparations that had the ventral temporal or dorsal nasal retina labelled with DiI. Counting of the growth cone number at the superficial and deep halves of the tract revealed a significant dispersion of growth cones from the subpial to the deep regions after the chondroitinase treatment (Fig. 9E) ($p < 0.05$, Mann-Whitney Test), supporting the findings that we obtained from the phalloidin staining studies. Furthermore, quantitative analyses of the growth cone morphology revealed a significant increase in the size of the DiI filled retinal growth cones at the tract after the chondroitinase treatment (Fig. 9F), suggesting that removal of the CS glycosaminoglycans triggered a change in response of these growth cones that might underlie their repositioning in this region of the retinofugal pathway.

DISCUSSION

In the present study, the regulating function of chondroitin sulfate on axon routings in the optic chiasm and tract was investigated. The major findings are: 1) Enzymatic removal of CS glycosaminoglycans in brain slice preparations of the retinofugal pathway leads to disruption of the chronotopic fiber order in the optic tract

of mouse embryos. Similar treatment of brain slices with keratanase does not produce comparable effect, indicating a crucial function of CS moiety of the proteoglycans in establishing the chronotopic fiber order at this position of the pathway. 2) The treatment of chondroitinase to brain slice preparations, however, does not give observable effect on the distribution of growth cones at the midline of the chiasm, where chondroitin sulfate is also found. These results imply a mechanism in which optic axons response specifically to external guidance cues in different regions of the retinofugal pathway in developing the chronotopic fiber order. 3) The thickness of the retinal fiber layer at both the midline of the chiasm and the optic tract was not significantly altered after the removal of CS.

Chondroitin sulfate proteoglycans and axon patterning at the optic tract

The existence of the age-related retinal axon order in the optic tract of mouse embryos (Colello and Coleman, 1997; Chung et al., 2001) was confirmed using rhodamine phalloidin as a marker for the retinal growth cones and anterograde filling of individual retinal axons. At the optic tract, the growth cones were restricted to the superficial region, while intense expression of CS epitope was observed in the deep region (Chung et al., 2000). After enzymatic removal of CS with chondroitinase ABC, the actin rich growth cones were dispersed across the thickness of the retinal fiber layer at the junction of the chiasm and the tract. Growth cone is the active growing structure of a neuron (Lockerbie, 1987). Its existence in the developing neural pathway represents the presence of newly arrived axons. The observation that growth cones lie predominantly next to the sub-pial glia implies that the advancing growth cones tend to move towards the pia as they approach the chiasm and tract. This deep

to superficial order of growth cones in the optic tract thus establishes a chronotopic order of retinal fibers in this region, with the youngest axons being closest to and the oldest farthest from the pial surface of the tract (Walsh and Guillery, 1985; Colello and Guillery, 1992). In the present study, we showed that this age-related order directly relied on a spatially restricted expression of the CS epitope. The tendency of growth cones deviating towards the subpial surface of the tract was removed after the enzymatic digestion of CS. The aggregation of actin rich growth cones at the superficial regions of the optic tract was abolished. This observation showed that CS epitopes was involved in the establishment of the chronotopic order of growth cones at the optic tract, confirming the suggestions from previous studies that the distribution of CS epitopes is related to the establishment of chronotopic order in the developing optic tract (ferrets: Reese et al., 1997; mouse: Chung et al., 2000). The disruption of the restricted growth cones in the subpial region by enzymatic removal of CS implicates an inhibitory role of CS moiety in axon guidance in the mouse optic pathway which repels advancing axons to the superficial regions of the optic tract. Different studies have also reported the inhibitory function of CSPGs in the central nervous system (Snow et al., 1991; Brittis et al., 1992; Snow and Letourneau, 1992; Dou and Levine, 1994; Hoffman-Kim et al., 1998). This age-related guidance effect at the optic tract is specific to the CS glycosaminoglycans, as the reordering is not affected by enzymatic treatment that removes the keratan sulfate glycosaminoglycan. The level of CS removal is very satisfactory that no detectable CS-56 antibody staining against CS epitope can be seen (Chung et al., 2000b; present result). It should be noted, however, that other than CS epitopes, the protein cores of the proteoglycans have been shown to regulate axon growth (Iijima et al., 1991; Grumet et al., 1994).

Two major brain CSPGs are present in the ventral diencephlon of fetal ferrets and in the advancing axons in the optic tract (Reese et al., 1997). Detailed studies of the expression of the two brain CSPGs, phosphacan and neurocan, in mouse optic pathway will be discussed in the next chapter.

Enzymatic treatment of tissues may be argued to cause retardation in axon growth or growth cone collapses in the chiasm, leading to false portrait of the absence of growth cones. However, our results show that the chondroitinase treatment does not lead to significant increase in growth cone collapses, nor redistribution or mobilization of actin from the growth cones, supporting the evidence that spatially regulated expression of CS glycosaminoglycan is essential for chronotopic fiber establishment at the mouse optic tract.

CS and axon patterning at the mouse chiasm

At the midline of the optic chiasm, the disruption of the fiber order was not obvious by the removal of CS. Axons crossing the midline are not sensitive to CS in the region and does not respond to it. The inhibitory role of CS in the optic tract seems not to be applicable to the decussating axons in the chiasmatic midline. It has been shown by Chung et al. (2000b) that CSPG acts as a functional barrier at the chiasmatic midline to stop the growth of uncrossed axons whilst allowing a group of crossed axons to pass through. The uncrossed axons respond to the abundant CS at the midline. They turn before hitting the CS raphe (Chung et al., 2000a) and project to the ipsilateral tract by interacting with axons from the other eye (Godement et al., 1990; Chan et al., 1999). However, the crossed axons decussate at the midline, despite the

presence of the CSPG. These axons disperse through the depth of the retinal fiber layer at the midline and their distribution is independent from the expression of the CS glycosaminoglycans. The guidance function of CS-PGs in the age-related order seemed to take place in the optic tract but not in the chiasm. The complexity of growth cone morphologies increases as they travel from the chiasm to the optic tract (Mason and Wang, 1997; Chan et al., 1998; Chung et al., 2000b; current results). The increase in the complexity of retinal growth cones suggests their changing responses to different guidance cues in successive regions in the retinofugal pathway.

The depths of the retinal fiber layer at the midline and at the tract were not affected by the removal of CS. Retinal axons travel down the surface of the diencephalon as bundles formed by fasciculation. Specific surface molecules stick axons together along their course. Cell adhesion molecules such as L1, TAG-1 and NCAM, expressed in the developing retinofugal pathway (Silver and Rutishauser, 1984; Sretavan et al., 1994; Lustig et al., 2001) may bind axons together to grow in unison. It is also possible that the expression of inhibitory molecules restrict the course of the axon pathway (Reese et al., 1997; Chung et al., 2000a). In fetal ferrets and mouse embryos, the radial glial cells ramify their processes into the retinal fiber layer (Reese et al., 1994, 1997; Marcus et al., 1995; Chan et al., 1999). These specific cellular elements may interact with each other to define the boundary of the optic pathway in the diencephalon. However, our results show that the removal of the CS from the diencephalon leads to straying of growth cones within the optic tract, but does not release the optic axons from the confinement of the retinal fiber layer in the chiasm and tract. Thus, CS glycosaminoglycans do not function to confine the axon

border in the ventral diencephalon.

Removal of chondroitin sulfates disrupted normal growth cone distribution at the threshold of the optic tract (see Fig 10). The restricted distribution of retinal growth cones (red) at the superficial region of the tract was abolished after removal of chondroitin sulfates from the deep regions of the chiasm and the tract. We concluded that the formation of chronotopic fiber arrangement at the threshold of the optic tract is controlled by a spatially restricted expression of chondroitin sulfate glycosaminoglycans, probably through an inhibitory action of these molecules to retinal axons in the retinofugal pathway.

Figure 1

Expression of chondroitin sulfate in the optic tract of E14 mouse embryos is complementary to the position of the retinal growth cones. **A**: Confocal micrograph of a whole-mount ventral diencephalon (outlined by broken line) of an E14 mouse embryo. DiI filled retinal axons have grown from the optic stalk (OS), through the midline of the chiasm (arrow) to the optic tract (OT). The dotted line indicates the level at the caudal region of the chiasm where frontal section of the diencephalon in **B** and **C** is taken. **B-C**: Confocal micrographs showing a frontal section of the ventral diencephalon that was labelled simultaneously with phalloidin for growth cones and CS-56 antibody for the CS epitope. The phalloidin staining (arrow heads in **B**) was largely confined to the superficial region of the optic tract (bordered by broken line), which was complementary to the immunostaining of the CS epitope (arrow heads in **C**) in deep regions of the tract. Midline is indicated by arrows. Anterior is up in **A**; dorsal is up in **B** and **C**. Scale bars: **A** = 100 μm; **B-C** = 50 μm.

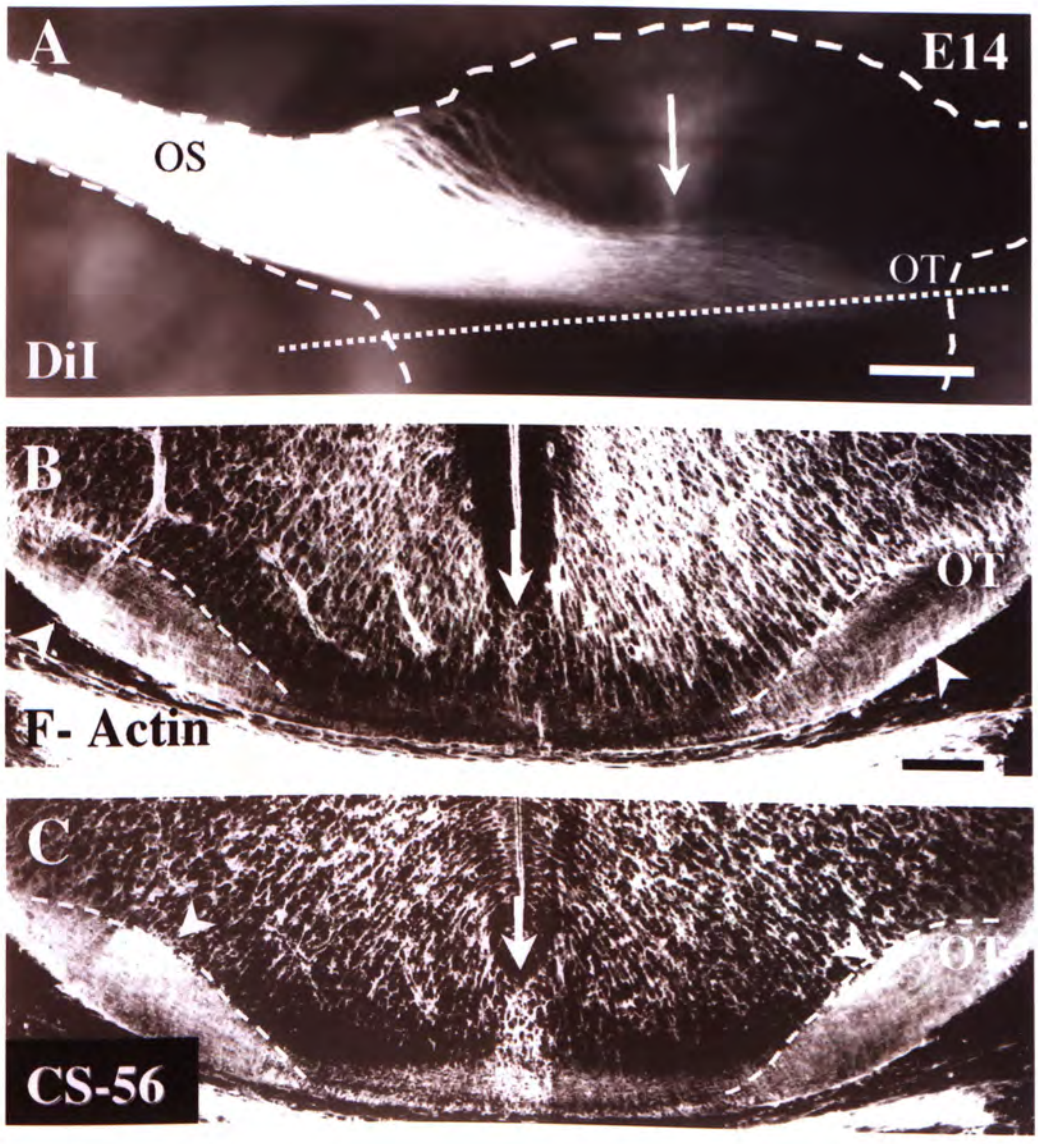
A
E14
OS
OT
DiI
B
OT
F- Actin
C
OT
CS-56

Figure 2

Confocal micrographs showing the phalloidin positive growth cone profiles in frontal sections of the chiasm and tract in slice preparations of the optic pathway from E14 mouse embryos. **A**: In control preparations, phalloidin positive staining was restricted largely to the superficial region of the retinal fiber layer (indicated by the broken line) at the threshold of the tract (OT). **B**: This accumulation of phalloidin positive growth cones was abolished by enzymatic digestion of CS (ABC). **C**: Treatment of the brain slices with keratanase did not produce a dispersion of phalloidin positive growth cones at the threshold of the optic tract. The dotted lines (in **A-C**) indicate the regions at the optic tract where intensity profiles of phalloidin stained growth cones from the subpial (A) to the deep (B) border of the retinal fiber layer were measured (see Figure 3). **D-E**: Treatment of the brain slices with chondroitinase removed CS immunoreactivity (small arrow in **C**) from the optic tract (outlined by broken lines) and other regions of the diencephalon. Midline is indicated by the large arrows. Dorsal is up. Scale bar in **C** = 100 μm, applied to **A-C**; scale bar in **D** = 100 μm, applied to **E**.

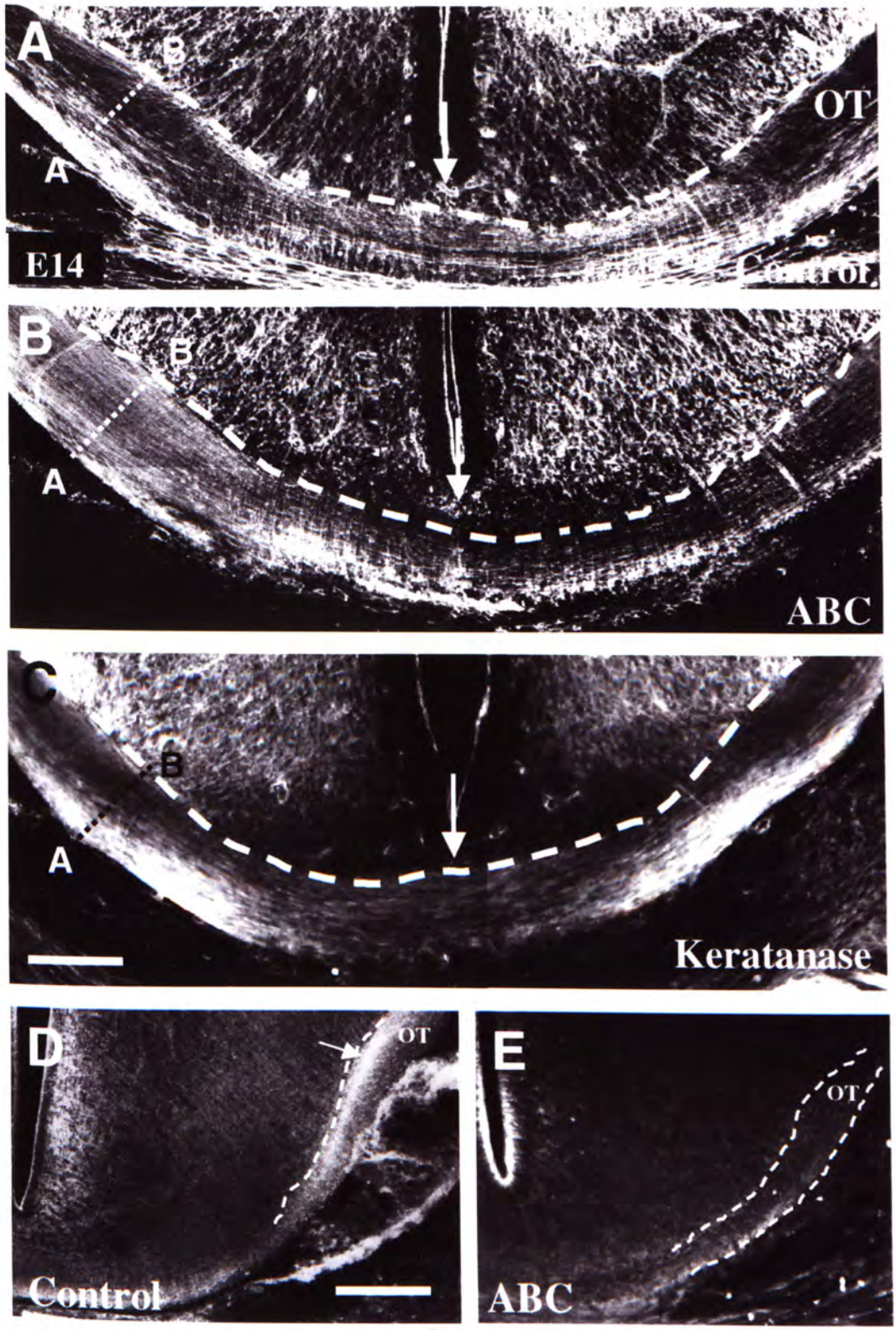
A
B
A
OT
E14
B
B
A
ABC
C
B
A
Keratanase
D
OT
Control
E
OT
ABC

Figure 3

Plots of intensity changes of phalloidin staining from the superficial (A) to deep (B) regions of the retinal fiber layer at the threshold of the optic tract in slice preparations of the optic pathway. **A**: In control preparations, the staining intensity consistently declined from the superficial to deep regions of the tract. **B**: Treatment of chondroitinase abolished the gradual decrease of staining intensity at the tract. The line that runs across each plot indicates the regression line generated by the statistic software.

(A) Control

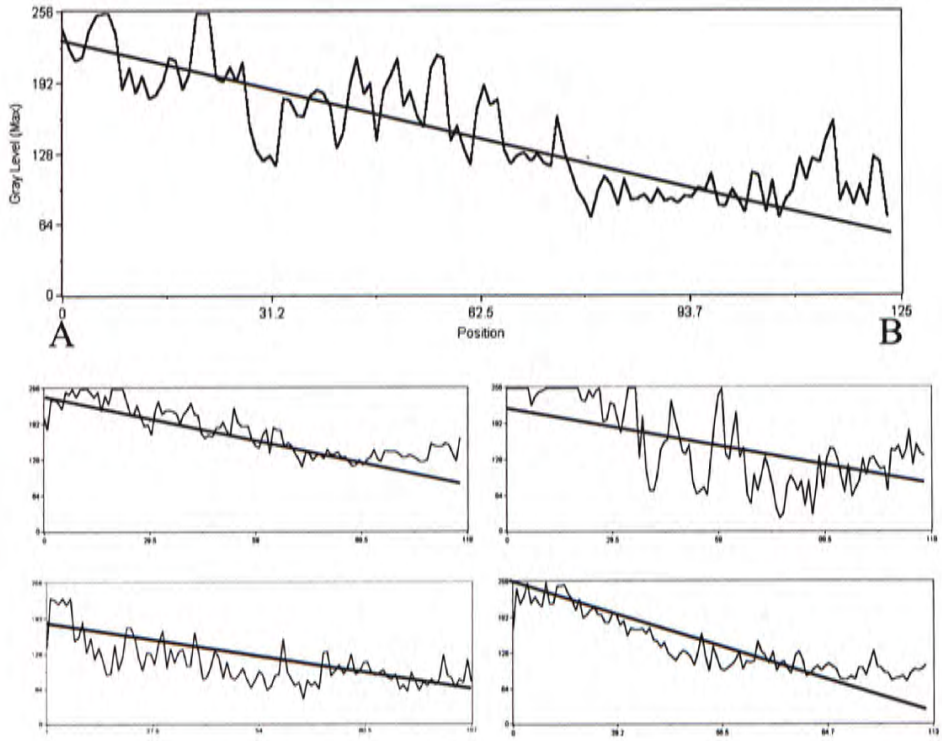

(B) Ch-ABC

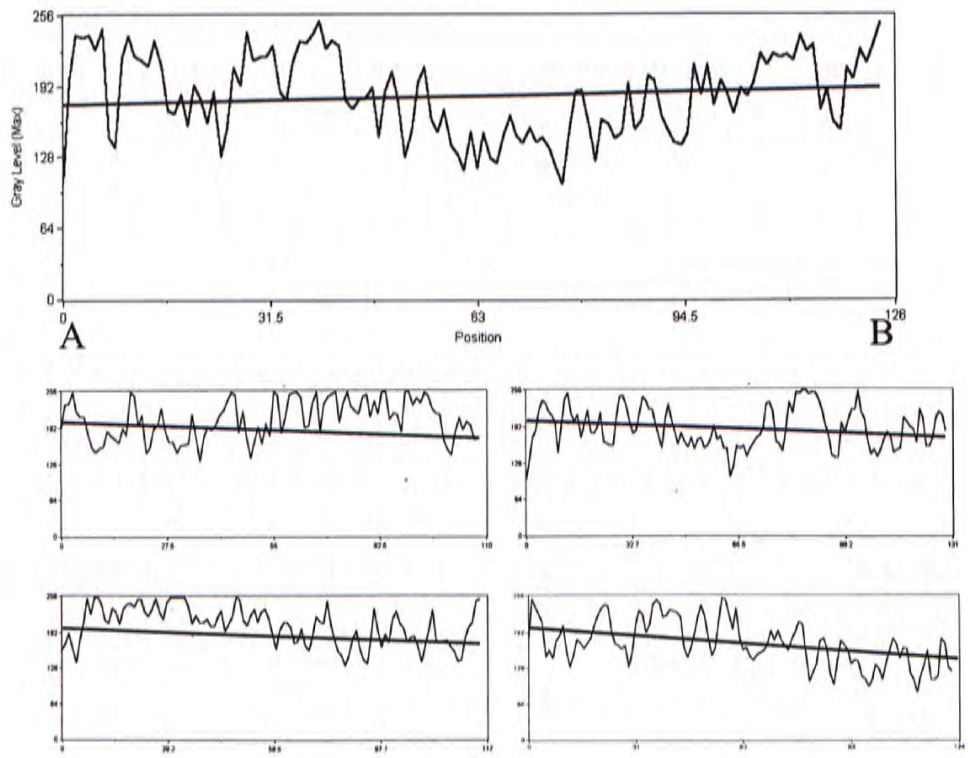

Figure 4

A: Plots showing the relative changes in fluorescence intensity of phalloidin staining from the subpial (A) to the deep (B) border of the optic tract (indicated by dotted lines in Figure 2) in control (dotted lines) and chondroitinase (ABC) treated (solid lines) preparations. Pixel intensity at the subpial region was denoted as 100%. Noted the removal of CS reduced the biased staining of phalloidin at the optic tract. **B**: Changes in slopes of these regression lines were analysed using ANOVA tests and the results showed a significant change (asterisk) in distribution of phalloidin postive growth cones in the optic tract after chondrointinase treatment (ABC) when compared with control or keratanase treated group. No statistical difference was found between the control and keratanase treated preparations. Data are presented as mean ± s.e.m.

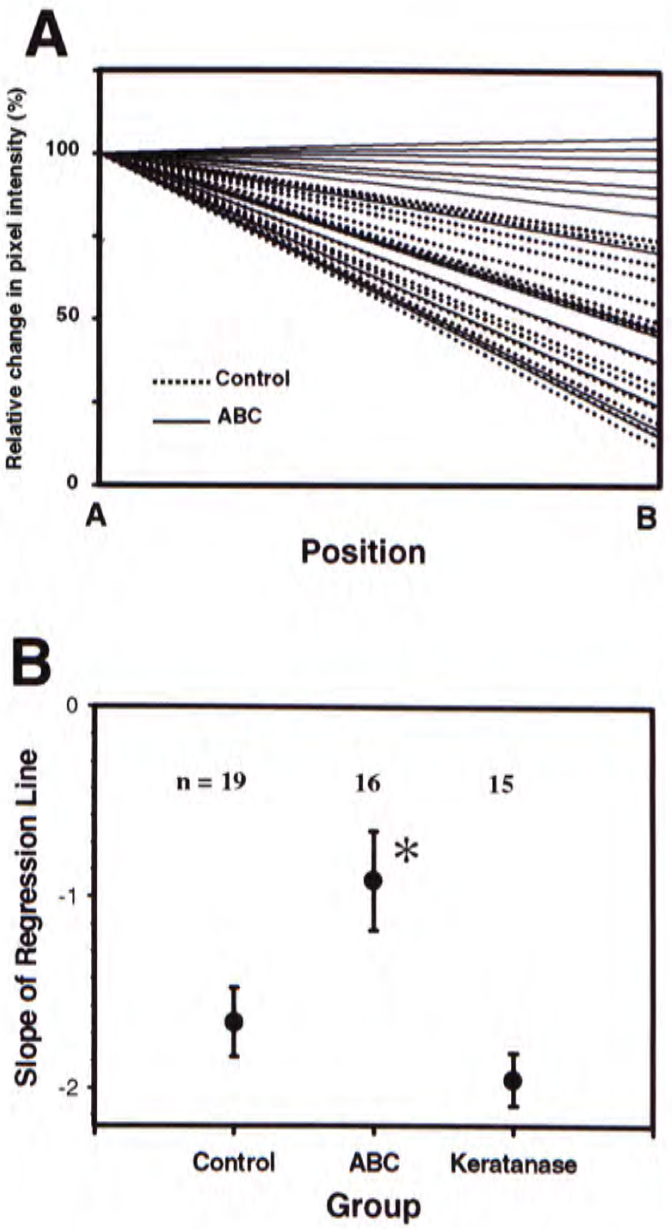
A
Relative change in pixel intensity (%)
100
50
0
Control
ABC
A
B
Position
B
Slope of Regression Line
0
-1
-2
n = 19
16
15
*
Control
ABC
Keratanase
Group

Figure 5

Confocal micrographs showing phalloidin positive growth cones at the midline (indicated by the dotted line) of the chiasm in frontal sections of the ventral diencephalon of E14 slice preparations. **A**: In control preparations, phalloidin stained growth cones dispersed through the depth of the retinal fiber layer. **B**: Enzymatic digestion with chondroitinase (ABC) did not produce obvious change in growth cone position at the midline. The dotted lines mark the position at the midline where intensity of phalloidin staining in the retinal fiber layer was measured. Dorsal is up. Scale bar = 50 μm.

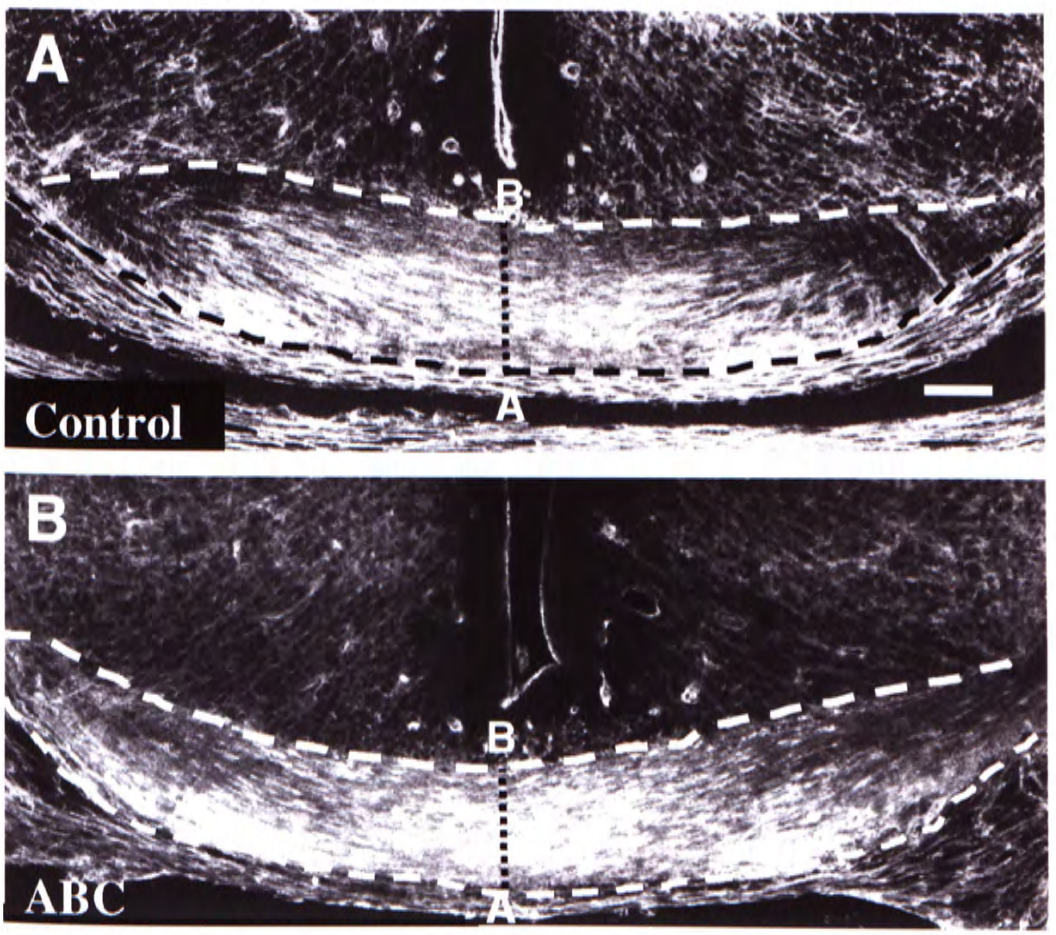
A
B
A
Control
B
B
A
ABC

Figure 6

Plots of intensity changes of phalloidin staining from the superficial (A) to deep (B) regions of the retinal fiber layer at the midline of the chiasm in slice preparations of the optic pathway. **A**: In most control preparations, the staining intensity was reduced gradually from superficial to deep region of the fiber layer. **B**: No obvious change in staining profile after treatment of brain slices with chondroitinase (ABC). The line that runs across each plot indicates the regression line.

(A) Control

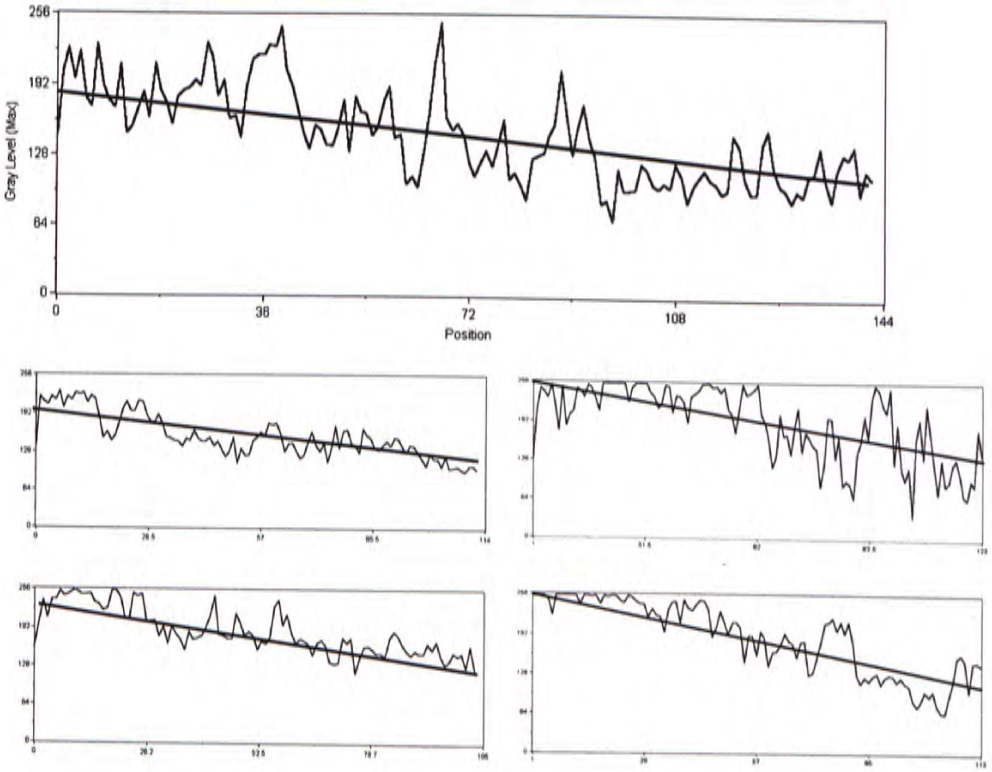

(B) Ch-ABC

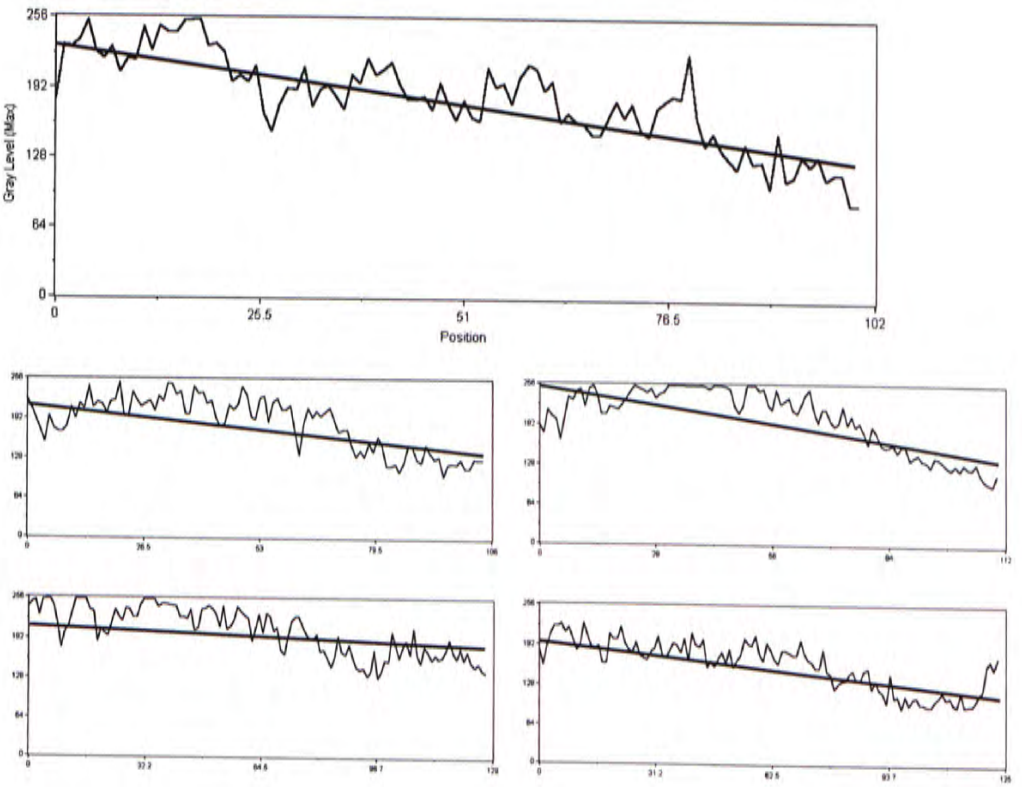

Figure 7

A: Graph showing the mean slope of the regression generated from measurements of intensity profiles across the retinal fiber layer at the midline of the chiasm. No significant difference was observed in growth cone distribution as reflected by the means of regression lines after chondroitinase treatment (ABC) when compared with control preparations. Such difference was not obvious in slices treated with keratanase. The data are presented as mean ± s.e.m. The number of preparations in each experimental group is indicated below the plot. **B**: Plots of measurements of the depth of the retinal fiber layers at the midline and at the threshold of the optic tract in slice preparations of the E14 optic pathway. There was no significant changes in thickness of the fiber layer at both regions after enzymatic digestion with chondroitinase (empty columns) when compared with those in control preparations (filled columns). Data are presented as mean + s.e.m.

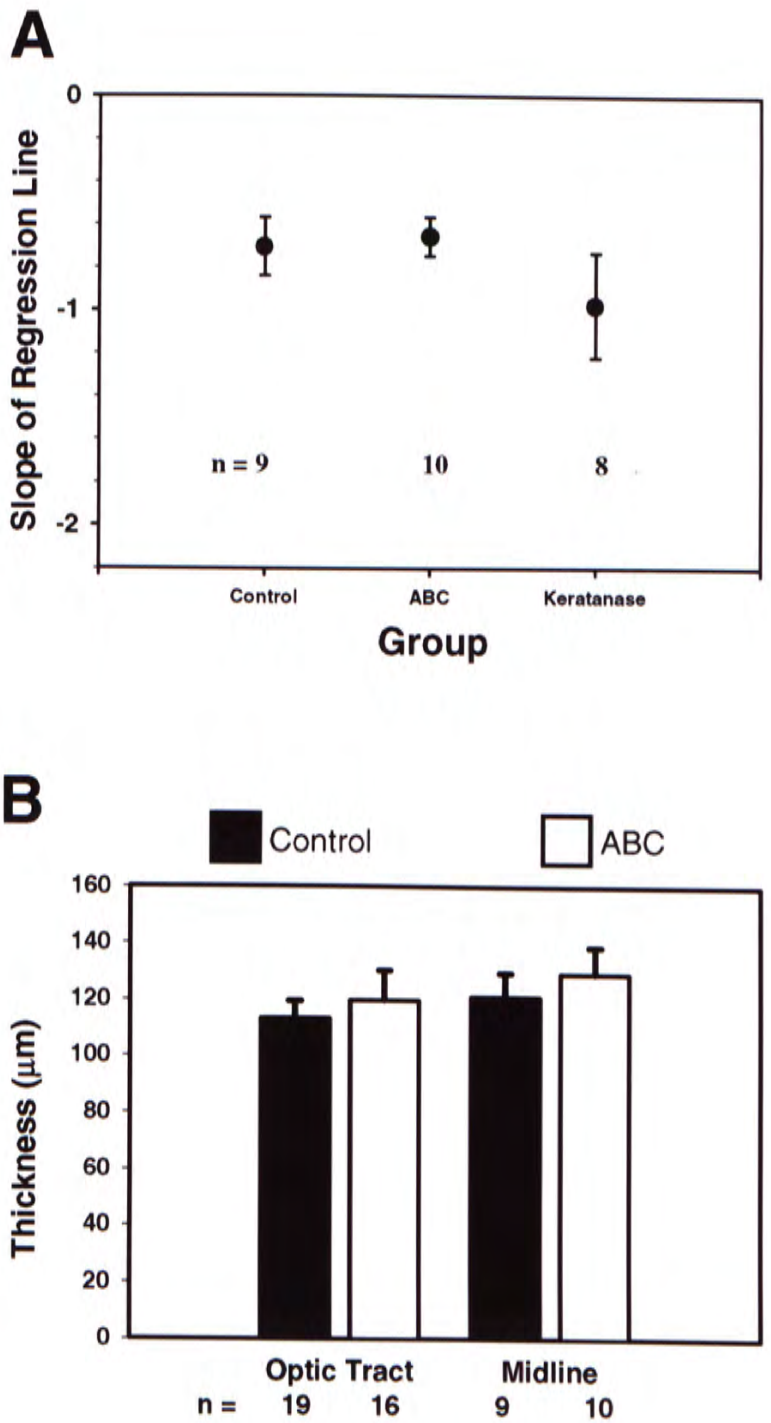
A
0
-1
-2
Slope of Regression Line
n = 9
10
8
Control
ABC
Keratanase
Group
B
Control
ABC
160
140
120
100
80
60
40
20
0
Thickness (μm)
Optic Tract
Midline
n = 19 16 9 10

Figure 8

Chondroitinase treatment did not produce obvious collapses or mobilization of actin from the retinal growth cone. **A-B**: Confocal micrographs showing the rhodamine phalloidin staining for F-actin-rich growth cones from E14 retinal explants on a laminin-polylysine substrate. The phalloidin positive staining is largely confined to the processes and core of the retinal growth cones. The axon shafts were only lightly stained. **C-D**: Chondroitinase treatment at concentration that abolishes the age-related order in the tract did not produce obvious changes in pattern of phalloidin staining within the growth cones. **E-F**: The neurite outgrowth from retinal explants was not obviously reduced after chondroitinase treatment. **G**: Assay of the percentage of neurites with collapsed growth cones in these cultures showed that chondroitinase treatment did not cause any significant increase in collapses of retinal growth cones. Scale bars in **A-D** = 10 μm; scale bar in **E-F** = 40 μm.

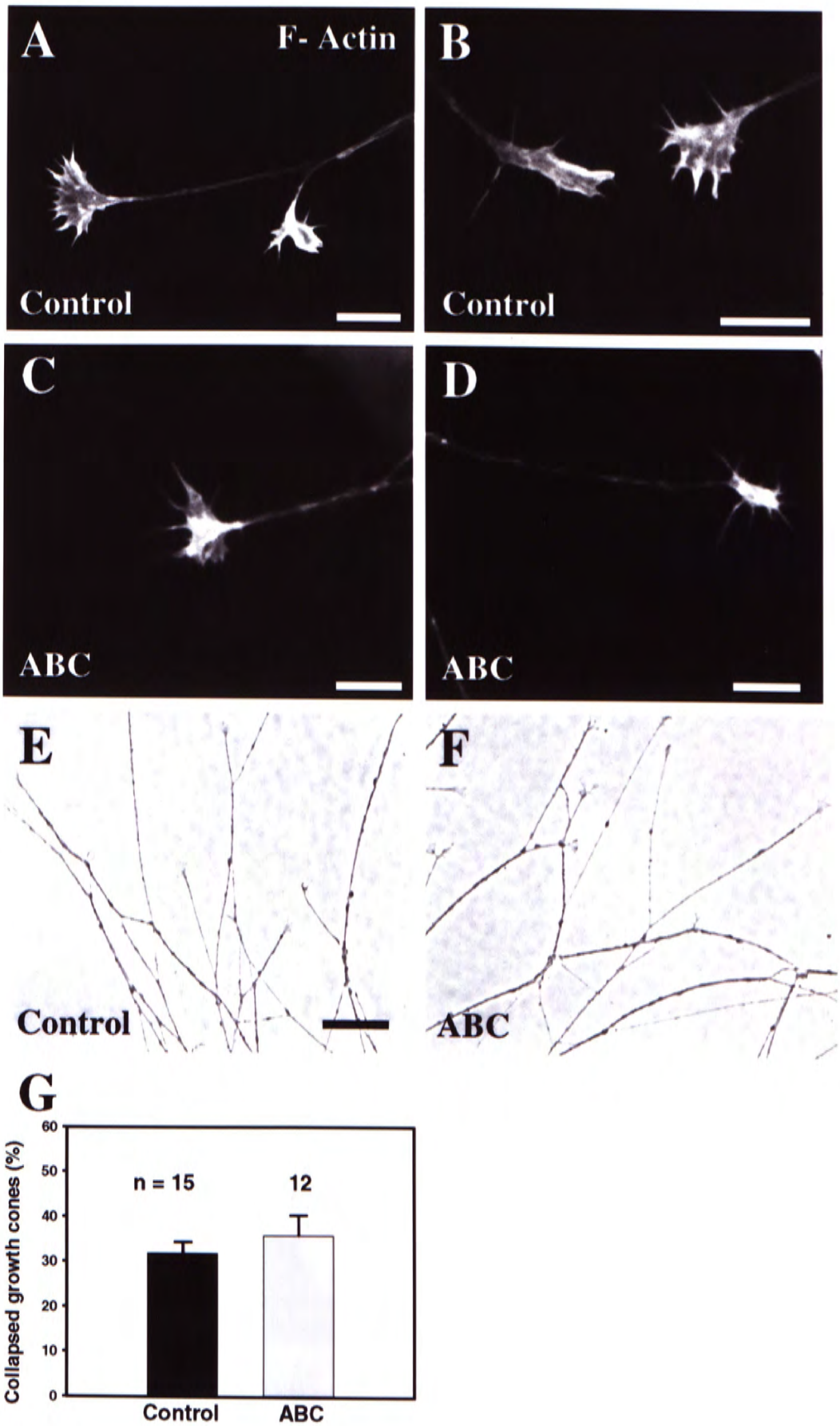
A
F- Actin
Control
B
Control
C
ABC
D
ABC
E
Control
F
ABC
G
Collapsed growth cones (%)
60
50
40
30
20
10
0
n = 15
12
Control
ABC

Figure 9

Removal of chondroitin sulfate produced a shift of dye-filled retinal growth cones from subpial to deep regions of the optic tract. **A-B**: Focal labels of retina either at the ventral temporal or dorsal nasal quadrant filled up growth cones (arrow heads) in the contralateral optic tract of E14 brain slices. Note the growth cones gathered at the subpial regions of the fiber layer in control preparations (**A**), but dispersed throughout the whole depth of the fiber layer after chondroitinase treatment (**B**). The pia is indicated by solid line and the deep margin of the optic tract is indicated by broken line in these confocal micrographs. **C-D**: Drawings to show the growth cones in other control (**C**) and chondroitinase treated (**D**) brain slices. Note the enzyme treatment causes a spread of growth cones from superficial to whole thickness of the fiber layer (bordered by broken lines) and did not produce substantial growth cone collapses in the optic tract. **E**: Counting growth cone number in the tract revealed a significant shift (asterisk) of growth cones from the superficial to deep half of the fiber layer after the removal of CS. **F**: Furthermore, enzymatic treatment produced a significant increase (asterisk) in size of retinal growth cones in the tract when compared with that in control preparations. Dorsal is up and midline is to the right in **A-D**. Scale bar in **A** = 25 μm; also applied to **B**.

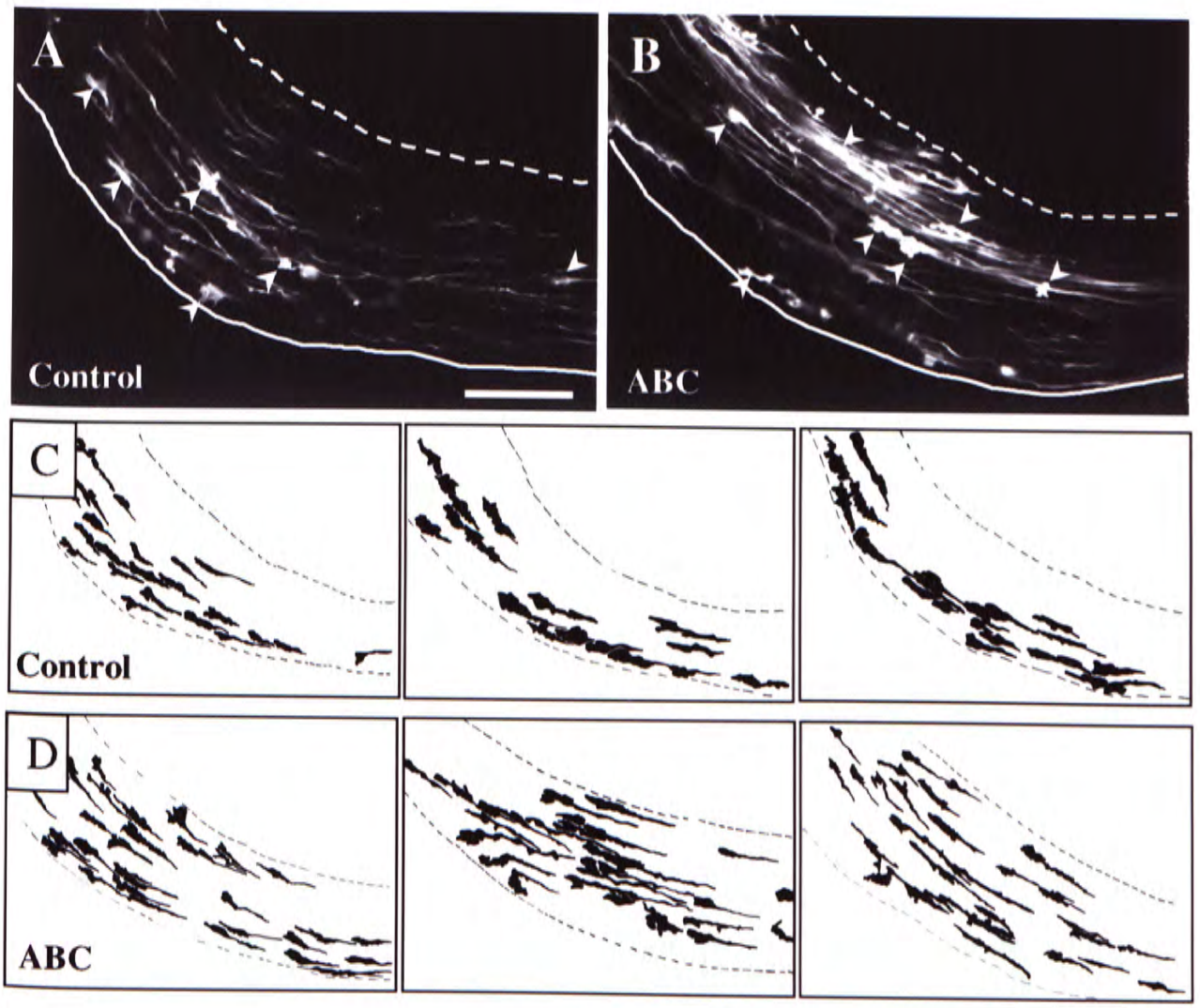
A
Control
B
ABC
C
Control
D
ABC

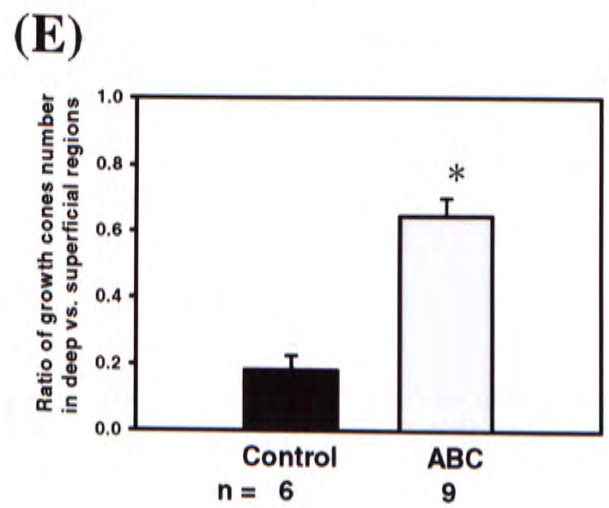
(E)
Ratio of growth cones number in deep vs. superficial regions
1.0
0.8
0.6
0.4
0.2
0.0
*
Control
ABC
n = 6
9

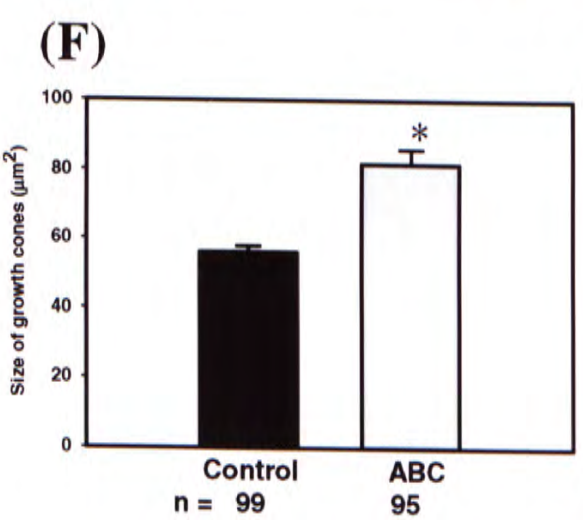
(F)
Size of growth cones (μm²)
100
80
60
40
20
0
*
Control
ABC
n = 99
95

Figure 10

Summary diagram showing the roles of the CS glycosaminoglycans in patterning the axon routing at the mouse chiasm. **A**: When retinal axons enter the chiasm, they first encounter the CS epitope (hatched area) at the midline (arrow). The uncrossed axons (green) respond to the CS and are halted and guided by other cues to the optic tract on the same side. Axons that crossed the midline (blue) do not have the response to the CS and continue to grow towards the contralateral optic tract (OT). **B**: At the threshold of the tract (empty arrow), axons change their response to the CS epitope (hatched area), which is present in abundance at the deep part of the retinal fiber layer, probably through a change in guidance molecules present on the axon surface (represented by a change from blue to red color). **C**: When the CS epitope is removed by a treatment of the pathway with chondroitinase ABC, the uncrossed axons (marked by asterisk in **C**) either halt or continue their journey across the midline without a stop, producing a highly reduced uncrossed pathway; whilst the crossed axons lose their age-related arrangement at the threshold of the optic tract.

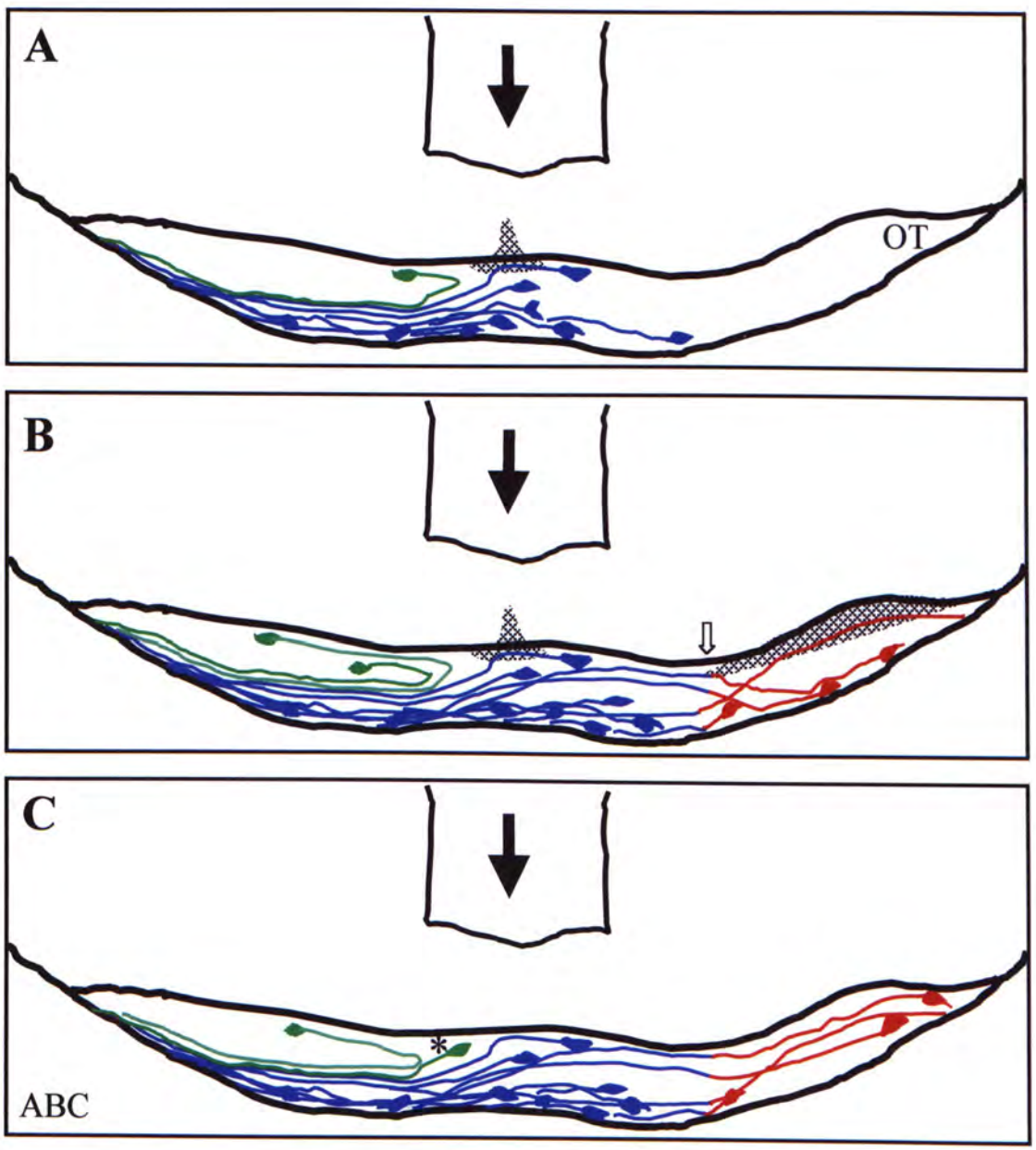
A
OT
B
C
ABC

CHAPTER 3

EXPRESSION OF PHOSPHACAN AND NEUROCAN IN THE DEVELOPING MOUSE RETINOFUGAL PATHWAY

INTRODUCTION

Among a number of proteoglycans, chondroitin sulfate proteoglycan (CSPG) has been shown to be involved in cell adhesion and migration, neurite outgrowth, mediating the effects of growth factors, and other developmental processes in nervous tissues (Margolis and Margolis, 1993; Friedlander et al., 1994; Grumet et al., 1994; Karthikeyan et al., 1994; Milev et al., 1994).

Neurocan, a nervous tissue–specific proteoglycan synthesized by neurons (Engel et al., 1996), is a multi-domain hyaluronic acid-binding chondroitin sulfate proteoglycans (Rauch et al., 1992; Margolis and Margolis, 1994). It has been shown previously that neurocan regulates neurite outgrowth and cell adhesion in neural tissues (Rauch et al., 1991; Friedlander et al., 1994). It has been reported that there are three proteolytic products of neurocan, including 90-kDa and 130-kDa N-terminal fragments and a 150-kDa C-terminal fragment, in postnatal rat brain (Meyer-Puttlitz et al., 1995; Inatani et al., 1999). Phosphacan, produced by astrocytes in the central nervous system, is a secreted form of receptor-type protein tyrosine phosphatase (RPTP zeta/beta), which consists of the extracellular domain (Maurel et al., 1994, 1995). These two molecules are major components of CSPG in the nervous tissues of the rodent brain (Rauch et al., 1991).

It was shown that localization of neurocan and phosphacan overlapped with that of neural cell adhesion molecules (L1 and NCAM), and the extracellular matrix (ECM) protein tenascin (Fridelander et al., 1994; Grumet et al., 1994; Milev et al., 1994). Neurocan and phosphacan were found to bind to L1 and NCAM and to tenascin. The binding was completely inhibited by antibodies against L1 and NCAM, indicating that these CAMs are major receptors for neurocan and phosphacan on neurons (Milev et al., 1994). Interactions of neurocan and phosphacan with neural cell adhesion and the extracellular matrix molecules have been demonstrated to modulate neuronal and glial adhesion neurite growth, and signal transduction across the plasma membrane during the development of the central nervous system (Grumet et al. 1993; Friedlander et al. 1994; Milev et al. 1994). Both supportive and inhibitory roles of CSPGs in patterning the axonal course have been reported. Rat superior colliculus-derived CSPG was reported to promote survival of retinal ganglion cells (Schultz et al., 1990). The molecules are regarded as one of the most important neurotrophic factors for retinal neuronal cells. It is likely that CSPG is a neurotrophic factor for retinal ganglion cells. In contrast to the findings of Schultz et al. (1990), many studies have suggested an inhibitory role of CSPGs to act as barriers for growing axons (e.g., posterior sclerotome: Oakley and Tosney, 1991; Perris et al., 1991; Landolt et al., 1995; retina: Snow et al., 1991; Brittis et al., 1992; optic tectum: Hoffman-Kim et al., 1998). In the rat, the centrifugal, receding CSPG expression has been related to inhibiting retinal axon growth in the retina (Brittis et al., 1992). Furthermore, the existence of phosphacan was demonstrated in rat retina (Inatani et al., 2000). Immunocytochemical results in rats showed that the expressions of neurocan and phosphacan follow different developmental time courses in the embryonic central

nervous system, indicating that these two proteoglycans may serve complementary or partially overlapping roles in axon guidance, cell interactions, and neurite outgrowth at specific sites and stages of central nervous system development (Meyer-Puttlitz et al., 1996). Thus it is possible that these brain CSPGs may be involved in the developing retinofugal pathway of mouse.

In this study, we asked if phosphacan, N-terminal and C-terminal neurocans were expressed in the retinofugal pathway of mouse embryos during the critical developmental stages when axons are actively growing and reorganizing in the optic chiasm.

MATERIALS AND METHODS

Animal and tissue preparations

Time-mated C57 pigmented mice were obtained from the University Animal House. The day that the vaginal plug was found was designated as embryonic day 0 (E0). Pregnant mice were killed by cervical dislocation. Embryos at E13-15 were removed by Cesarean section. The embryos were killed by decapitation. The heads were fixed in 4% paraformaldehyde in 0.1M phosphate buffer (pH 7.4) overnight at 4°C. The tissues were embedded in a gelatin-albumin mixture and sectioned either frontally or horizontally at a thickness of 100μm using a vibratome. Serial sections of the retinofugal pathway from the eyes to the proximal parts of the optic tract were collected in 0.1M phosphate buffered saline (PBS, pH 7.4).

Immunohistochemistry

The expression patterns of phosphacan, C- and N-terminal neurocan were detected using polyclonal antisera to phosphacan and to the N- and C- terminal portions of neurocan (kindly provided by Prof. R.U. Margolis). The sections were washed three times with PBS, incubated in 10% normal goat serum (NGS) in PBS for 1 hour at room temperature. The sections were then incubated in the primary antibodies (diluted 1:1000 in PBS with 1% NGS and 0.5% Triton X-100) overnight at 4°C. After washing with PBS, the sections were incubated in fluorescein isothiocyanate (FITC)-conjugated secondary antibody (anti-rabbit IgG, diluted 1:100 in PBS, from Jackson ImmunoResearch, West Grove, PA) for 3 hours at room temperature. The control sections were processed with the same procedures but without the addition of primary antibodies. No positive staining was detected in all control preparations. The sections were washed in PBS and coverslipped with 50% glycerol in PBS for confocal microscopy.

Confocal microscopy

The immunofluorescent staining of the sections was examined with a confocal imaging system (MRC600, Bio-Rad, England) connected to a Zeiss Axiophot photomicroscope (Oberkochen, Germany) using a blue excitation filter set (BHS, 488 nm excitation and 515 nm emission long pass). The digital images were processed by the Confocal Assistant software (Bio-Rad, UK).

RESULTS

Expression pattern of phosphacan, N- and C- terminal neurocans in the retina

At E13, expression of phosphacan was localized in the lens and in radial neuroepithelial cells in most retinal regions. Intense staining of phosphacan was found in the peripheral regions of the retina while the staining at the central retina around the optic disk was reduced substantially (Fig. 1A). At this stage, prominent expression of phosphacan was detected in the retinal fiber layer and at the optic disk. However, the neurocan expression was weak. N- (Fig. 1B) and C- (Fig. 1C) terminal neurocans immunoreactivity was only detected in lens, peripheral retina and only a weak staining was found in the retinal fiber layer and the optic disk.

At E14, expression of phosphacan was found in the inner layer of the retina, the peripheral retina, the lens and the optic nerve head (Fig.1D). However, the uneven distribution of phosphacan between the peripheral and central retina became less apparent when compared to that at E13. At this stage, immunoreactivity for N-terminal neurocan was distinct, showing an intense staining in the peripheral retina and the lens, and a centrifugal, receding gradient of N-terminal neurocan expression in other region of the retina (Fig. 1E). In the contrary, C-terminal neurocan still only expressed mainly in the inner retinal layer at a comparatively low level (Fig. 1F). While the optic disk was virtually devoid of staining of both neurocans, the immunoreactivity for both phosphacan and neurocans were found in the ganglion cell layer at this stage.

Similar staining pattern for phosphacan was observed in retinas at E15, with phosphacan expressed in the lens, peripheral retina and optic disk. A laminated pattern of staining was seen in the inner layer of the retina (Fig. 1G). Higher magnification showed that immunostained phosphacan was localized at the innermost retinal fiber layer and a cellular layer in the inner region of the retina, which sandwiched an adjacent cellular layer with weak immunostaining (Fig. 1J). At this developmental stage, the expression of N-terminal neurocan in retinas was found, again, in the lens and peripheral retina. Increased immunoreactivity for this epitope was detected in the inner retinal layer, optic disk and optic stalk (Fig. 1H). More detailed N-terminal neurocan expression was revealed under a higher magnification of the retinal layer, where prominent staining was observed in the presumptive ganglion cell layer but not in the deepest layer where retinal fiber layer located (Fig. 1K). The weak staining of phosphacan observed in the inner region of the retina seemed to overlap with the strong immunostaining of N-terminal neurocan (compared 1J with 1K). For C-terminal neurocan, expression pattern was similar to that of E14, where weak immunoreactivity for the epitope was found in the periphery and the inner layer of the retina, as well as the lens (Fig. 1I).

Expression pattern of phosphacan, N- and C- terminal neurocans in the ventral diencephalon

At E13, when the retinal axons start to grow into the chiasm and optic tract (Godement et al., 1987; Chung et al., 2000b), compartmentalization of the two brain CSPG expression was observed in the anterior regions of the diencephalon (Fig. 2A, 2D and 2G). In horizontal section of the ventral diencephalon cutting through the

level of optic stalks, the expression of phosphacan (n = 4) was found adjacent to the end of optic stalk, expressing on the lateral sides of the anterior part of the chiasm and was particularly intense in the paraventricular region (Fig. 2A and 2B). Complementary to this observation, an intense staining of N-terminal neurocan (n = 3) was found in the whole optic stalk, terminated right at the entry zone to the chiasm (Fig. 2D and 2E) This expression of the phosphacan and N-terminal neurocan could also be observed in coronal sections of the preparations (phosphacan: n = 4; N-terminal neurocan: n = 4). The optic stalk was very faintly labeled with immunoreactive phosphacan (Fig. 2J), yet prominent staining of N-terminal neurocan was found throughout the optic stalk (Fig. 2K). At the terminal of the optic stalk, phosphacan started to express intensely in the paraventricular region in the diencephalon (Fig. 2J). However, this region was completely devoid of N-terminal neurocan expression (Fig. 2K). While the immunoreactivities for phosphacan and N-terminal neurocan were found as two domains on both sides of the posterior diencephalon in horizontal sections (Fig. 2A and 2D), the expressions of these two brain CSPGs were shown as an inverted V-shaped structure in the posterior diencephalon in sections 100μm ventral to Figure 2A (Fig. 2C, 2I and 2F). At the rostral tip of this structure, an extension stemmed out into the midline of the chiasm. It was noted that immunoreactivity for N-terminal neurocan was clearly detected in the fiber layer of the ventral diencephalon (Fig. 2F), where the other two CSPG antibodies did not show. In contrast to the regulated expression pattern of phosphacan and N-terminal neurocan, extremely weak immunoreactivity for C-terminal neurocan (horizontal: n = 4; coronal; n = 3) was detected only in the posterior diencephalon (Fig. 2G and 2H).

At E14, more retinal axons enter the chiasm and the optic tract (Chan et al., 1998). At this stage, horizontal preparation of the diencephalon revealed a regulated expression of phosphacan. In the anterior part of the diencephalon cutting through the optic stalk and optic tract, the expression of phosphacan (n = 4) was found in these two regions (Fig. 3A-3C) and a down-regulation was observed at the midline of the chiasm. A prominent immunoreactivity was detected at the lateral regions of the mid-chiasm (Fig. 3B), which merged with the expression shown in the optic tract in a section 100 μ m ventral to Figure 3B (Fig. 3C) to form a band at the posterior boundary of the optic chiasm (Fig. 3D). It was noted that there were two circular regions posterior to the band of staining in the chiasm, which was devoid of phosphacan expression (Fig. 3C and 3D). The inverted V-shaped expression of phosphacan in the posterior diencephalon was also found at this stage, with a rostral extension pointed into the midline of the chiasm (Fig. 3C). For N-terminal neurocan (horizontal: n = 2; coronal; n = 4), the immunostaining was largely localized at the posterior region of the diencephalon in an inverted V-shape. Only a basal level of immunoreactive N-terminal neurocan was detected in the optic stalk (Fig. 3E). At this stage, virtually no signal of C-terminal neurocan immunoreactivity (horizontal: n = 2; coronal; n = 2) was detected in the ventral diencephalon (Fig. 3F).

In E14 embryos, coronal preparations (n = 6) from the rostral regions of the chiasm showed a prominent expression of phosphacan in the paraventricular region on the lateral sides of the diencephalon (Fig. 4A). A basal level of immunostaining against phosphacan was detected in the optic stalks. Frontal sections of the mid-

chiasm showed a very intense staining of immunoreactive phosphacan in the deep regions of the retinal fiber layer at the lateral sides of the chiasm (Fig. 4B). A slight elevation in the signal of immunoreactive phosphacan was found at the midline. In a more caudal section cutting through the optic tracts, dense labeling of anti-phosphacan was detected in the deep regions of the optic tracts (Fig. 4C). A band of prominent immunostaining of phosphacan was found in the deep region of the posterior chiasm, which may overlap with its band expression found in the posterior boundary of the chiasm in the horizontal sections (compared Fig. 4C with 3D). It could be seen from these coronal preparations (Fig. 4A-4C) that the retinal axons and the radial glial cells were both stained by the immunoreactive phosphacan.

At E15, the characteristic expression pattern of phosphacan, which was found in the anterior part of the chiasm in horizontal sections at E14, was also observed. Immunoreactivity for phosphacan (n = 3) was detected in the optic stalks and tracts in this region and a down-regulation of signal was observed in the paramidline regions of the chiasm (Fig. 5A and 5B). The dense labeling of phosphacan immunoreactivity on the lateral regions of the mid-chiasm was detected (Fig. 5B). In more ventral section, the prominent band of the expression of phosphacan still existed in the posterior boundary of the optic chiasm (Fig. 5C). The reduction in phosphacan expression at regions posterior to the boundary of the chiasm was also observed (Fig. 5A and 5C). At this stage, dense labeling of N-terminal neurocan (n = 3) was found at the junction of optic stalk and chiasm (Fig. 5D). A regulated band-shaped expression of N-terminal neurocan was detected at the posterior boundary of the optic chiasm, which was similar to the pattern of phosphacan staining (Fig. 5E). For C-terminal

neurocan (n = 3), the expression of the epitope was detected in the fiber layer of the chiasm, with an up-regulation of the expression shown at the midline of the chiasm (Fig. 5F).

In coronal sections of E15 embryos, immunoreactive phosphacan staining (n = 6) was found in the paraventricular regions on the lateral sides of the diencephalon (Fig. 6A). This staining was extended into more caudal sections (Fig. 6B). Immunoreactivity for phosphacan was also detected in the retinal fiber layer on the lateral sides of the caudal chiasm (Fig. 6C). For frontal sections stained against N-terminal neurocan (n = 3), prominent signal was detected at the junction of the optic stalk and chiasm (Fig. 6D). Intense staining of N-terminal neurocan was found in the fiber layer of the optic chiasm (Fig. 6E), which may overlap with the band-shaped expression detected in the horizontal section at the posterior boundary of the optic chiasm (compared Fig. 6E with 5E). On the lateral sides of the retianl fiber layer in the tract, immunostained N-terminal neurocan was found (Fig. 6F). In coronal preparation reacted with antibody against C-terminal neurocan (n = 5), only a basal level of immunoreactivity was detected in the section cutting across the optic stalk (Fig. 6G) and chiasm (Fig. 6H). It was noteworthy that an intense immunostaining of the C-terminal neurocan was found in the superficial region of the optic tract (Fig. 6I), where retinal growth cones were located (see chapter 4; Guillery and Walsh, 1987; Colello and Guillery, 1992).

DISCUSSION

In the present study, we have investigated the expression pattern of nervous

tissue–specific chondroitin sulfate proteoglycans (CSPGs), neurocan and phosphacan, in the retinofugal pathway of mouse embryos. We have shown that phosphacan and neurocan are expressed in a spatiotemporally regulated pattern in the retinofugal pathway.

Role of phosphacan, N- and C-terminal neurocan in the retina

In mouse embryos, retinal ganglion cells begin to send axons into the optic stalk at E12. By E13, the axons start to grow into the ventral diencephalon (Silver, 1984). Phosphacan expression was detected in the retinal fiber layer and optic disk in the retina at E13. However, neurocans were expressed at a low level in the retina. In the later developmental stage at E15, a well-organized expression pattern of both CSPGs was found. We have shown that a laminated expression pattern of phosphacan was found in the inner retinal layer. The middle layer, which was weak in phosphacan expression, showed a positive staining of N-terminal neurocan at the same stage. Beyond this presumptive ganglion cell layer, a phosphacan immunopositive layer was defined. However, the identity of this structure remains to be clarified. CSPGs have been suggested to have inhibitory functions for growing axons (Snow et al., 1990, 1991; Oakley and Tosney, 1991; Perris et al., 1991; Brittis et al., 1992; Pindzola et al., 1993; Landolt et al., 1995; Hoffman-Kim et al., 1998; Inatani et al., 2001). However, instead of the commonly suggested inhibitory function to axon growth, the neurocan and phosphacan may cooperate to set up the laminated pattern in the mouse retina. We suggest that the CS glycosaminoglycan plays the inhibitory function on axon growth (Snow et al., 1990, 1991; Fichard et al., 1991; Chung et al., 2000b), but the protein core may be responsible for setting up the laminated pattern in the retina.

Role of phosphacan, N- and C-terminal neurocan in the chiasm

Phosphacan and N-terminal neurocan were found to coincide with the distribution of SSEA-1 neurons as an inverted V-shaped pattern (see next chapter). This suggests that these neurons are one of the major sites of production of phosphacan and neurocan in the ventral diencephalon. At E13, when most retinal axons are traveling in the optic stalk (Silver and Sidman, 1980) and the first retinal axons start to enter the chiasm (Godement et al., 1987), a rostral raphe of phosphacan and N-terminal neurocan expression was seen to extend into the midline of the chiasm from the inverted V-shaped expression. Moreover, it has also been shown that retinal axon growth slows down when axons enter the chiasm (Godement et al., 1994; Chan et al., 1998). At the midline region, the frequency of pauses in axon growth is particularly high (Godement et al., 1994). This may be related to the presence of this thin raphe of phosphacan and N-terminal neurocan expression at the chiasmatic midline, suggesting an inhibitory role of the molecules that stops the growth of uncrossed axons before they hit the midline and allows the crossed axons to pass through (Guillery et al., 1995; Chan et al., 1998). Similar staining pattern of CS using CS-56 antibody has been reported (Chung et al., 2000a).

At E14, the characteristic expression of phosphacan shown in the lateral regions of the mid-chiasm in the present study suggested another inhibitory role of the molecule. The intense staining of phosphacan at these regions may be responsible for channeling the axons towards the midline and preventing most axons from entering the optic tract before crossing the midline, except the early uncrossed axons. Also, the

expression of these molecules may function to prevent the crossed axons from entering the optic stalk after crossing the midline. The posterior band expression of phosphacan was seen at the caudal region of the chiasmatic fiber layer, which is correlated to prevent the retinal axons from invading the posterior diencephalon. Asher et al. (2000) have shown that neurocan inhibits neurite outgrowth of cerebellar axons in the central nervous system. Phosphacan is also shown to inhibit neurite outgrowth of dorsal root ganglion cells (Garwood et al., 1999). The repulsive effects of 6B4 proteoglycan/phosphacan have been demonstrated previously on cortical and thalamic neurons by growing dissociated neurons on substratum absorbed with phosphacan, which did not support neuronal cell adhesion (Maeda and Noda, 1996). CSPGs prepared from rat brain inhibit the NGF-induced neurite outgrowth from PC12D pheochromocytoma cells irreversibly in a dose-dependent manner (Oohira et al., 1991). Another study has reported that neurocan and phosphacan inhibited neurite outgrowth from retinal ganglion cells of postnatal rat (Inatani et al., 2001) *in vitro*.

Some studies suggested that removal of CS glycosaminoglycans (GAGs) has little effect on the inhibitory property (Milev et al., 1994) or does not relieve the inhibitory effects of mouse phosphacan (Garwood et al., 1999), indicating that the effects are associated with the core glycoprotein. However, we have previously demonstrated that enzymatic removal of the CS GAGs in brain slice preparations of the retinofugal pathway results in a diffuse axon course at the chiasm and a diminution of the uncrossed axon component (Chung et al., 2000b), as well as abolishes the accumulation of phalloidin positive growth cones at the subpial region of the optic tract (see previous chapter). All of which may be due to the removal of

the potential inhibitory property of CSPG by digesting CS. However, it is noted that an interesting complementary expression of phosphacan and N-terminal neurocan was found in the optic stalk at E13. N-terminal neurocan was expressed intensely in the whole optic stalk and the fiber layer in the chiasm when the retinal axons are traveling within these regions (Silver, 1984). These observations suggest that it is difficult to classify neurocan (and/or phosphacan) clearly as supportive or inhibitory to axon growth. Instead, the spatial and temporal expression of the molecules may define their properties on axon growth.

At the threshold of the optic tract, immunoreactivity of the anti-phosphacan was most prominent in the deeper parts of the chiasm and tract at E14. C-terminal neurocan, however, expressed intensely on the subpial regions of the optic tract at E15. This specific expression of C-terminal neurocan in the retinal fiber layer was only seen in the optic tract but not in the optic stalk and the chiasm. These restricted distributions of phosphacan and neurocan were observed at the time when most axons are navigating across the midline of the chiasm toward the optic tract. Many studies have reported that there is a deep to superficial order according to time of arrival in the pathway. The youngest axons grow closest to the subpial surface of the tract and the oldest axons lie in the deep region (Guillery and Walsh, 1987; Colello and Guillery, 1992; Colello and Coleman, 1997; Colello and Guillery, 1998). This age-related order in the optic tract may be related to the different CSPGs expressed in the retinal fiber layer, each of which has its own characteristic patterns. While intense restricted expression of phosphacan in the deep parts of the optic tract may repel the arriving growth cones away from the pial surface, C-terminal neurocan in the subpial

surface of the tract may exert stimulatory effect by providing a relatively favorable environment to direct advances of growth cones. Similar finding of the CSPG distribution being densest in the deeper parts of the optic tract of developing ferrets has been reported (Reese et al., 1997). Enzymatic removal of chondroitin sulfate glycosaminoglycans in mouse brain slice preparations of the retinofugal pathway was shown to abolish the age-related axon order in the optic tract (see Chapter 2). These studies, together, suggest a role of CSPG in establishing the age-related fiber order in the tract.

CSPGs are generally regarded as barriers for neurite outgrowth (Snow et al., 1990; Oohira et al., 1991; Dou and Levine, 1994; Milev et al., 1994; Reese et al., 1997; Hoffman-Kim et al., 1998). *In vitro* studies show that CSPGs inhibit neurite outgrowth and elongation (Snow et al., 1990, 1991; Fichard et al., 1991; Oohira et al., 1991; Brittis et al., 1992; Snow and Letourneau, 1992; Dou and Levine, 1994; Katoh-Semba et al., 1995; Canning et al., 1996; Maeda and Noda, 1996). Some studies report that the inhibitory effects of CSPGs are alleviated when CS chains are removed (Snow et al., 1990, 1991; Fichard et al., 1991; Chung et al., 2000b), whereas others show that the effects are associated with the protein cores (Iijima et al., 1991; Oohira et al., 1991; Grumet et al., 1993; Katoh-Semba and Oohira, 1993; Dou and Levine, 1994; Maeda and Noda, 1996). However, CSPGs are also found to be expressed in regions of the developing nervous system where axon pathways form (Flaccus et al., 1991; Sheppard et al., 1991; Bicknese et al., 1994; Ring et al., 1995). Some *in vitro* studies indicate that brain CSPGs, as well as CS GAG chains can enhance neurite

outgrowth (Iijima et al., 1991; Lafont et al., 1992; Faissner et al., 1994; Fernaud-Espinosa et al., 1994; Maeda and Noda, 1996).

In conclusion, we have demonstrated that the expressions of neurocan and phosphacan are regulated spatiotemporally in different ways, suggesting overlapping or complementary roles in axon guidance in the developing retinofugal pathways. Since both neurocan and phosphacan were present in regions where neurites avoid and grow actively, it suggests that neurocan and phosphacan may play a regulatory role of axon growth through interactions with other cellular and molecular factors like neurons, glia, NCAM and other ECM molecules.

Figure 1

Confocal photomicrographs showing immunoreactivity for phosphacan, N- and C-terminal neurocans in horizontal sections of the retinas in C57 mouse embryos. Anterior is up. **A**: At embryonic day 13 (E13), phosphacan is expressed in most retinal regions (R) and lens (L), but preferentially in the inner layer of the retina. Substantial staining of phosphacan is found in the peripheral regions of the retina and the expression of phosphacan is very prominent in the optic nerve head (ON). **B-C**: At this stage, only weak immunoreactivities for N- (**B**) and C-terminal neurocans (**C**) are detected. **D-F**: At E14, expression of phosphacan (**D**), N- (**E**) and C-terminal neurocans (**F**) is found in the inner layer of the retina, the peripheral retina and the lens. **G-K**: At E15, a laminated pattern of phosphacan staining is seen in the inner layer of the retina (**G,** higher magnification in **J**), where the innermost retinal fiber layer and a cellular layer in the inner region of the retina sandwich a weakly stained cellular layer. This weak staining of phosphacan seemed to overlap with the strong immunostaining of N-terminal neurocan observed in the inner region of the retina (**H,** higher magnification in **K**). Expression pattern of C-terminal neurocan at this stage is weak (**I**). Scale bars in A, D, G = 100 μm, applied to A-I; scale bars in J, K = 25 μm.

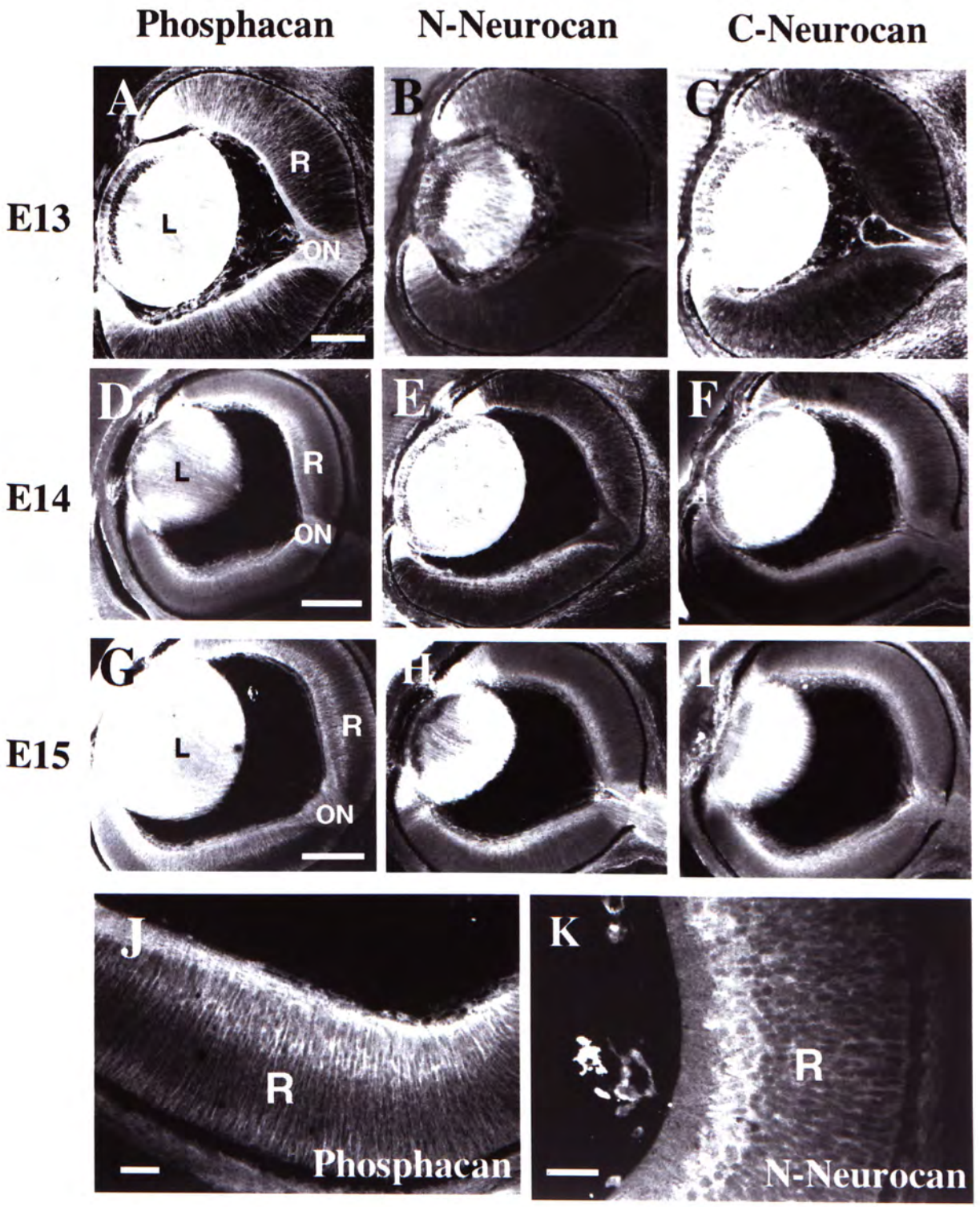
Phosphacan
N-Neurocan
C-Neurocan
E13
E14
E15
A
B
C
D
E
F
G
H
I
J
K
R
L
ON
R
L
ON
R
L
ON
R
Phosphacan
R
N-Neurocan

Figure 2

Confocal photomicrographs showing immunoreactivity for phosphacan, N- and C-terminal neurocans in the ventral diencephalon of E13 mouse embryos. In horizontal sections of the ventral diencephalon (A-I), anterior is up; whereas in the frontal section (J, K), dorsal is up. The arrows point to the midline of the brain. **A-B**: The expression of phosphacan is found adjacent to the end of the optic stalk (indicated by arrow head in **B**) on the lateral sides of the anterior part of the chiasm. It is particularly intense in the paraventricular region. **D-E**: An intense staining of N-terminal neurocan is found in the whole optic stalk, terminates right at the entry zone to the chiasm (indicated by arrow head in **E**), which is complementary to the staining of phosphacan in this region. **J-K**: The complementary expression pattern (indicated by empty arrow in **K**) of the phosphacan and N-terminal neurocan can also be observed in coronal sections of the preparations (positions indicated by the dash lines in **A** and **D**). **C, F**: The expressions of phosphacan (**C**) and N-terminal neurocan (**F**) were shown as an inverted V-shaped structure (outlined by broken lines) in the posterior diencephalon in sections 100 μm ventral to **A**. In the fiber layer of the chiasm, immunoreactivity for N-terminal neurocan was detected (asterisk in **F**). **I**: A higher magnification of the boxed area in **C** shows the phosphacan staining in a V-shaped configuration (outlined by broken lines). At the rostral tip of this structure, an extension of phosphacan staining stems out into the midline of the chiasm (indicated by arrow head). **G-H**: In contrast to the regulated expression patterns of phosphacan and N-terminal neurocan, extremely weak immunoreactivity for C-terminal neurocan is detected only in the posterior diencephalon. Scale bars = 100 μm (D also applied to A, G, H; B applied to E, I-K; C applied to F).

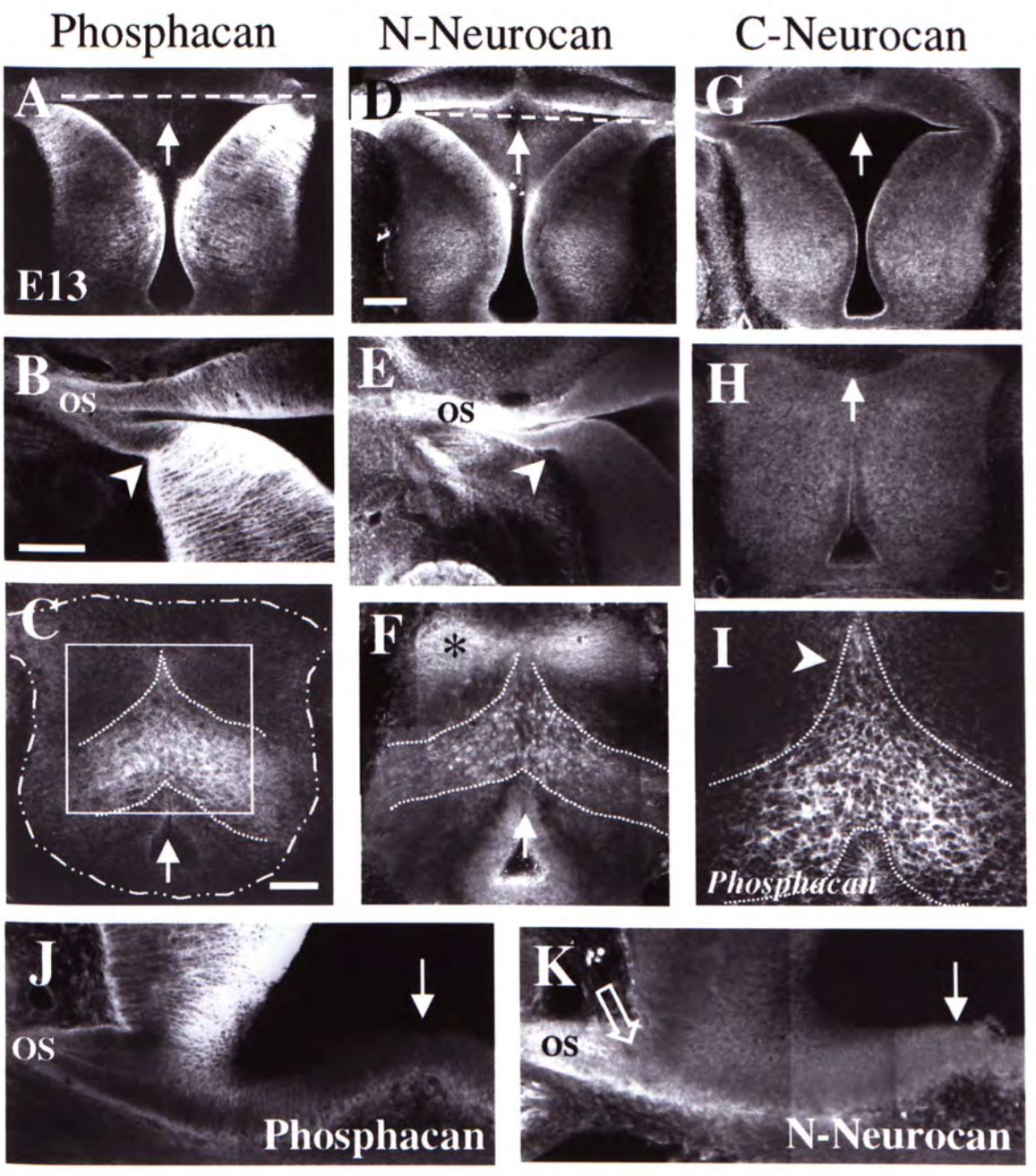
Phosphacan
N-Neurocan
C-Neurocan
A
E13
D
G
B
OS
E
OS
H
C
F
*
I
Phosphacan
J
OS
Phosphacan
K
OS
N-Neurocan

Figure 3

Confocal photomicrographs showing immunoreactivity to phosphacan, N- and C-terminal neurocans in the ventral diencephalon of E14 mouse embryos in horizontal sections. Anterior is up. The arrows point to the midline of the brain. **A-B**: At E14, immunoreactive staining of phosphacan is detected in the optic stalk (OS) and optic tract (OT) and a down-regulation is observed at the midline of the chiasm. A prominent immunoreactivity for phosphacan is detected at the lateral regions of the mid-chiasm (**B**; boxed area in **A**), which merges with the expression shown in the optic tract (**C**; a section 100 μm ventral to **A**), to form a band at the posterior boundary of the optic chiasm (**D**). **C**: The inverted V-shaped expression of phosphacan in the posterior diencephalon (bordered by dash-lines) is found, with a rostral extension pointed into the midline of the chiasm. **D**: Two circular regions devoid of phosphacan expression (indicated by arrow heads in **C**, **D**) are found posterior to the band of phosphacan staining in the chiasm. **E**: The immunostaining for N-terminal neurocan is largely localized at the posterior region of the diencephalon in an inverted V-shaped. **F**: Virtually no signal of C-terminal neurocan immunoreactivity is detected in the ventral diencephalon. Scale bar in A = 200 μm, applied to C and F; scale bar in B = 100 μm; scale bar in D = 200 μm, applied to E.

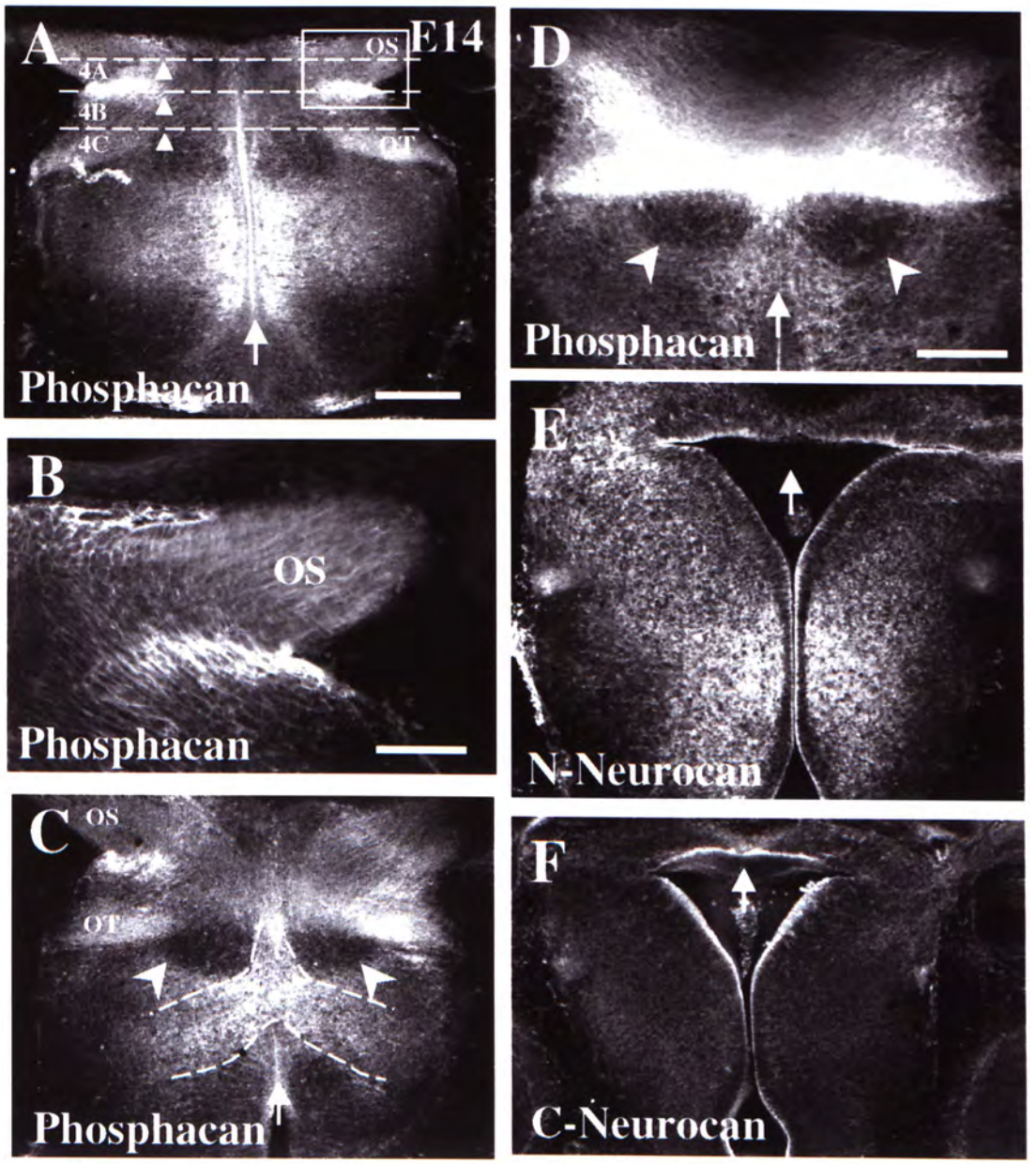
A
E14
OS
4A
4B
4C
OT
Phosphacan
B
OS
Phosphacan
C
OS
OT
Phosphacan
D
Phosphacan
E
N-Neurocan
F
C-Neurocan

Figure 4

Confocal photomicrographs showing phosphacan immunoreactivity in the coronal sections of the ventral diencephalon of mouse embryos at E14, corresponding to the regions indicated by the dash lines in Figure 3A. Dorsal is up. The arrows point to the midline of the brain. **A**: A prominent expression of phosphacan is found in the paraventricular region on the lateral sides of the diencephalon. In the optic stalks (OS), a basal level of immunostaining against phosphacan is detected. **B**: In a section cutting across the mid-chiasm, an intense staining of phosphacan is detected in the deep regions of the retinal fiber layer at the lateral sides of the chiasm (indicated by arrowheads). A slight elevation in the signal of immunoreactive phosphacan is found at the midline. **C**: In a section cutting across the optic tracts (OT), dense labeling of anti-phosphacan is detected in the deep regions of the optic tracts (indicated by arrowheads). A band of prominent immunostaining of phosphacan is found in the deep region of the posterior chiasm. Scale bar = 100 μm, applied to A-B.

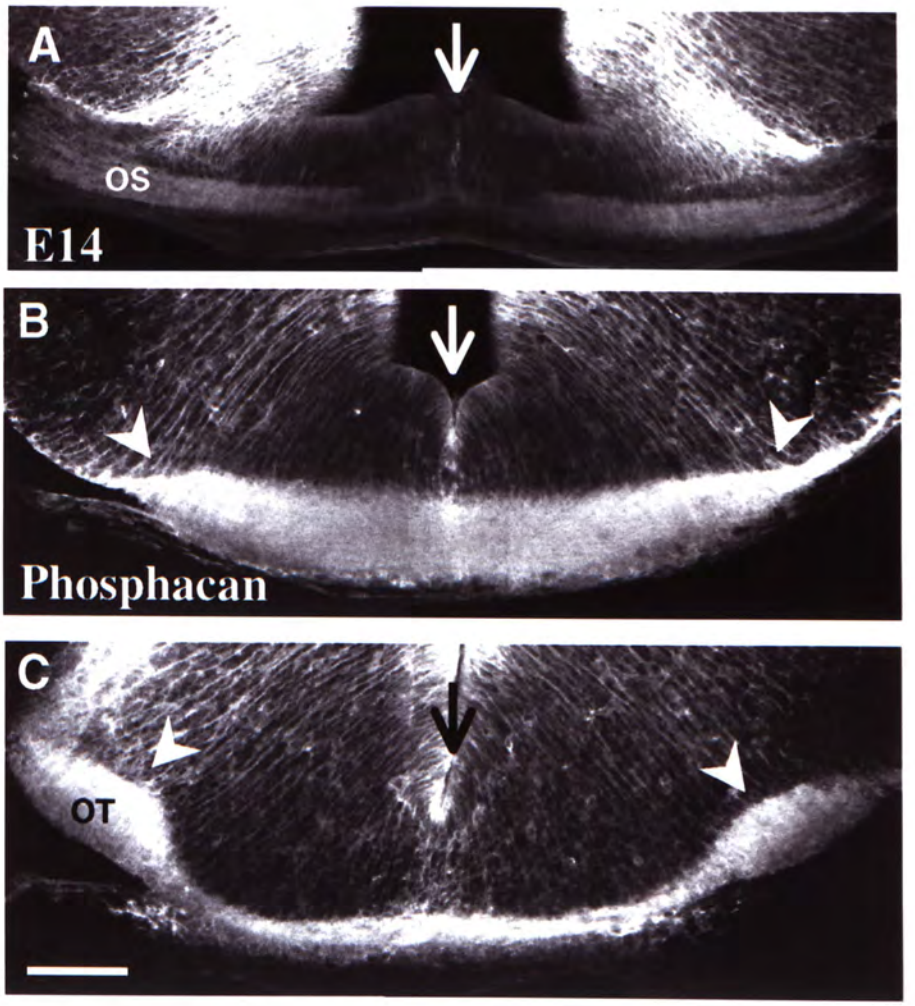
A
OS
E14
B
Phosphacan
C
OT

Figure 5

Confocal photomicrographs showing immunoreactivity to phosphacan, N- and C-terminal neurocans in the ventral diencephalon of E14 mouse embryos in horizontal sections. Anterior is up. The arrows point to the midline of the brain. **A**: At E15, immunoreactivity for phosphacan is detected in the optic stalks (OS) and tracts in the ventral diencephalon. A down-regulation of the signal is observed in the paramidline regions of the chiasm. **B**: Higher magnification of the boxed area in **A**. The dense labeling of phosphacan immunoreactivity on the lateral regions of the mid-chiasm is detected. **C**: In a more ventral section, the prominent band of the expression of phosphacan exists in the posterior boundary of the optic chiasm. The down-regulation of phosphacan expression in the two circular regions posterior to the boundary of the chiasm is found. **D**: Dense labeling of N-terminal neurocan is found at the junction of the optic stalk (OS) and the chiasm. **E**: A regulated band-shaped expression of N-terminal neurocan is detected at the posterior boundary of the optic chiasm, which is similar to the pattern of phosphacan staining. **F**: The expression of C-terminal neurocan is detected in the fiber layer of the chiasm, with an up-regulation of the expression shown at the midline of the chiasm. Scale bars in A, B = 100 μm; scale bar in C = 200 μm, applied to E, F; scale bar in D = 200 μm.

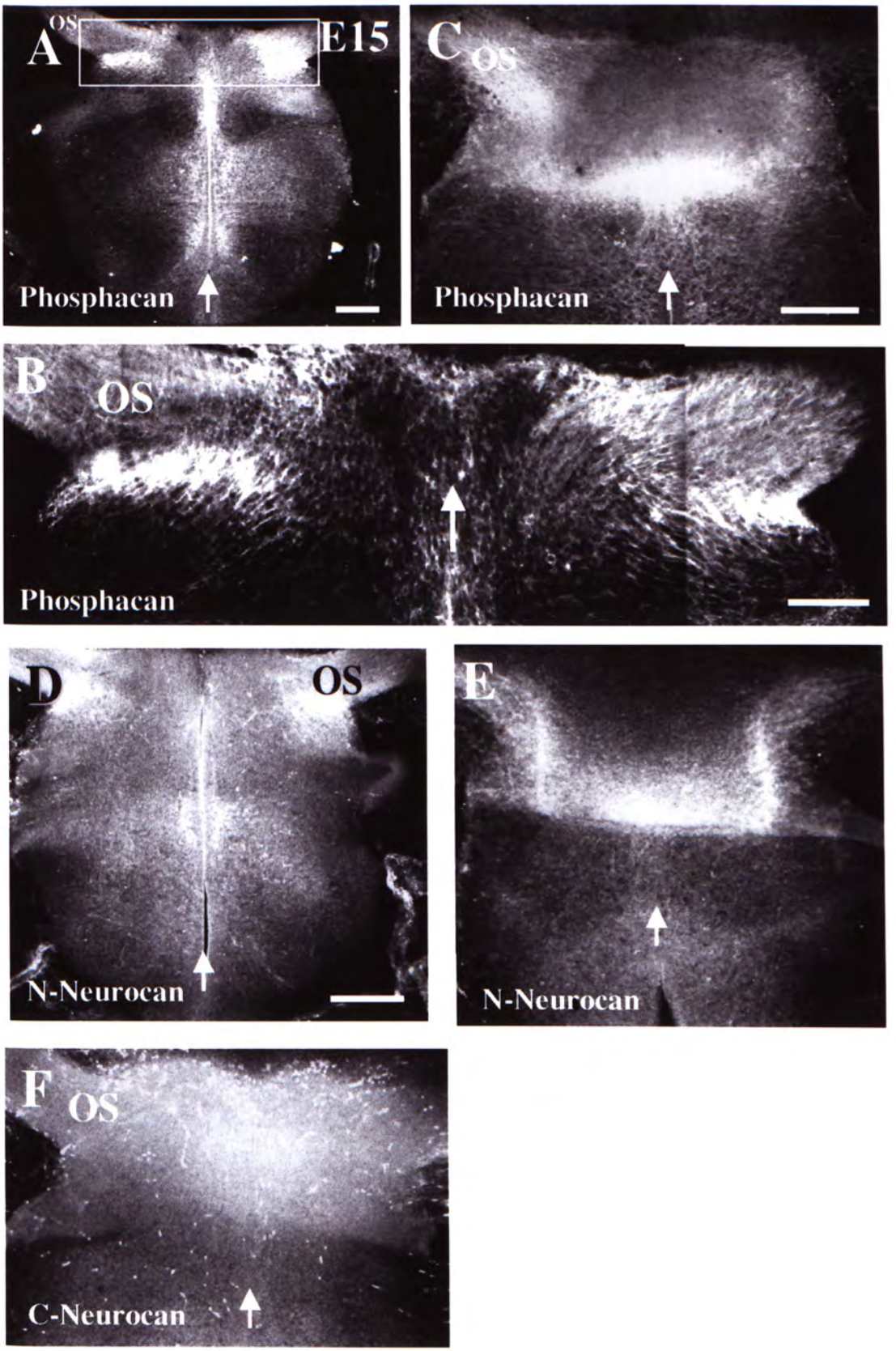
A
OS
E15
Phosphacan
C
OS
Phosphacan
B
OS
Phosphacan
D
OS
N-Neurocan
E
N-Neurocan
F
OS
C-Neurocan

Figure 6

Confocal photomicrographs showing phosphacan, N- and C-terminal neurocans immunoreactivity in the coronal sections of the ventral diencephalon of mouse embryos at E15. Dorsal is up. The arrows point to the midline of the brain. **A**: Immunoreactive phosphacan staining is found in the paraventricular regions on the lateral sides of the diencephalon. **B**: This staining is extended into more caudal sections. **C**: Immunoreactivity for phosphacan is also detected in the retinal fiber layer on the lateral sides of the caudal chiasm. **D**: Staining against N-terminal neurocan shows prominent signal at the junction of the optic stalk and the chiasm. **E**: Intense staining of N-terminal neurocan is found in the fiber layer of the optic chiasm, which may overlap with the band-shaped expression detected in horizontal section at the posterior boundary of the optic chiasm (see Figure 5E). **F**: Immunoreactivity is found on the lateral sides of the optic fiber layer in the tract. **G-H**: Only a basal level of immunoreactivity for C-terminal neurocan is detected in the sections cutting across the optic stalk (**G**) and the chiasm (**H**). **I**: An intense immunostaining of the C-terminal neurocan was found in the superficial region of the optic tract, where retinal growth cones were located. Scale bar = 100 μm.

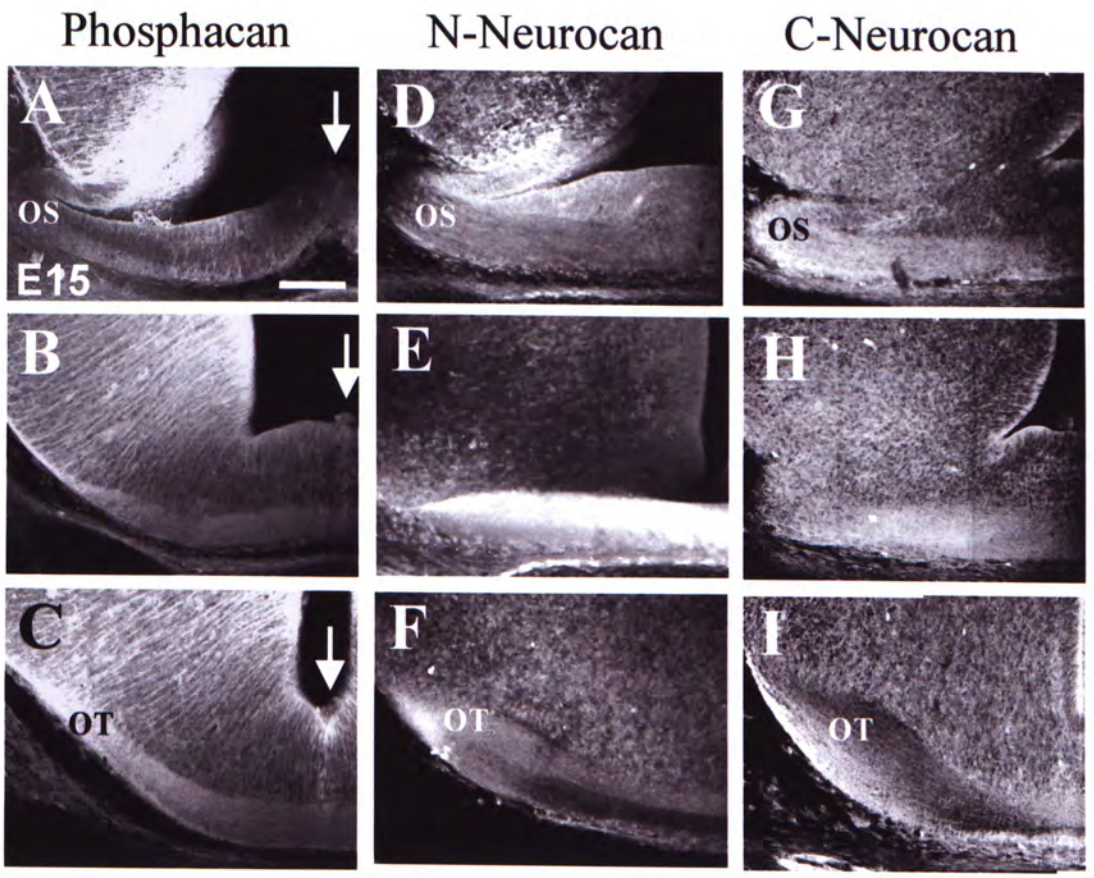
Phosphacan
N-Neurocan
C-Neurocan
A
OS
E15
D
OS
G
OS
B
E
H
C
OT
F
OT
I
OT

CHAPTER 4

HEPARAN SULFATE PROTEOGLYCAN EXPRESSION IN THE OPTIC CHIASM OF MOUSE EMBRYOS

INTRODUCTION

In addition to chondroitin sulfate (CS), there is another group of glycosaminoglycan (GAG), heparan sulfate (HS), which is covalently attached to a protein to form proteoglycans (PGs). Different molecules, including growth factors, cell adhesion molecules, proteases and receptors, have been reported to interact with HS sidechains to play a part in a variety of developmental processes in the nervous system (Hardingham and Fosang, 1992; Lander, 1993; Margolis and Margolis, 1993; Small et al., 1996; Iozzo, 1998; Bernfield et al., 1999). The HS chains bind to fibroblast growth factor (FGF) (which stimulates a variety of cell types to proliferate) both *in vitro* and in tissues (Vlodavsky et al., 1987; Rapraeger et al., 1991; Yayon et al., 1991; Nurcombe et al., 1993; Walker et al., 1994; Brickman et al., 1995; Lin et al., 1999). For some cells, this binding seems to be a required step for FGF to activate its cell-surface receptor (which is a transmembrane tyrosine kinase) (Klagsbrun and Baird, 1991; Rapraeger et al., 1991; Yayon et al., 1991; Schlessinger et al., 1995). Moreover, the spatiotemporal overlap of HSPGs with growing axons suggests that HSPGs are likely to play a supportive role in the development of various axon pathways (Herndon and Lander, 1990; Halfter, 1993; Treloar et al., 1996; Watanabe et al., 1996; Halfter et al., 1997; Ivins et al., 1997). While there are *in vitro* studies showing that HSPGs promote neurite outgrowth on different substrates, indicating a positive role of these molecules in axon growth (Hantaz-Ambroise et al., 1987; Verna

et al., 1989; Dow et al., 1991; Haugen et al., 1992; Isahara and Yamamoto, 1995), there is an *in vivo* study of the retinotectal projection in *Xenopus* demonstrating the importance of HSPGs in regulating axon growth in the optic tract and targeting of axons in the tectum (Walz et al., 1997). However, it is not clear whether these proteoglycans are involved in axon growth and formation of distinct fiber orders at the mouse chiasm. In this study, we used a monoclonal antibody against the HS moieties to find out whether HSPGs are expressed in the retinofugal pathway of mouse embryos at the period when axons grow through the optic chiasm, and correlate the expression of HSPGs to the distinct axon routing patterns in the chiasm.

MATERIALS AND METHODS

Animal and tissue preparations

Pregnant C57 mice were killed by cervical dislocation. Embryos at E11 to E16 were taken out by Caesarian section, washed briefly in 0.1 M phosphate buffered saline (PBS) at pH7.4 and decapitated. The heads were fixed and embedded in a gelatin-albumin mixture as described in previous chapters. The blocks were sectioned at either 50 μm (E11 to E13) or 100 μm (E14 to E16) with a Vibratome to yield both horizontal and coronal sections. Serial sections of the retinofugal pathway from the eyes to the proximal parts of the optic tract were collected in PBS.

Immunocytochemistry

A monoclonal antibody (clone F58-10E4, from Seikagaku Co., Tokyo, Japan) that is specific for an epitope occurs in native heparan sulfate chains has been used to analyze the cellular distribution of this glycosaminoglycan during development. This

antibody recognizes the N-sulfated glucosamine residues of heparan sulfate and does not react with hyaluronate, chondroitin sulfate, or dermatan sulfate (David et al., 1992). The sections were washed and incubated in blocking buffer using the same methods as in chapter 3. After that, the sectioned were reacted with primary antibody (diluted 1:150 in PBS with 1% NGS and 0.5% Triton X-100) overnight at 4°C. Some sections were incubated with a primary antibody against stage-specific antigen-1 (SSEA-1; diluted 1:5, from Developmental Studies Hybridoma Bank, IA, under contract N01-HD-6-2915 from NICHD; Solter and Knowles, 1978) that reacts with a population of early neurons in the ventral diencephalon (Marcus and Mason, 1995). After rinsing in PBS, both groups of sections were incubated in a fluorescein isothiocyanate (FITC) -conjugated secondary antibody (anti-mouse IgM, diluted 1:200 in PBS, from Sigma, St. Louis, MO) for 3 hours at room temperature. Control sections, which did not show any detectable immunostaining in our preparations, were prepared using the same procedures without the addition of primary antibodies. The sections were washed briefly in PBS and cover-slipped with a mounting medium containing 90% glycerol.

Rhodamine phalloidin staining

To study the age-related order of axons in the chiasm and the optic tract, a dye-conjugated rhodamine phalloidin (R415, Molecular Probes, Eugene, OR) that binds specifically to F-actin-rich regions in the retinal growth cones (Wulf et al., 1979; Colello and Guillery, 1992) was used to stain frontal sections of the brain in embryos at E14. To reveal the relationship of the HS expression with this age-related order, simultaneous staining of rhodamine phalloidin and antibody against heparan

sulfate was carried out. After sectioning with a Vibratome, sections for single-label studies were washed twice with PBS, incubated in 0.1% Triton-X 100 in PBS for 30 minutes, washed with PBS again and then incubated in 1 unit/ml rhodamine phalloidin solution in PBS at 4°C overnight. For double-label studies, sections were first incubated overnight in the antibody against the HS epitope, then in a goat anti-mouse secondary antibody conjugated to Alexa Fluor 488 (Molecular Probes) for 3 hours (IgM, 1:200 in PBS pH 7.4). The sections were then washed with PBS and incubated with Alexa Fluor 568-conjugated phalloidin (1:40 in PBS pH 7.4, Molecular Probes) overnight at 4°C. This combination of fluorophores gives a better separation of signals in our preparations than by using FITC and rhodamine. The sections were cover-slipped in 50% glycerol in PBS.

Confocal microscopy and image analyses

The images were captured using a confocal imaging system (Bio-Rad MRC 600, Hertford, England) connected to a Zeiss Axiophot photomicroscope (Oberkochen, Germany). A blue excitation filter set (BHS, 488-nm excitation and 515-nm emission long pass) was used for HS immunoreactivity, and a green excitation filter set (GHS, 514-nm excitation and 550-nm long pass) was used for dye-conjugated phalloidin which stained actin-rich growth cones in the retinal fiber layer of the retinofugal pathway. The images were acquired using the COMOS software (Bio-Rad) and stored in Zip disks (Iomega). The confocal images were then processed using the Confocal Assistant software (Bio-Rad). Images collected from the same sections double-stained with both antibody against HS and dye-conjugated phalloidin were merged using the Confocal Assistant software.

RESULTS

Expression pattern of heparan sulfate at the retina

Throughout the stages examined (from E11 to E16) in the present study, expression of the HS epitope was first detected in the retina of mouse embryos at E11, the time when most ganglion cells are generated (Dräger, 1985) but have not yet entered the optic stalk (Silver and Sidman, 1980). At this stage, HS immunoreactivity was found in most retinal regions and a consistent weaker staining in the central regions around the optic disk was observed (Fig. 1A). Positive staining of the antibody was observed in the inner limiting membrane, vitreous, and the lens. At later developmental stages, HS expression in the retina was downregulated. Immunostaining for the HS epitope at E13 was largely restricted to the peripheral regions of the retina, whereas a weak immunoreactivity for HS was found in the inner regions of the retina (Fig. 1B, C). In the retinal fiber layer and at the optic nerve head, a prominent HS immunoreactivity was detected, implying a possible involvement of HSPGs in regulating axon growth in the retina (Fig. 1C). At E15 and E16, similar expression pattern of the HS epitope was found in the retina, where intense staining was detected in the inner retinal layer, peripheral retina and in the optic stalk (Fig. 1D, E).

Heparan sulfate expression at the ventral diencephalon

In the ventral diencephalon, the HS expression was first detected at E11 (n = 6, not shown). At E12 (n = 6), when most of the retinal axons are growing into the optic stalk but have not yet entered the chiasm (Silver and Sidman, 1980), immunoreactive HS was mainly found in two symmetrical domains at the caudal

regions of the ventral diencephalon (Fig. 2A), which stained the surface and pericellular space of the cells within these domains, as well as the basement membrane of blood vessels and the pia that is rich in HS content (Fig. 2B). At E13, HS immunoreactivity was also prominent in the lateral diencephalon (Fig. 2C). At this developmental stage, several retinal axons have already arrived at the chiasm and optic tract (Godement et al., 1987; Chung et al., 2000b). In horizontal sections of the ventral diencephalon (n = 6), HS-rich regions were found to coincide with the SSEA-1 immunopositive regions, suggesting that these SSEA-1-positive neurons expressed the HS epitope (compare Fig. 2C with 2D). In the proximal part of the optic tract at the lateral region of the diencephalon caudal to the optic stalk, immunostaining for the HS epitope was also found (Fig. 2C). This staining appeared to be confined to the deep regions in the cross-section of the tract (Fig. 2E). In a more ventral section where the retinal fiber layer runs across the optic chiasm, immunoreactive HS was most prominent in the optic fiber layer. Though the signal was much weaker, an inverted V-shaped array posterior to the chiasm showed the HS immuoreactivity (Fig. 2F). It is noteworthy that at the rostral tip of this array, there was an intense staining for the immunoreactive HS at the midline of the chiasm where axons decussate (Fig. 2F, G). This staining appeared to mark the cells and their extracellular space. From the coronal sections (n = 9), this staining labeled the retinal fiber layer at the midline of the diencephalon (Fig. 2H).

At E14, more retinal axons were added to the chiasm and the optic tracts (Chan et al., 1998). Obvious staining of immunoreactive HS in the optic stalk and the chiasm was found in horizontal preparations (n = 8) of the ventral diencephalon at this

stage (Fig. 3A). While the staining in the stalk was evenly distributed, it was found to bias to the deep regions of the cross-section at the threshold of the optic tract (Fig. 3B). In a more ventral position, which cuts the retinal fiber layer of the chiasm, a prominent staining for the immunoreactive HS was noted at the midline and in the optic axons, whereas a weak label was detected in the inverted V-shaped region posterior to the chiasm (Fig. 3C and 3D). When we looked at the coronal sections of the ventral diencephalon, which cut the rostral half of the chiasm (n = 9), this prominent label at the midline of the ventral diencephalon was also observed (Fig. 3E and 3F). Intense immunoreactivity for HS was found in the optic axons in their initial course at the lateral regions of the chiasm (Fig. 3E and 3F). As optic axons continue to grow towards the more caudal part of the diencephalon, an obvious reduction in HS immunoreactivity was consistently detected in regions approximately 100 μm flanking both sides of the midline (Fig. 3F). In a more caudal section, at the level that contains the caudal parts of the chiasm and the threshold of the optic tract, the expression of HS was restricted to the deep parts of the retinal fiber layer leaving the subpial regions of the tract virtually devoid of staining (Fig. 3G).

At E15 (n = 4) and E16 (n = 3), most retinal axons have arrived at the chiasm and entered the optic tract, including the major uncrossed axons from the ventral temporal retina (Godement et al., 1990; Chan et al., 1999). At both ages, intense staining for immunoreactive HS in the retinal fiber layer was detected as in the E14 chiasm (Fig. 4A). From the coronal sections of the rostral half of the chiasm, an intense staining of HS was detected at the midline of the chiasm where fibers decussate. This staining was substantially reduced on both sides approximately 100

μm from the midline (Fig. 4A-C). At the level of the caudal chiasm and the tracts, a high level of HS immunostaining was restricted to the deep regions at threshold of the optic tract (Fig. 4D).

Changes of growth cone positions at the mouse chiasm

To investigate the possible relationship between the expression pattern of the HS epitope and the changes in age-related order in the mouse chiasm (Colello and Coleman, 1997; Colello and Guillery, 1998), rhodamine phalloidin was used to stain the F-actin-rich growth cones to reveal its distribution in the retinal fiber layer of the E14 chiasms (n = 3) (Wulf et al., 1979; Forscher and Smith, 1988; Colello and Guillery, 1992). In frontal sections of the chiasm, the phalloidin staining appeared to mark the growth cones through the whole thickness of the retinal fiber layer at the junction of the stalk and the chiasm (Fig. 5A). In a section 100 μm caudal to Figure 5A, phalloidin-stained growth cones were shown to be restricted at the subpial regions of the lateral part of the chiasm and start to spread to whole thickness of the axon layer at the midline (Fig. 5B). This shifting of growth cone positions appeared to coincide with the regions (approximately 200 μm from the midline) where down-regulation of HS expression was observed (compared Fig. 5B with 3F). In the optic tract, the phalloidin staining was confined to the subpial regions where newly arrived growth cones traversed (Fig. 5C). At this part of the retinofugal pathway, HS immunoreactivity was found to be restricted to the deep parts of the tract (compared with Fig. 3G).

More detailed studies of the spatial relation of HS immunoreactivity and growth cone position in the retinal fiber layer of the chiasm was carried out by the use of double staining for dye-linked phalloidin and antibody against the HS epitope on frontal sections of E14 diencephalon (n = 4). At the junction of the optic stalk and the ventral diencephalon, phalloidin-labeled growth cones were observed in whole thickness of the fiber layer (Fig. 6A). However, most retinal growth cones shifted ventrally and gathered at the subpial surface of the retinal fiber layer in a section 100 μm caudal to Figure 6A (Fig. 6B). At this position, complementary staining of HS immunoreactivity to the phalloidin staining was observed at deep regions of the fiber layer (Fig. 6B). At regions flanking the midline, a spread of growth cones across the whole thickness of the fiber layer at the midline was observed, accompanying by a dramatically decrease of HS expression (Fig. 6B). In a more caudal section, it could be seen that at the level cut across the optic tract, phalloidin-stained growth cones and immunoreactive HS epitopes occupied the superficial and deep regions of the optic tract respectively and complementarily (Fig. 6C).

DISCUSSION

In the present study, the expression patterns of heparan sulfate (HS) proteoglycans (PGs) in the retinofugal pathway of mouse embryos has been characterized by the use of a monoclonal antibody specific for the HS epitope. The current results show that immunoreactive HS epitope exists at E11, the earliest stage that we examined, in the retina and the ventral diencephalon. Moreover, immunoreactive HS was found in the retinal axons and, to a lesser extent, the resident neurons at the chiasm from E12 to E16, the time when retinal axons are actively

growing across the optic chiasm. Also, intense HS immunoreactivity was detected at the midline over the period of major axon growth and there was a substantial decrease of this immunoreactivity in a region approximately 100 μm flanking both sides of the midline. This down-regulation of HS expression coincides with the dispersion of some actin-rich growth cones from the subpial region to deeper parts of the retinal fiber layer at the midline. In addition, restricted expression of HS epitope was observed in only the deep regions of the optic tract, which shows a complementary pattern to the position of the growth cones, suggesting a regulatory function of HS to the establishment of chronotopic order of retinal axons in this segment of the retinofugal pathway.

Heparan sulfate proteoglycans in the retina

In the retina of mouse embryos, immunopositive HS epitope was strongly expressed at E11, when most retinal ganglion cells are generated (Dräger, 1985). At this early stage, the HS epitope was found in all regions of the retina. After that, the staining pattern of this HS epitope is changed gradually. At E16, the staining of HS epitope was reduced at the central retina and was restricted to the periphery of the retina. This receding gradient of HS expression from the central to peripheral retina appears to go along closely with the expression pattern of chondroitin sulfate (CS) PG in the mouse retina (Brittis et al., 1992; Chung et al., 2000a). The intraretinal growth of ganglion cell axons has been suggested to be regulated by the expression of CSPGs, probably through its inhibitory role in retinal axon growth (Snow and Letourneau, 1992). The similarity of the expression of these two groups of molecules raises the possibility that HS is also involved in putting an inhibitory function to axon

growth in the retina. However, in contrast to the virtually nil expression of CS epitope in the retinal fiber layer and at the optic disk (Chung et al., 2000a), HS showed a prominent expression in these regions. Similar staining patterns of HS were also reported in the retina of rat and chick embryos (Karthikeyan et al., 1994; Halfter et al., 1997), suggesting a supportive role of HSPGs, rather than inhibitory, to axon growth in the retina. Although the functions of HSPGs in the retina of mouse embryos are still not clear, it is very likely that these proteoglycans pose their functions by interacting with growth factors and their receptors to regulate axon growth in the retina. Some studies have reported that binding of fibroblast growth factors (FGFs) to HSPG is an essential step for signal transduction of FGFs and the initiation of the corresponding cellular responses (for review, see Klagsbrun and Baird, 1991; Gallagher and Turnbull, 1992; Ornitz, 2000). For cells lacking expression of HS, they do not bind to FGF-2, even if they express the high affinity fibroblast growth factor receptor (FGFR) (Rapraeger et al., 1991; Yayon et al., 1991). Binding of HSPG and FGF-2 triggers the growth stimulating and differentiation inhibiting responses. It was reported that FGFs regulate proliferation and differentiation of retinal progenitor cells and are associated with the first appearance of ganglion cells in the retina (Park and Hollenberg, 1989; Pittack et al., 1991, 1997; Guillemot and Cepko, 1992; De Iongh and McAvoy, 1993; McFarlane et al., 1998; McCabe et al., 1999). Moreover, the orderly axonal projection pattern towards the optic disk in the developing retina of rats involves the activation of FGFR signaling cascade. Defasciculation and misrouting of ganglion cell axons to inappropriate regions in the retina were reported if defined steps in the FGFR signal transduction cascade were blocked (Brittis et al., 1996). Until now, no direct evidence has been put forward that these FGF

receptor-induced activities in the developing retina are mediated through a binding to HSPGs. However, these proteoglycans are very likely to be candidates which play a role in most of these developmental events.

Heparan sulfate proteoglycans in the chiasm neurons

We have shown that before and during the major period of axon growth into the chiasm, HSPGs expression are found in the ventral diencephalon of mouse embryos. Similarity of the expression of these PGs and the distribution of SSEA-1 positive neurons suggests that these early neurons may produce HSPGs in the ventral diencephalon. A previous study in our laboratory has shown that this specialized cellular domain is immunoreactive to CS-56, an antibody against the chondroitin sulfate (CS) PGs (Chung et al., 2000a). These two groups of PGs may act together for the biological properties of these chiasm neurons. In the mouse, the proteoglycan CD44 in the chiasm neurons is a potential inhibitory molecule to retinal axon growth (Sretavan et al., 1994). Different sulfated glycosaminoglycans, including CS, HS, and keratin sulfate are involved in the modification of CD44 into various isoforms (Brown et al., 1991; Greenfield et al., 1999). These modifications of the carbohydrate contents are resulted from various splicing of exons coding for the polypeptide of CD44. These processes are developmentally regulated, tissue specific and contribute to the diverse biological functions of these molecules (Peach et al., 1993; Piepkorn et al., 1997). We suggest that the immunostaining for the HS and CS epitopes recognize the carbohydrate moieties on the CD44 in the mouse ventral diencephalon. However, it is also possible that other proteoglycans which are essential for the axon guidance in the developing nervous system are expressed in these chiasm neurons.

In this study, an obvious staining for HS is observed at the midline of the chiasm throughout the major period of axon growth (E13-E16). When compare this to the immunoreactivity for CS, which is substantially reduced at later stages of pathway development (at E15 and E16) (Chung et al., 2000a), different expression patterns of the CS and HS glycosaminoglycans in the mouse chiasm were found. It is possible that the cellular elements at the midline may modify the functional constituents of these glycosaminoglycan chains on the PG molecules to regulate retinal axon growth in the chiasm. However, the function of HS at the midline is unknown. Previous studies have shown that HS is involved in the nonpermissive role of the midline glia in the tectum to the growth of midbrain neurites (Garcia-Abreu et al., 2000). Purified agrin, a HSPG, was shown to inhibit retinal neurite outgrowth in chick embryos (Halfter et al., 1997). Furthermore, the HSPG syndecans have been related to defining tissue boundaries in developing *Xenopus* embryos through an inhibitory function (Teel and Yost, 1996). However, the exact function of HS in retinal axon guidance and its control over axon divergence as CS GAG does in the mouse optic chiasm remains to be determined.

Heparan sulfate proteoglycans and chronotopic fiber order in the chiasm

Other than chiasm neurons, optic axons at the chiasm and the tract also show the expression of HS epitope. In this study, an important spatial relationship between HS immunoreactivity and chronotopic arrangement of retinal axons in the chiasm and the tract was observed. This correlation is most obvious in the retinal fiber layer in the chiasm and at the optic tract. In the optic tracts, when growth cones gather in the

subpial regions, HS immunoreactivity is found intensely in the deep regions of the retinal fiber layer (Guillery and Walsh, 1987; Colello and Guillery, 1992). Furthermore, the HS immunoreactivity is substantially down-regulated in regions that palisade the midline, where a gradual shift of retinal growth cones from the subpial surface to the whole retinal fiber layer is found (Colello and Coleman, 1997; Colello and Guillery, 1998). This observation is further confirmed by using a dual-label technique. The complementary changes of the immunoreactive HS and the position of retinal growth cones in the retinal fiber layer at the mouse chiasm and tract suggest that the development of the chronotopic order of the retinal axons in these regions may be related to the expression of HSPGs.

While the function of HSPGs to axon growth in the mouse chiasm remains undetermined, many studies have demonstrated the participation of the molecules in different developmental events. *In vivo* studies showed that there is a promoting property of HSPGs to neurite outgrowth (Hantaz-Ambroise et al., 1987; Haugen et al., 1992; Isahara and Yamamoto, 1995). The spatiotemporal overlap of HS expression with growing axons in the developing axon pathways also suggest a supportive role of HSPGs in axon growth (Herndon and Lander, 1990; Watanabe et al., 1996; Halfter et al., 1997; Ivins et al., 1997). Interaction of HSPGs with cell adhesion molecules (CAMs) and extracellular matrix proteins was also suggested to be involved in axon elongation and fasciculation in the chiasm and tract (Cole and Glaser, 1986; Cole et al., 1986; Raulo et al., 1994; Rauvala et al., 1994; Burg et al., 1995; Storms et al., 1996; Kinnunen et al., 1998, 1999). Enzymatic removal of native HS in the diencephalon of developing *Xenopus* optic pathway produces a retardation of retinal

axon elongation in the optic tract (Walz et al., 1997). However, addition of FGF-2 to these heparitinase-treated embryos resumes the axon growth, indicating that the growth promoting property of HS is probably mediated by an interaction with the FGF signaling system (Walz et al., 1997). Despite the resumption of axon extension after addition of FGF-2, axons still lose their directionality after heparitinase treatment. It suggests a possible function of HS in promoting fasciculation of axons in the developing optic tract through a growth factor-independent mechanism. In the mouse retinofugal pathway, fasciculation of axons in deep regions of the fiber layer in the chiasm and in the tract may be mediated by HS epitope by similar mechanism. When function together with other inhibitory molecules, such as CS-PGs, these protoglycans regulate the development of age-related fiber order in different regions of the retinofugal pathway. Specific HS structures were shown to be essential in retinal axon targeting, suggesting that the sequences of HS, instead of the gross structure of the proteoglycans, are important for axon guidance (Irie et al., 2002). However, it should be noted that HSPGs may perform a similar inhibitory rather than supportive role to the retinal axon growth as that of CSPGs in the mouse chiasm (Chung et al., 2000a, b) and of HSPGs in other developing systems (Teel and Yost, 1996; Garcia-Abreu et al., 2000).

Figure 1

Confocal photomicrographs showing immunoreactivity to heparan sulfate (HS) in horizontal sections of the retinas in C57 mouse embryos. Anterior is up. **A:** At embryonic day 11 (E11), HS immunoreactivity is found in most retinal regions (R). Positive staining is also observed in the lens (L) and vitreous. **B:** At E13, substantial staining of HS is restricted to the peripheral regions of the retina, whereas a week immunoreactivity for HS is found at the inner layer of other retinal regions. **C:** Prominent expression of HS is found in the optic nerve head (ON) and in the layer of optic axons (indicated by arrowheads). **D:** Similar expression pattern of HS is found at E15, in which the HS immunoreactivity is found in the inner retinal layer and at the peripheral retina. **E:** The optic nerve head (asterisk in **D**) shows an intense staining for HS, as shown here at higher magnification. Scale bars = 50 μm in A, 100 μm in B, C, E, 200 μm in D.

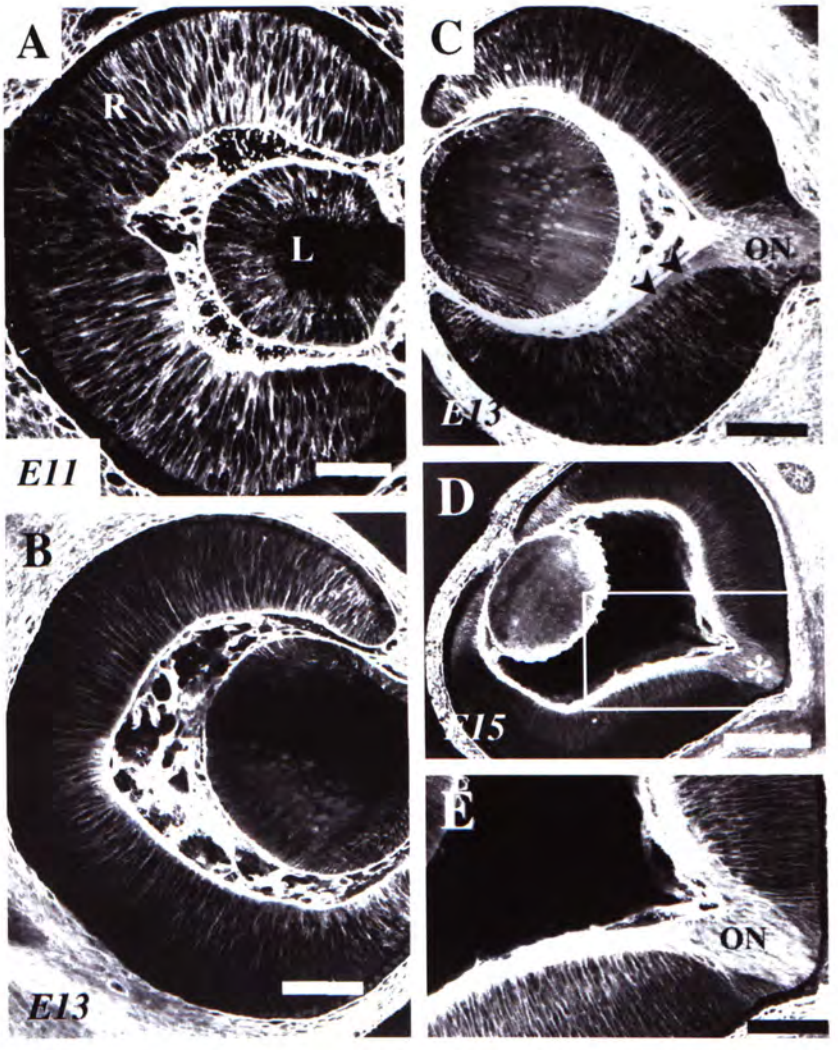
A
R
L
E11
B
E13
C
ON
E13
D
E15
E
ON

Figure 2

Confocal photomicrographs showing immunoreactivity for heparan sulfate (HS) in the chiasm of embryonic day 12 (E12) (**A**, **B**) and E13 (**C-H**) mouse embryos. In the horizontal sections of the ventral diencephalon (**A-G**), anterior is up; whereas in the frontal section (**H**), dorsal is up. The arrows point to the midline of the brain. **A**: At E12, immunoreactive HS is found in two groups of cells in the caudal regions of the ventral diencephalon, which stains the surface and the pericellular space of these cells (as shown at higher magnification in **B**). The blood vessels are indicated by the arrowheads in **A**. **C**: At E13, staining of HS is most intense at the caudal regions of the ventral diencephalon, which coincides with regions that contain neurons immunopositive for SSEA-1 as shown in **D**. Noted the section in **C** is cut more dorsally on the left than on the right. The ventral diencephalon is outlined by a white broken line in **D**. **E**: A higher magnification of the boxed area in **C** shows the HS staining in the deep regions of the optic tract (outlined by the dotted white line). **F**: At the chiasm, the HS staining is found in the optic axons and in the cellular domain caudal to the optic axons. **G**: A higher magnification of the boxed area in **F**, indicating the immunoreactive HS at the midline (indicated by the arrowheads) where axons decussate to the opposite side of the brain. **H**: Frontal section of the chiasm shows that the midline region is immunopositive to the HS antibody. The staining extends from the ventricular surface to the pial surface of the chiasm. Scale bars = 200 μm in A, 50 μm in B, E, G, H, 200 μm in C, D, F.

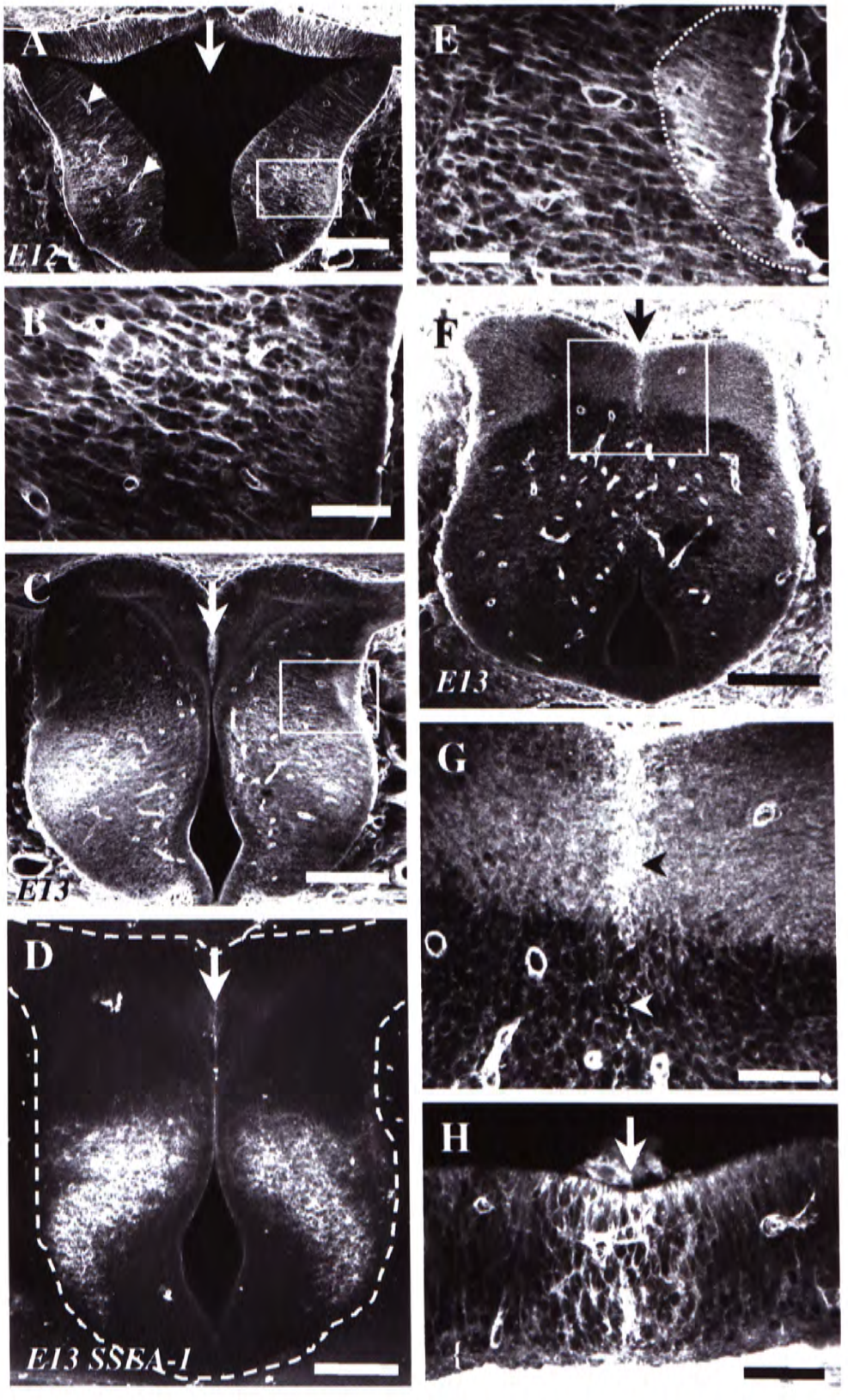
A
E12
B
C
E13
D
E13 SSEA-1
E
F
E13
G
H

Figure 3

Confocal photomicrographs showing immunoreactivity for heparan sulfate (HS) in the chiasm of embryonic day 14 (E14) embryos. In the horizontal sections of the diencephalon (A-D), anterior is up; whereas, in the frontal sections (E-G), dorsal is up. The arrows point to the midline of the brain. **A:** The staining of HS is most prominent in both the optic stalk (OS) and the optic tract (OT), as indicated in a higher magnification in **B**. Although the staining at the stalk appears to mark the structures at all positions, the staining in the tract is restricted to the deep regions (arrowhead). The dotted lines in A correspond to the level where frontal sections in E, F, and G are collected. **C:** In a more ventral section, prominent staining for HS is also detected at the midline of the chiasm (indicated by the arrowheads in D). **D:** Higher magnification of the boxed area in C. **E:** In a frontal section of the ventral diencephalon, substantial label of HS is found at the midline. The optic axons in the stalk (indicated by the arrowhead) at this position are also positive to HS. **F:** At a more caudal section, the immunostaining is confined at the midline region and in the retinal fiber layer at the lateral regions of the chiasm (arrowheads). Note that the staining marks the deep regions of the retinal fiber layer (indicate by the bracket) and is reduced in regions flanking the midline. **G:** Intense staining of HS is detected in deep parts of the optic tract (arrowhead). Scale bars = 200 μm in A, 100 μm in B, 200 μm in C, 50 μm in D, 100 μm in E-G.

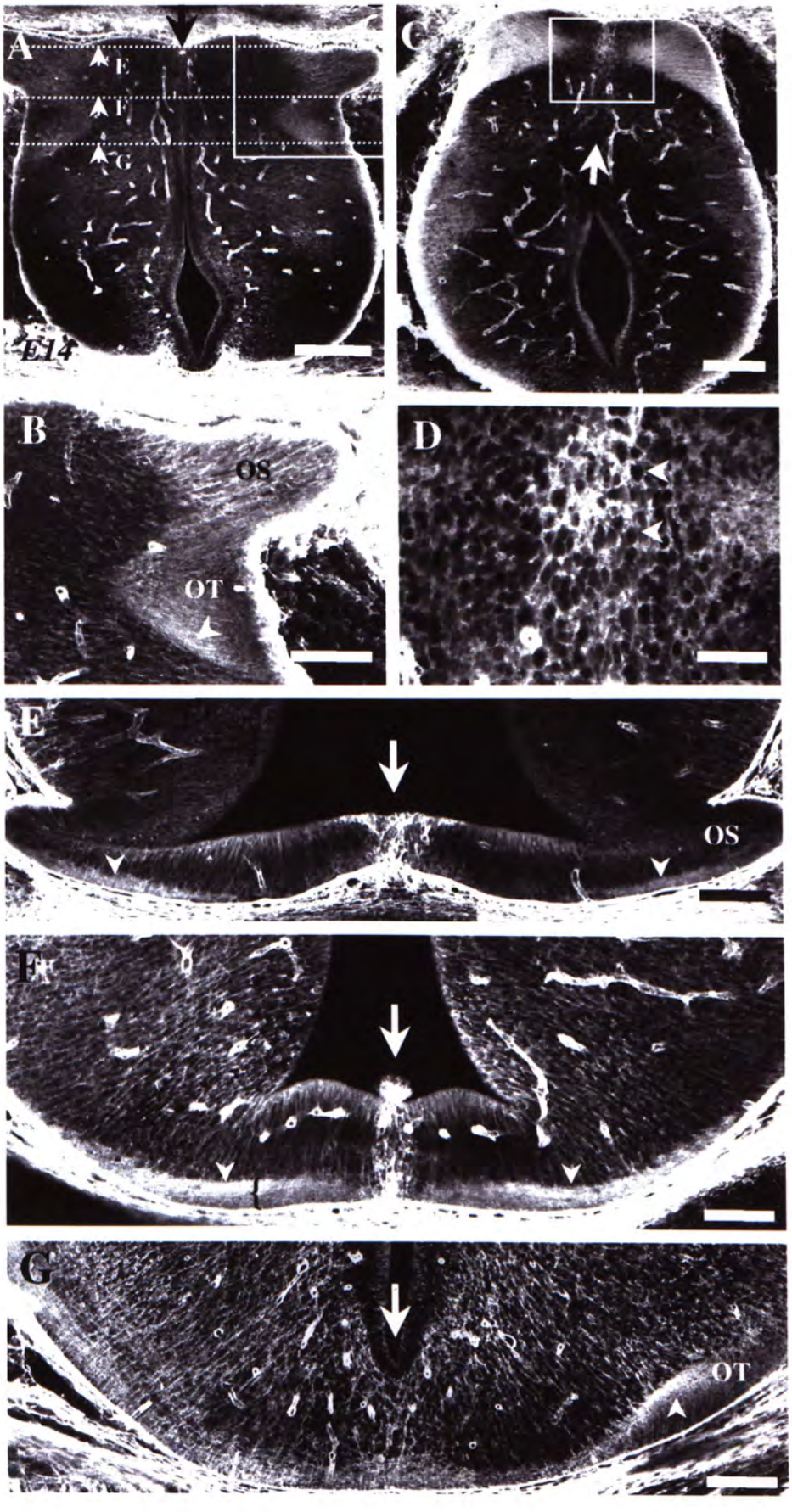
A
E
F
G
E14
C
B
OS
OT
D
E
OS
F
G
OT

Figure 4

Confocal photomicrographs showing immunoreactivity for heparan sulfate (HS) in the chiasm of embryonic day 15 (E15) embryo. Anterior is up in the horizontal section of the ventral diencephalon (A); and dorsal is up in the frontal sections (B-D). The large arrows point to the midline of the brain, and the brackets indicate the retinal fiber layer. **A:** The retinal fiber layer at rostral regions of the diencephalon shows a substantial labeling of HS. It is noted that the immunoreactivity is reduced substantially at a region approximately 100 μm from the midline (indicated by the open arrow). The cellular regions caudal to the chiasm show a weak HS immunoreactivity. **B:** In frontal sections of the chiasm, HS immunoreactivity is found largely in the optic stalk (OS) and at the midline. **C:** In a more caudal position, the staining for HS is substantially reduced at regions on both sides of the midline. **D:** At the optic tract, the immunostaining is detected in the deep regions of the optic axons (arrowhead). Scale bars = 100 μm in A-D.

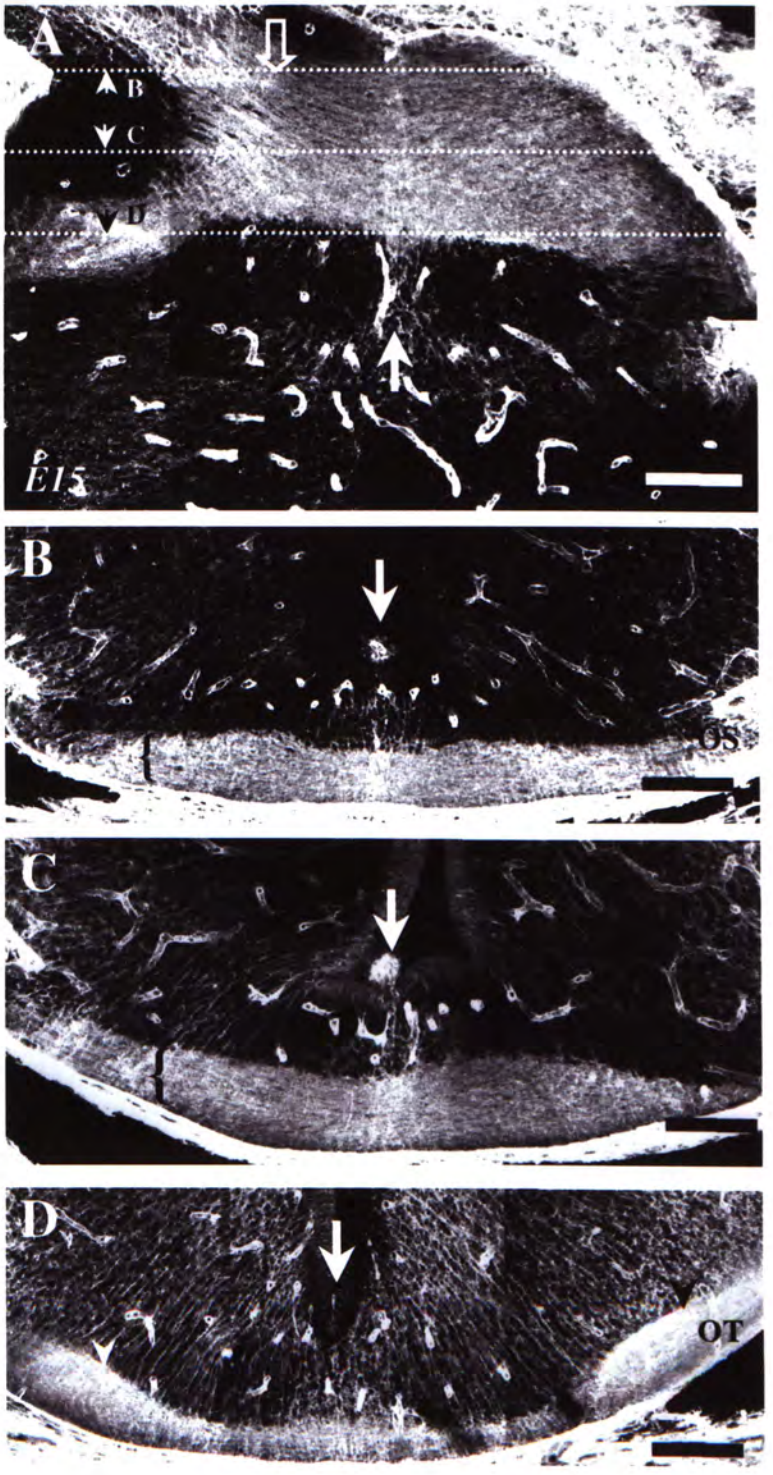
A
B
C
D
E15
B
OS
C
D
OT

Figure 5

Confocal photomicrographs showing the frontal sections of the ventral diencephalon stained with rhodamine phalloidin, which marks the F-actin-rich growth cones in the chiasm of an embryonic day 14 (E14) embryo. Structures on the left are slightly rostral to those on the right in these sections. Dorsal is up, and the arrows point to the midline of the brain. The retinal fiber layer of the chiasm is marked by the dotted lines. **A:** The phalloidin staining appears to mark the whole optic stalk (OS). **B:** In a section 100 μm caudal to A, phalloidin-positive growth cones concentrate at the superficial region of the retinal fiber layer (bracket) in the lateral region of the chiasm (indicated by asterisk) and start to spread to deeper positions at the midline. This shifting of growth cone position appears to coincide with regions where reduction in heparan sulfate immunoreactivity is observed (see Fig. 3F). **C:** Phalloidin staining is restricted to the superficial regions of the optic tract (OT) (arrowheads). Scale bar = 100 μm in A-C.

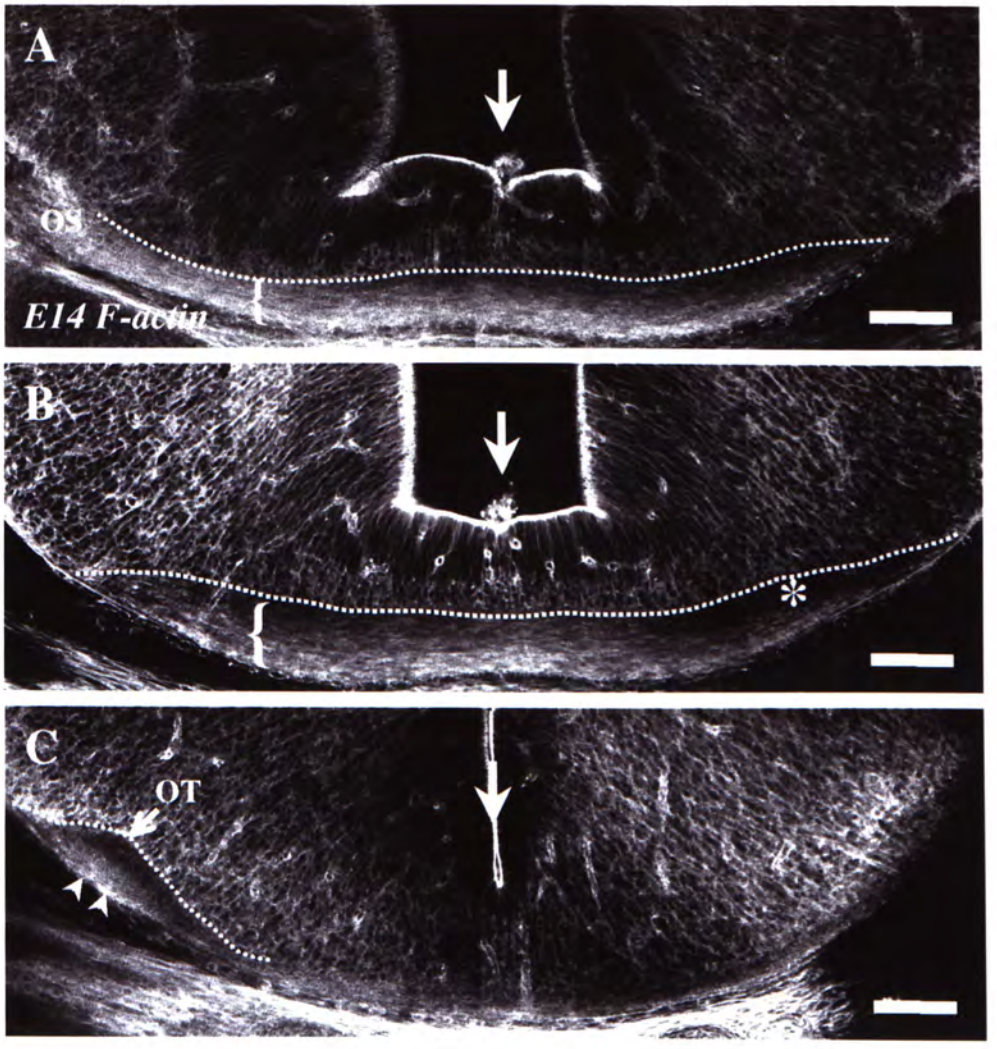
A
OS
E14 F-actin
B
*
C
OT

Figure 6

Confocal photomicrographs showing the frontal sections of the ventral diencephalon stained with dye-conjugated phalloidin for actin-rich growth cones (red in color) and a monoclonal antibody against the heparan sulfate (HS) epitope (green in color) in the optic chiasm of an embryonic day 14 (E14) embryo. The retinal fiber layer is enclosed by the broken lines. Dorsal is up, and the arrows point to the midline of the brain. **A:** The phalloidin staining is found in the axons at the optic stalk (OS). **B:** In the section 100 μm caudal to A, phalloidin-positive growth cones are restricted to the superficial region of the retinal fiber layer in the chiasm and start to spread to deeper parts in a region approximately 100 μm from the midline (indicated by the arrowhead), which has a substantial reduction of HS immunoreactivity. **C:** In the optic tract (OT), the phalloidin staining is again restricted to the superficial regions and the HS immunoreactivity is localized in the deep regions of the retinal fiber layer. Scale bars = 100 μm in A,B (applied to C).

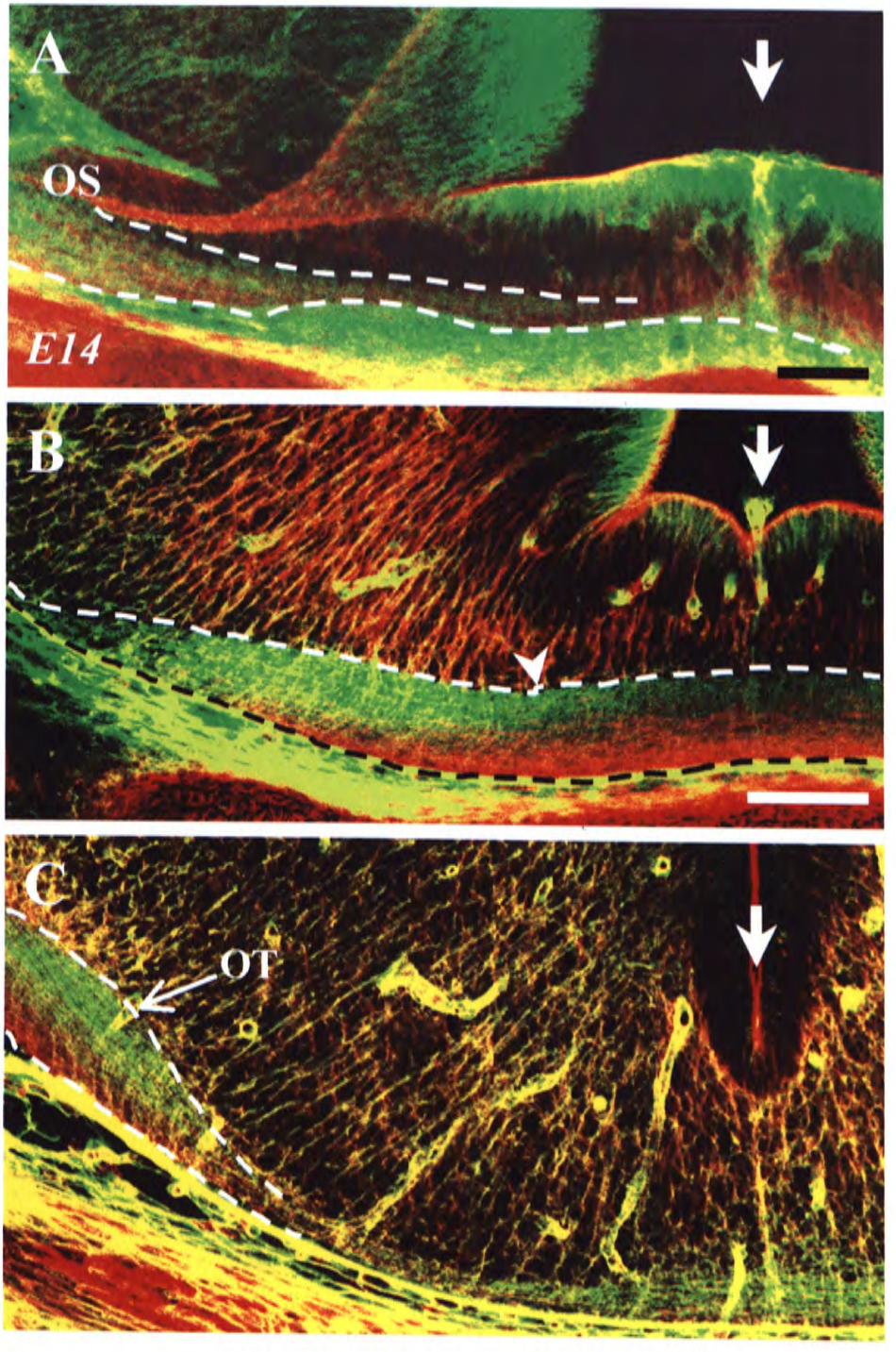
A
OS
E14
B
C
OT

CHAPTER 5

EXPRESSION OF NEURAL CELL ADHESION MOLECULES (NCAM) IN THE CHIASM OF MOUSE EMBRYOS

INTRODUCTION

Retinal axons undergo different rearrangement throughout the mouse retinofugal pathway. These fiber sortings include the partial decussation pattern of crossed and uncrossed axons at the midline of the chiasm (Silver, 1984; Godement et al., 1990; Sretavan, 1990), the segregation of dorsal from ventral fibers in the optic tract (Torrealba et al., 1982; Cucchiaro and Guillery, 1984; Reese and Baker, 1993; Chan and Guillery, 1994; Chan and Chung, 1999), and the reordering of axons according to the time of arrival of their growth cones (Walsh and Guillery, 1985; Colello and Guillery, 1992).

In the previous chapters, we have disscussed the possible roles of proteoglycans in regulating the chronotopic order of retinal axons in the retinofugal pathway of developing mouse embryos. In this chapter, we will shift our focus to another molecule: neural cell adhesion molecule (NCAM), which is a possible candidate in guiding the proper establishment of the retinofugal pathway in the mouse.

NCAM, which is expressed by most neurons, is one of the Ca^{2+}-independent cell adhesion molecules in vertebrates. This molecule has been shown abundantly on developing axons and the glial environment (Silver and Rutishauser, 1984; Brittis et al., 1995). It is thought to bind adjacent cells, as well as neurites and their

environment together by a homophilic mechanism (Rutishauser et al., 1982; Hoffman and Edelman, 1984; Dodd and Jessell, 1988). Some NCAM molecules, however, use a heterophilic binding activity (with CSPG: Grumet et al., 1993; with Phosphacan: Milev et al., 1994). There are at least 20 forms of NCAM, each of which is generated by alterative splicing of RNA transcript produced from a single gene (Cunningham et al., 1987; Santoni et al., 1987). Some forms of NCAM arise from glycosylation (Rougon et al., 1982), which carry different amounts of sialic acid. Polysialic acid (PSA) is not an independent molecular entity, but a post-translational modification of NCAM (Rutishauser and Landmesser, 1991). By virtue of their negative charge, the long sialic acid chains hinder cell adhesion, thereby modifying the adhesive function of NCAM (Rothbard et al., 1982; Hoffman and Edelman., 1983; Rutishauser et al., 1985). Therefore, NCAM that is heavily loaded with sialic acid may, sometimes, serve to prevent adhesion rather than cause it. N-CAM is present in mouse brain and rat neural tissue (Chuong et al., 1982). It exists as many embryonic (E) forms and three major adult (A) forms (Edelman and Chuong, 1982; Rougon et al., 1982). In early embryonic cells, PSA is present in large amount in NCAM and decreases with age in a tissue-dependent manner with concomitant increase in NCAM binding (Hoffman and Edelman, 1984).

With the homophilic and heterophilic binding abilities of and also the presence of PSA, NCAM is involved in the facilitation of axon elongation (Dodd and Jessell, 1988; Brittis et al., 1995) and fasciculation of axons into bundles (Silver and Rutishauser, 1984; Rutishauser and Landmesser, 1991).

In previous studies, NCAM was found in the retinofugal pathway in goldfish and chick (chick: Silver and Rutishauser, 1984; goldfish: Bastmeyer et al., 1990). In this study, we will investigate NCAM expression in the retinofugal pathway of mouse embryos during the major growth period of retinal axons and discuss how expression pattern of NCAM in the diencephalon is correlated to the routing of axons in the pathway.

MATERIALS AND METHODS

Animal and tissue preparations

Time-mated C57 mouse embryos were used in this study. Pregnant mothers were killed by cervical dislocation. Embryos at the age of E13-15 were taken out by Caesarian section and stored temporarily in cold 0.1M phosphate buffered saline (PBS). The heads of each embryo were cut, and immersed in freshly prepared 4% paraformaldehyde in 0.1M phosphate buffer (PB) and were stored overnight at 4°C. The fixed heads were embedded in a gelatin-albumin mixture. The orientation of the embryo within the gelatin-albumin block was marked by a cut at the block. The blocks were then sectioned using a vibratome at 100μm thickness. Some blocks were sectioned horizontally while others were sectioned parasagittally. Serial sections of the ventral diencephalon, from the level of eyeballs to the chiasm, were collected from the horizontal sections. Serial sections of the retinofugal pathway from retina to optic tract were collected in PBS from the parasagittal sections. After N-CAM immunostaining, the serial sections were examined under a confocal microscope.

Retinal labeling with lipophilic dyes

In order to reveal the course of retinal axon growth, a lipophilic dye was implanted into the retina of the aldehyde-fixed mouse embryos to label the retinal axons (Godement et al., 1987). Fluorescent carbocyanine dye DiI (1,1'-dioctadecyl-3,3,3',3'-tetramethylindocarbocyanine perchlorate) (Molecular Probes, USA) was used. The dye labels axons by incorporating into the plasma membrane of retinal ganglion cells and diffusing along the axons (Honig and Hume, 1986; Godement et al., 1987; Thanos et al., 1993; Chan and Guillery, 1994).

After fixation of the embryo heads overnight, the cornea and lens of the fixed embryos were removed. Tiny crystals of DiI were applied to all quadrants of the retina in order to fully label all retinal axons. The embryos were then immersed in 2% buffered formalin, sealed from light and stored in 37°C water bath for 4 days before sectioning. Cross sections of the optic tract at a thickness of 200μm were obtained by first sectioning the head horizontally on a Vibratome to approximately 400-600μm above the ventral floor of the diencephalon. The block was then reembedded in gelatin-albumin, and serial cross sections of the retina, optic stalk, and chiasm at 200μm thickness were obtained in parasagittal sections of the head (Chan and Guillery, 1994). The sections were then double-stained with NCAM antibody.

Preparation of brain slices

While some of the *in vivo* tissues were stained with DiI and/or by immunocytochemistry directly after fixation, brain slices were prepared to be incubated with 5A5 anti-NCAM antibody (mouse IgM; Developmental Studies Hybridoma Bank, U.S.A.). C57 mice embryos at E14 were decapitated and kept in

chilled Dulbecco's modified Eagle's medium (DMEM)/F12 medium containing penicillin (1000 U/ml) and streptomycin (1000 μg/ml). Brain slice preparations of the retinofugal pathway comprising the eyes, optic stalks, chiasm and proximal parts of the optic tract were prepared as described in the chapter 2. A tiny DiI crystal dye was incorporated into the dorsal quadrants of the retina. The DiI-stained brain slices were then cultured in DMEM/F12 with 10% foetal bovine serum (Life Technologies, USA) at 37°C in a rolling incubator for 5 hours. Within the incubation period, the cultures were supplied with pure oxygen three times, as a jet of oxygen directed into the air space above the culture medium. In experimental brain slices, 5A5 antibody against sialylated form of N-CAM was added at a final concentration of 1:1000 during incubation. For control, brain slices were kept under the same condition, except no addition of 5A5 antibody. After the incubation period, the brain slices were fixed in 4% paraformaldehyde overnight and sectioned parasagittally. These sections were cover-slipped in PBS and imaged for DiI signal by a confocal imaging system directly.

Immunostaining of Neural Cell Adhesion Molecules (NCAM) in the retinofugal pathway

The serial sections obtained from *in vivo* tissues were blocked in 10% normal goat serum (NGS) for 1 hour. After several washes with PBS, the sections were incubated overnight at 4°C in the primary antibody. Monoclonal antibody 5A5 (Dodd et al., 1988), an IgM, was used to detect highly polysialylated NCAM (PSA-NCAM) at a dilution 1:1000 in PBS (at pH7.4 with 1% NGS and 0.5% Triton X-100). After several rinses in PBS, the serial sections were incubated in a fluorescein isothiocyanate (FITC)-conjugated secondary antibody (goat anti-mouse IgM; Jackson

ImmunoResearch Laboratories, Inc., U.S.A.) at 1:200 dilution in PBS (at pH7.4 with 1% NGS and 0.1% Triton X-100) for 3 hours. The sections were rinsed again in PBS before being mounted in 1:1 PBS and glycerol. For DiI-5A5 double-staining sections, after blocking with NGS, the sections were incubated with 0.1% Triton X-100 for 10 minutes followed by several rinses in PBS. The sections were incubated overnight in 5A5 primary antibody (same concentration without Triton X-100), then in goat anti-mouse IgM secondary antibody (1:200 in PBS with 1%NGS and 0.1% Triton X-100) conjugated to Alexa Fluor 488. All sections were cover-slipped and investigated under confocal imaging system directly.

Confocal microscopy and image analyses

The images were captured with a confocal imaging system (Bio-Rad MRC 600, Hertford, England) connected to a Zeiss Axiophot photomicroscope (Oberkochen, Germany). A blue excitation filter set (BHS, 488nm excitation and 515nm emission long pass) was used to image the immunoreactivity of 5A5 antibody. A green excitation filter set (GHS, 514 nm excitation and 550 nm long pass) was used to reveal the DiI labeled optic axons. The digital images were processed using the Confocal Assistant software (BioRad, USA). Images collected from the same sections double-stained with both antibody against HS and DiI labeling were merged using the Confocal Assistant software.

RESULT

The expression pattern of PSA-NCAM in the retina and optic stalks

From the horizontal sections of the retina at E13 to E16, the fibers in the optic

stalk and the inner retinal layer were immuno-labeled by the 5A5 antibody (Fig. 1A-1D). Moreover, from the cross-sections of the optic stalk at E14 and E15, PSA-NCAM was clearly found on all bundles of the fibers (Fig. 1E and 1F).

The expression pattern of PSA-NCAM in the chiasm

From the results of horizontal sections at E13 and E14, the posterior region of the ventral diencephalon was stained. An inverted V-shaped PSA-NCAM expression pattern was labeled (Fig. 2A and 2B), with the opening pointed caudally. The anterior part of the ventral diencephalon, where the axons from the optic stalk enter the chiasm, also showed the expression of PSA-NCAM. However, the expression of PSA-NCAM in the anterior part of ventral diencephalon was weaker than that in the posterior region.

The result of the horizontal sections of the ventral diencephalon at E15 and E16 showed different PSA-NCAM expression pattern when compared with the results at E13 and E14. At E15 and E16, a clear C-shaped expression pattern of PSA-NCAM was found at the posterior region of the ventral diencephalon with the opening pointed caudally (Fig. 2C and 2D). Moreover, when compare the expression patterns between optic stalks and the chiasm, we could find that there was a down regulation of PSA-NCAM from optic stalks to optic chiasm (Fig. 2E and 2F). From the results of the frontal sections at E14 to E16, we could also find the down regulation of the PSA-NCAM expression from the optic stalks to the chiasm (Fig. 3; compared A with B, C with D, E with F). Moreover, an intense staining of the 5A5 antibody was found at the midline region of the glial cell layer in the chiasm in anterior sections (Fig. 3A, 3C

and 3E).

In frontal sections of the diencephalon, expression of PSA-NCAM was found in similar pattern at the junction of the optic chiasm and tract at E14 to E16. In caudal chiasm, a band shape expression of PSA-NCAM laid on the ventral region of the fibrous layer (Fig. 4A-4C). At E15 and E16, the band expression of PSA-NCAM seen in the chiasm extended into the optic tracts (Fig. 4B-4D). At further posterior position, the expression of PSA-NCAM shifted to the deep region of the optic tracts (Fig. 4B and 4D).

In cross sections of the optic chiasm, the obvious down-regulation of PSA-NCAM in the optic chiasm was also detected (Fig. 5C and 5E) when compared the expression patterns with that in the cross section of optic stalks (Fig. 1F). The expressions of PSA-NCAM in optic stalks were stronger than that in the optic chiasm. It is noteworthy that there was a group of axons populated at the caudal side of the chiasm, which showed strong PSA-NCAM immunoreactivity. When the tissues were double-stained with DiI to reveal the location of retinal axons (Fig. 5A and 5B), it confirmed that these axons were not originated from retinal ganglion cells (Fig. 5E and 5F).

The expression pattern of PSA-NCAM in horizontal sections of optic tract

At E13, only a few retinal axons reached the optic tracts. At E14, most optic fibers entered the optic tracts and the shape of optic tracts was clear to observe. In horizontal sections at E14, the expression of the PSA-NCAM was restricted at the

posterior region of the optic tracts (Fig. 6A), where the optic stalks are originated from the dorsal retina of both eyes. Sections obtained at E15 (Fig. 6B) showed similar results as that of E14. Such expression pattern agreed with the result from the horizontal sections that the expression of PSA-NCAM in the optic tract is restricted at the posterior region of the optic tracts.

To verify the origin of this group of axons, which co-localized the expression of PSA-NCAM at the posterior region of the optic tracts, double-staining of DiI and 5A5 was performed. The whole retina, at the age of E15, was labeled by DiI and the characteristic shape of the cross section of the optic tract was shown (Fig. 6A and 6D). The same sections were double-stained with 5A5 and the PSA-NCAM expression was clearly found in only the posterior region of the optic tracts (Fig. 6E and 6F). Merge of the corresponding figures demonstrated that fibers at the posterior region of the optic tracts, where PSA-NCAM exists, are retinal axons (Fig. 6G and 6H).

Dorsal-ventral order of optic fiber in the tract after 5A5 incubation

Since retinal axons sending from dorsal retina occupy the posterior region of the optic tracts (Chan and Guillery, 1994), where PSA-NCAM locates, this suggests a possible role of PSA-NCAM in modulating the dorsal ventral order of optic fibers in the tract. Effect of binding of anti-PSA-NCAM to the tissues along the optic pathway was demonstrated by incubating brain slices at E14 with 5A5 antibody. In horizontal sections of optic tract in control brain slices (n = 10), axons from dorsal retina (stained with DiI) occupied the posterior region of the tract (Fig. 7A to 7C). After incubation

of the brain slices with 5A5 (n = 8), the restricted location of these dorsal retinal axons disappeared consistently. These axons spreaded rostrally to occupy also the anterior position of the optic tract. The dorsal ventral order of retinal fibers in the optic tract is disrupted (Fig. 7D to 7F).

DISCUSSION

The functions of NCAM in the optic stalk

NCAM is abundantly expressed on axons and often found in the glial environment (Silver and Rutishauser, 1984; Brittis et al., 1995). In the present results, we find from cross sections of the optic stalk that PSA-NCAM is expressed on the axon bundles throughout the optic stalk. NCAM influences neurite extension (Dodd and Jessell, 1988; Brittis et al., 1995) and fasciculation of axons into bundles (Silver and Rutishauser, 1984; Rutishauser and Landmesser, 1991) by homophilic binding and interactions to other molecules (Grumet et al., 1993; Hankin and Lagenaur, 1994; Doherty and Walsh, 1994; Brittis et al., 1995). When antibodies against NCAM are injected into the primitive eye rudiment, they disturb the normal growth pattern of the nerve processes in chick (Silver and Rutishauser, 1984). These antibodies inhibit the tendency of developing nerve cell processes to perform fasciculation. Therefore, we suggest that NCAM expressed in optic stalk of developing mouse can have the same ability in fasciculating the axons.

The down regulation of PSA-NCAM may be related to the loss of retinotopic fiber order at the chiasm

It has been reported that there is a retinotopic fiber order, demonstrating a

quadrant-specific relationship with retina, when axons enter the optic stalk (Chan and Chung, 1999). However, as axons enter the chiasm, this order is lost and the fasciculated bundles of axons in the optic stalk become defasciculated (Silver 1984; Silver and Rutishauser, 1984). Since NCAM demonstrates its role of axon fasciculation in the optic stalk, the defasciculation of the axon bundles is related to the change in NCAM expression. The functions of NCAM are modulated by the amount of PSA on the molecule (Rutishauser and Landmesser, 1991; Storms and Rutishauser, 1998; Monnier et al., 2001). PSA expression appears to have a negative effect on membrane-membrane binding (Cunningham et al., 1983; Hoffman and Edelman, 1983; Rutishauser et al., 1985). It has been proposed that the large size and the abundance of PSA can impede the ability of membranes to get close enough for effective receptor-receptor interaction (Rutishauser et al., 1988). Thus, a variety of contact-dependent cell interactions can be affected by changes in the amount of PSA on the cell surface. These effects are likely to represent a quantitative change in interaction rather than an all-or-nothing transition (Rutishauser and Landmesser, 1991). It seems that PSA-NCAM contributes to the regulation and fine-tuning of adhesions of cells during development. Direct evidence shows that the presence of PSA on the surface membrance can affect both cell-cell and cell-substrate interactions (Acheson et al., 1991). Fasciculation can be interpreted as an outcome from net forces that promote axon-axon association and that promote axon-environment interaction (Rutishauser and Landmesser, 1991). When NCAM with a low PSA content is expressed, cell-cell interaction responsible for bundling is increased (Rutishauser et al., 1988). However, removal of PSA from NCAM increases cell-substrate interactions, leading to defasciculation in axon bundling of mouse embryos (Acheson

et al., 1991). Thus, the patterns of bundling and defasciculating are attributed to a balance between axon-axon and axon-substratum interactions (Yin et al., 1995). Optic axons are exposed to an environment that includes other PSA-positive cells and processes. Enzymatic removal of PSA from the optic axons caused them to defasciculate in the tract/tectal region (Yin et al., 1995). This enzyme treatment affects both optic axons and their environment. Thus, the results would suggest that removal of PSA causes a relative increase in axon-environment interactions, implicating that the PSA may serve to mask them from responding prematurely to some guidance cues in their target region (Yin et al., 1995). At later developmental stage in chicks, the normal down-regulation of PSA in tectum might serve to expose the environmental cues for the development of optic axons (Yin et al., 1995). We suggest that the down regulation in PSA-NCAM expression in the chiasm leads to increase in heterophilic interactions of axon and molecules in the environment (e.g. CSPG: Grumet et al., 1993; HSPG: Storms et al., 1996), which outweigh axon-axon interactions in the chiasm. Thus, defasciculation in the chiasm occurs, which leads to the separation of the axon bundles and in turn distorts the fiber order. The retinotopic fiber order is lost at the same region where the defasciculation occurs, and PSA-NCAM is thought to be involved in both arrangements of the axon fibers. Therefore, down regulation of PSA-NCAM in the chiasm occurs with the defasciculation of the axon bundles, may hence be related to the loss of the retinotopic order in the chiasm. However, the identity of the axons expressing PSA-NCAM caudal to the chiasm in cross sections is still to be determined.

PSA-NCAM may be involved in the establishment of the retinotopic order in the optic tracts

The retinotopic fiber order in the optic stalk is lost as retinal axons travel through the optic chiasm (Naito 1986,1989; Reese and Baker, 1993; Chan and Chung, 1999). However, when the retinal axons enter the optic tracts, a new retinotopic order of these fibers is re-established in which axons from the dorsal retina are segregated from ventral retinal axons (Torrealba et al., 1982; Cucchiaro and Guillery, 1984; Reese and Baker, 1993; Chan and Guillery, 1994; Chan and Chung, 1999). In contrast to the quadrant-specific order in the optic stalk, axons in optic tract show segregation between origins from dorsal and ventral retina (Chan and Guillery, 1994). The axons sending from the dorsal and ventral retina occupy the posterior and anterior regions of the optic tract respectively. This fiber segregation is established after the axons cross the midline of the optic chiasm. Dorsal axons shift caudally while ventral axons travel rostally to their future position in the tract (Chan and Chung, 1999). Some guidance signals in the corresponding environment should be responsible for the establishment of this order. In the present results, PSA-NCAM expression in the optic tract is restricted to the posterior part, where dorsal retinal axons localize. PSA-NCAM may have repulsive properties in setting this retinotopic organization of retinal axons. Axons from the ventral retina may be more responsive to PSA-NCAM and so they are limited to the anterior part of the tract (Chan and Chung, 1999). Further verification of the function of PSA-NCAM on this dorsal-ventral fiber order in the optic tract was shown by our preliminary results of brain slice culture with 5A5 antibody.

Figure 1

Confocal photomicrographs showing PSA-NCAM immunoreactivity in horizontal sections of the retina in C57 mouse embryos. Anterior is up. **A-D:** At embryonic day 13-16 (E13 to E16), PSA-NCAM is expressed in the inner part of the retina (R) and the fibers in the optic stalk (OS). **E-F:** At E14 and E15, brightly stained fibers are seen in all fascicles in the optic stalk and are separated by unlabelled interfascicular septa. Scale bars: **A** = 100 μm; **C** = 200 μm, applied to **B-D**. **E-F** = 50 μm.

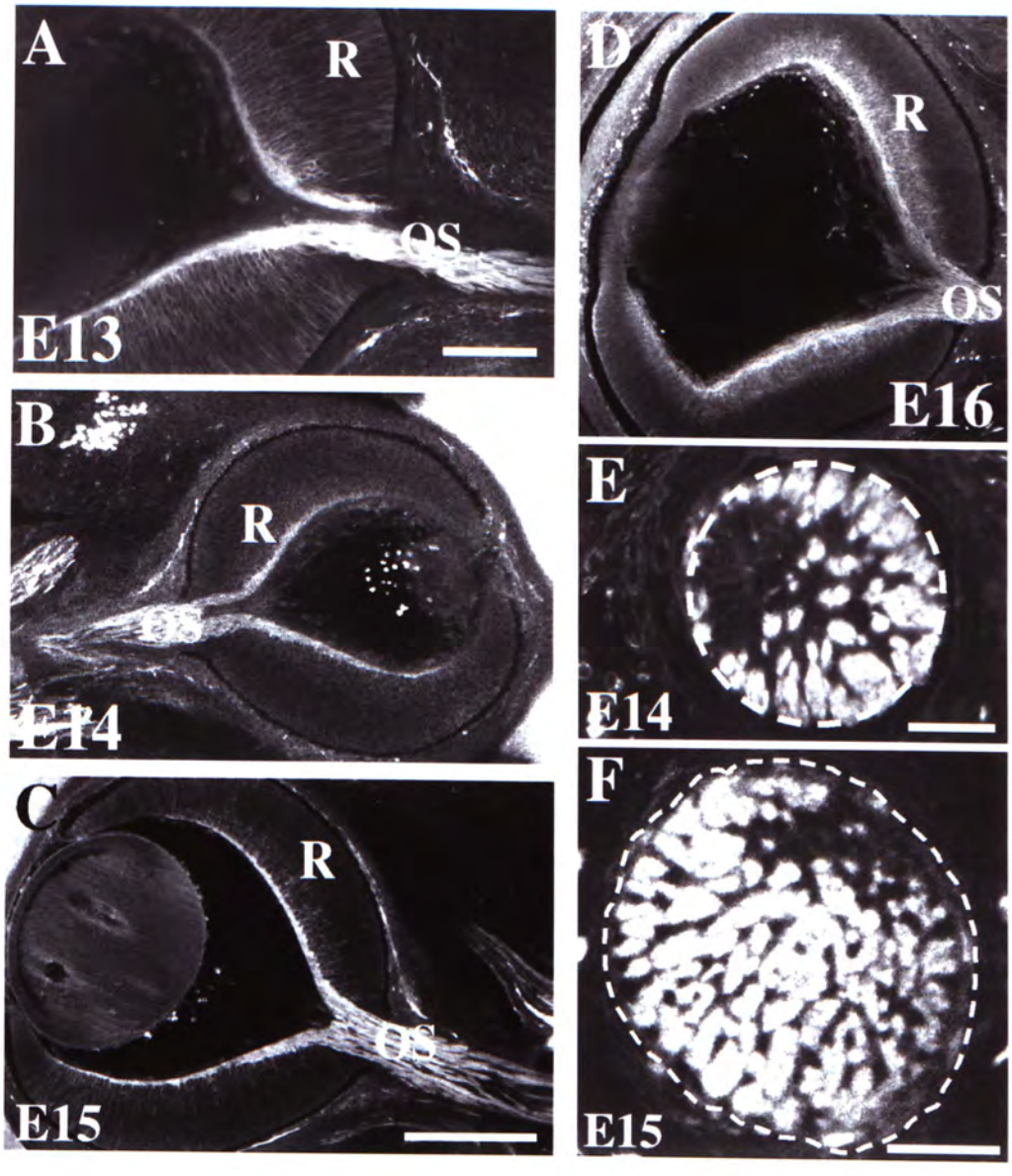
A
R
OS
E13
B
R
OS
E14
C
R
OS
E15
D
R
OS
E16
E
E14
F
E15

Figure 2

Confocal photomicrographs showing PSA-NCAM immunoreactivity in horizontal sections of the ventral diencephalon in C57 mouse embryos. Anterior is up. **A-B**: At E13 and E14, immunostaining for PSA-NCAM is seen as a broad, inverted, V-shaped array opening caudally in the posterior region of the ventral diencephalon. Weak immunostaining for PSA-NCAM is also detected in the anterior part of the ventral diencephalon, where the axons from the optic stalk enter the chiasm. **C-D**: At E15 and E16, PSA-NCAM expression is detected in a C-shaped pattern with the openings pointing caudally. **E-F**: Horizontal sections of the anterior part of the ventral diencephalon under higher magnification show that there is a down-regulation of PSA-NCAM expression from the optic stalk (OS) to the optic chiasm. Midline is indicated by arrows. Scale bars: **A** = 200 μm, applied to **B**; **C** = 250 μm, applied to **D**; **E** = 100μm, applied to **F**.

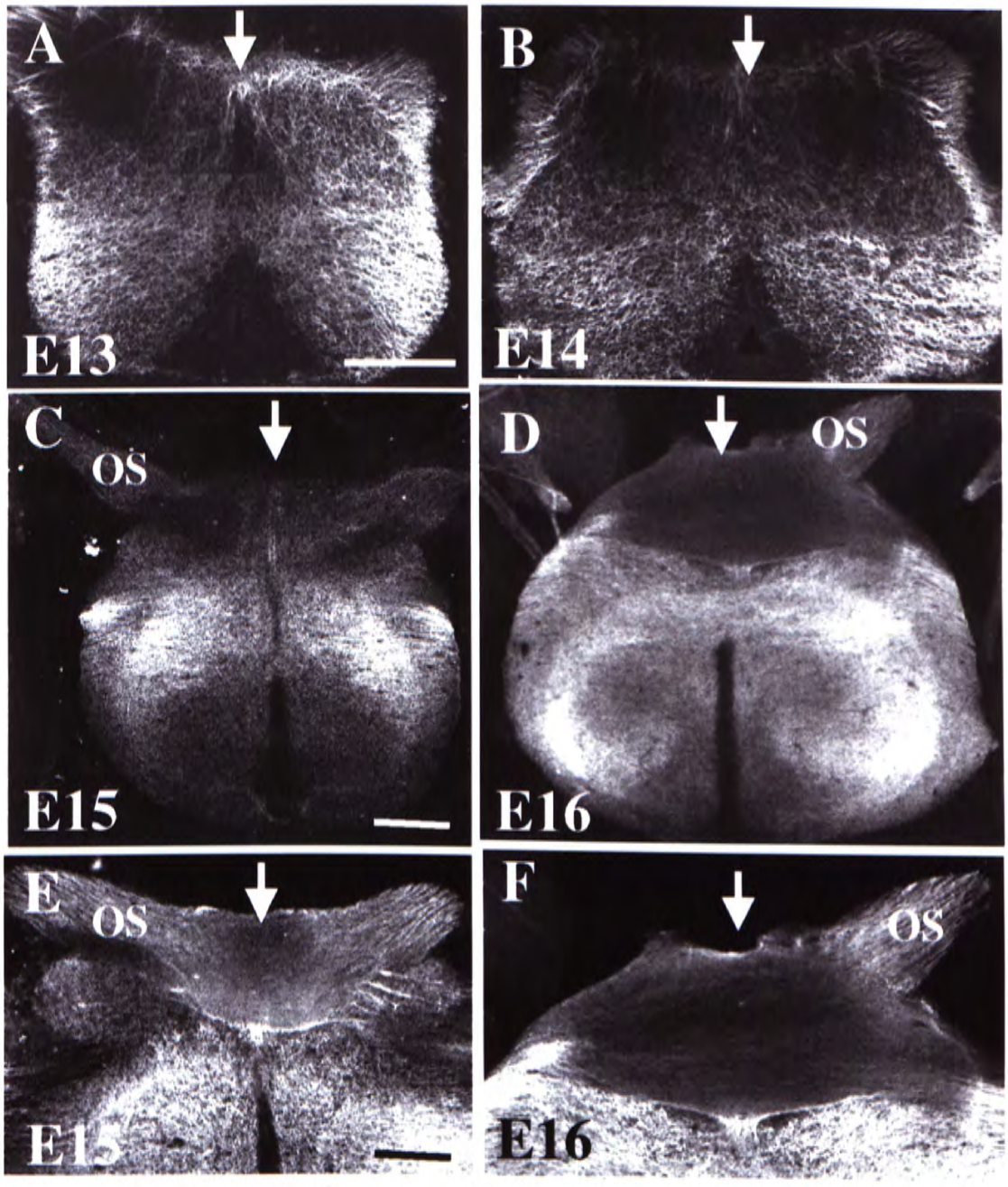
A
E13
B
E14
C
OS
E15
D
OS
E16
E
OS
F
OS
E16

Figure 3

Confocal photomicrographs showing PSA-NCAM immunoreactivity in coronal serial sections of the ventral diencephalon in C57 mouse embryos. Dorsal is up. **A-B**: At E14, the immunostaining for PSA-NCAM is detected in the optic stalks (OS) (indicated by the arrow heads in **A**). There is a down-regulation of the PSA-NCAM expression from the optic stalks to the chiasm (**B**). **C-F**: PSA-NCAM (arrow heads in **C** and **E**) is expressed in the optic stalks at E15 (**C**) and E16 (**E**). The characteristic down-regulation pattern of the PSA-NCAM from the optic stalks to the chiasm is also seen at E15 (**D**) and E16 (**F**). The immunoreactivity for PSA-NCAM is detected at the midline region of the glial layer of the chiasm (**A**, **C** and **E**). Midlines are indicated by arrows. Scale bars = 100 μm, **A** also applied to **B, D**.

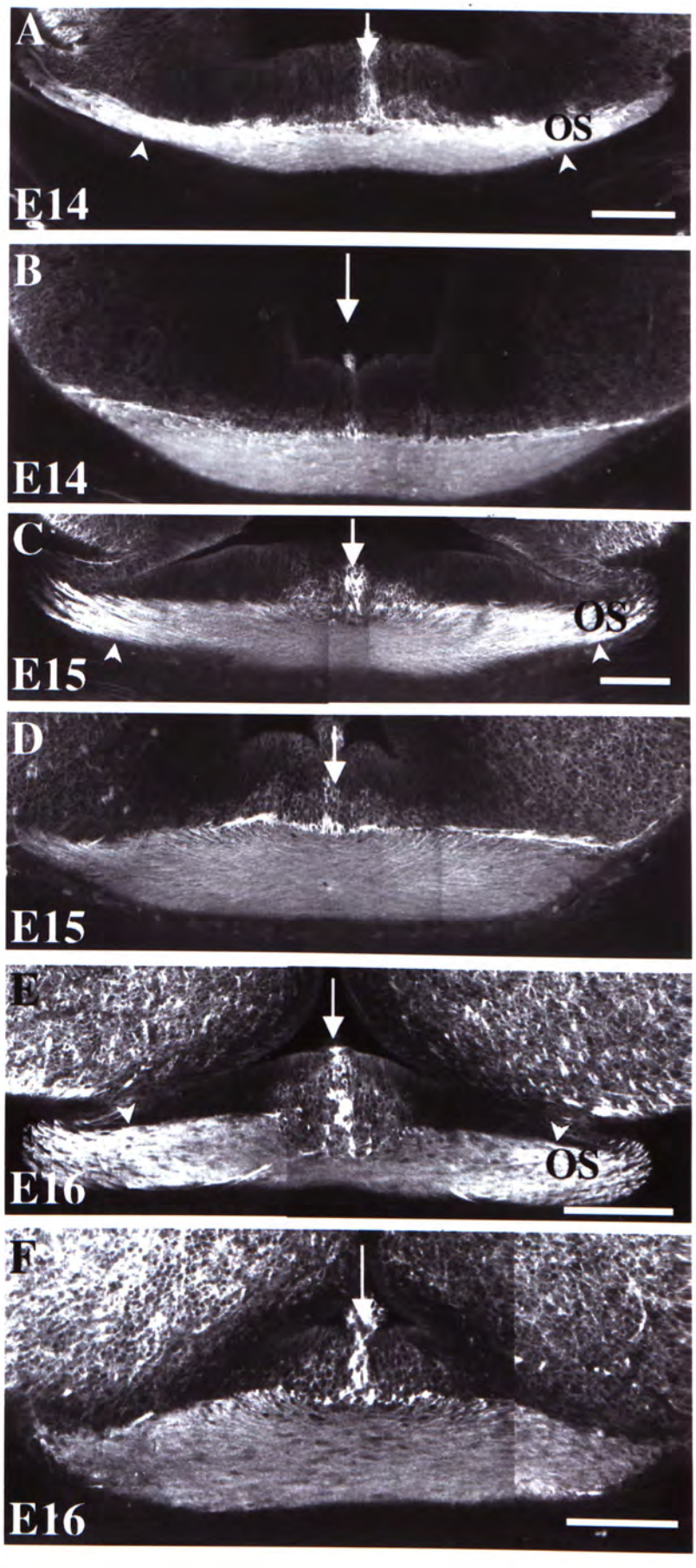
A
OS
E14
B
E14
C
OS
E15
D
E15
E
OS
E16
F
E16

Figure 4

Confocal photomicrographs showing PSA-NCAM immunoreactivity in coronal sections of the ventral diencephalon in C57 mouse embryos. Dorsal is up. **A**: At E14, immunostaining for PSA-NCAM is found in the deep region of the optic tracts. **B**: At E15, a band shape expression of PSA-NCAM is found at the bottom of the fiber layer of the chiasm in the section of the caudal chiasm, where retinal axons leave the chiasm into the optic tracts. The band shape expression of PSA-NCAM extends into the optic tracts. **C-D**: At E16, the expression of PSA-NCAM is in a band shape located at the bottom of the fiber layer of the chiasm (**C**). The PSA-NCAM is found in the deep region of the optic tracts in a more caudal section (**D**). Midlines are indicated by arrows. Scale bars = 100 μm, **A** also applied to **B, D**.

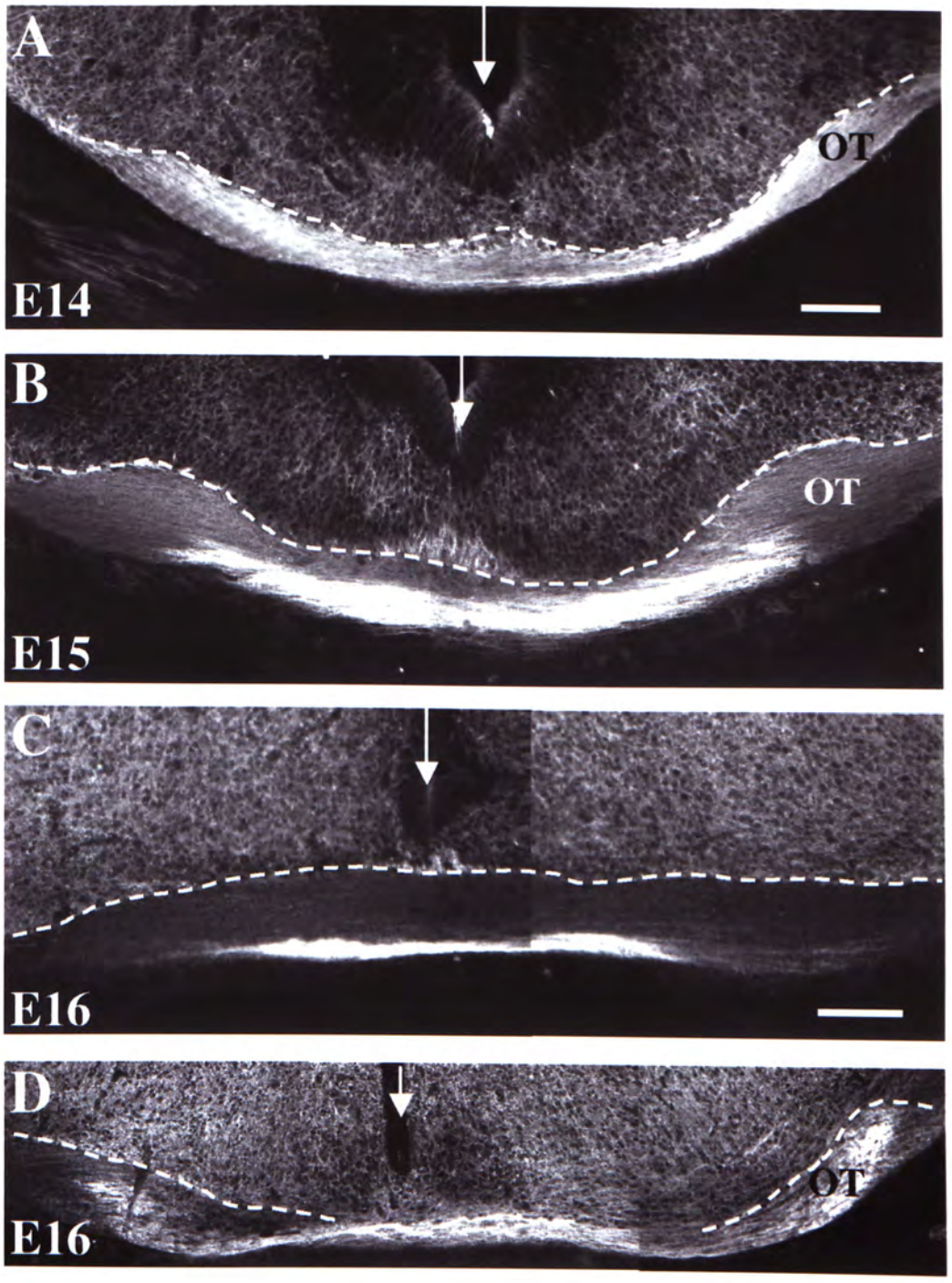
A
OT
E14
B
OT
E15
C
E16
D
OT
E16

Figure 5

Confocal photomicrographs showing pseudocolor images of axons labeled with DiI (red) and PSA-NCAM immunoreactivity (green) in transverse sections of the optic chiasm in C57 mouse embryos at E15. These micrographs are taken near the midline of the chiasm. Dorsal is up. **A-B**: The solid lines indicate the ventral pial surface of the chiasm and the deep margin of the chiasm is indicated by the broken lines. All axons from the eye fully filled with DiI are labeled. **C-D**: The same sections are reacted with 5A5 antibody against PSA-NCAM. Most of the area within the fiber layer is only slightly labeled, while a group of axons populated at the caudal side of the chiasm (indicated by arrow heads) show strong PSA-NCAM immunoreactivity. **E-F**: The two groups of images are merged to generate final images, which show the co-localization (yellow) of retinal axons (red) and PSA-NCAM (green). These images clearly show that the axons strongly stained at the caudal side of the chiasm are not sent from retinal ganglion cells. D, dorsal; R, rostral. Scale bar in **A** = 100 μm, applied to **B-F**.

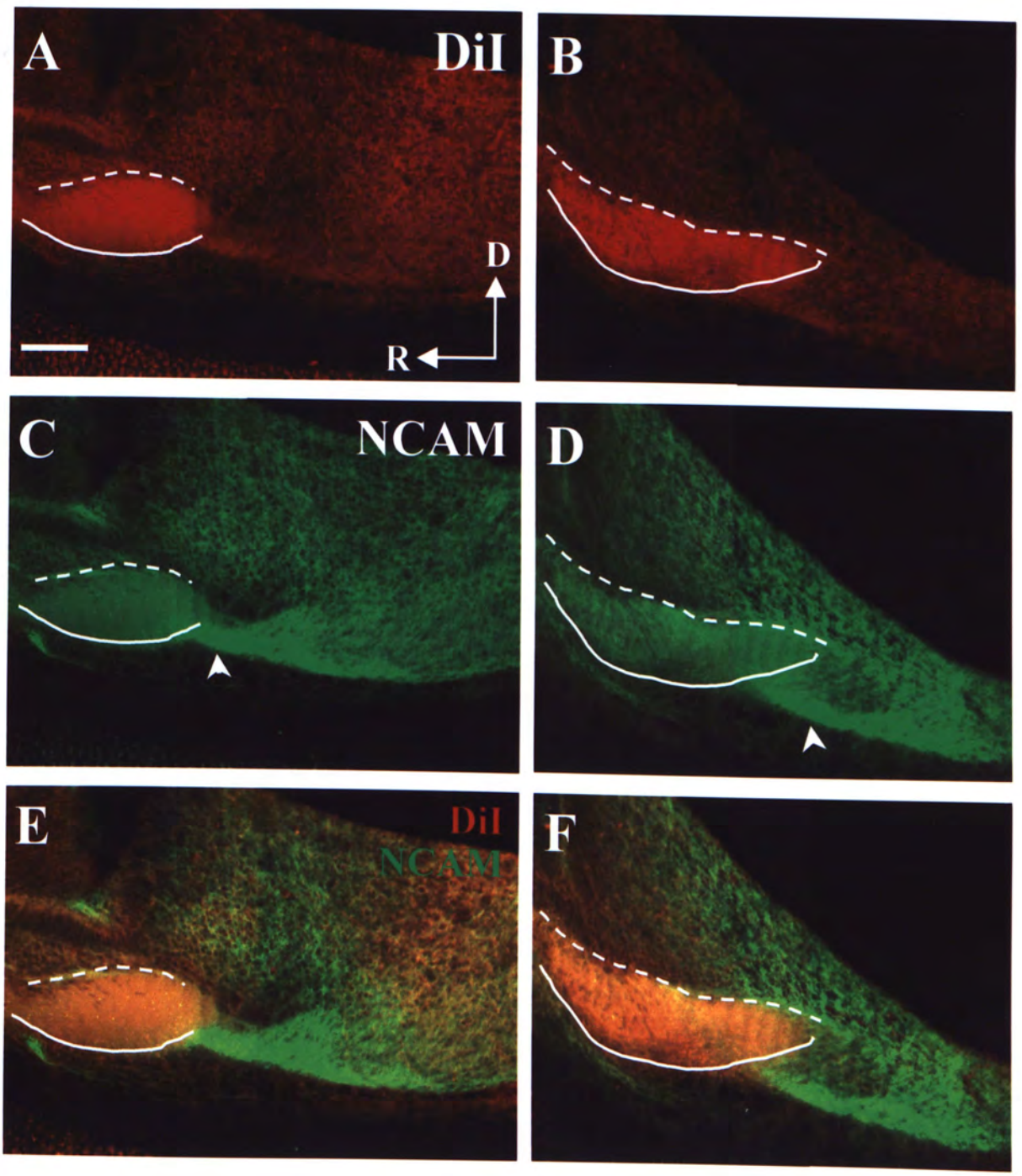
A
DiI
D
R
B
C
NCAM
D
E
DiI
NCAM
F

Figure 6

Confocal photomicrographs showing transverse sections of the optic tract in C57 mouse embryos. The dash lines outline the fibers in the optic tract. **A-B**: At E14 and E15, immunoreactivity of PSA-NCAM is found in the caudal tail of the optic tract. **C-D**: Retinal axons sending from retinal ganglion cells in the optic tract are stained with DiI (red), which is diffused from the fully labelled eye. **E-F**: The same sections are double-stained against PSA-NCAM (green), which is found to be restricted in the posterior region in the optic tract. **G-H**: Merged images of **C** with **E** and **D** with **F** confirm that PSA-NCAM is expressed only in the caudal tail of the optic tract. The co-localizaion of PSA-NCAM and DiI staining is shown in yellow color. D, dorsal; R, rostral. Scale bar in **H**= 100 μm, applied to **A-H**.

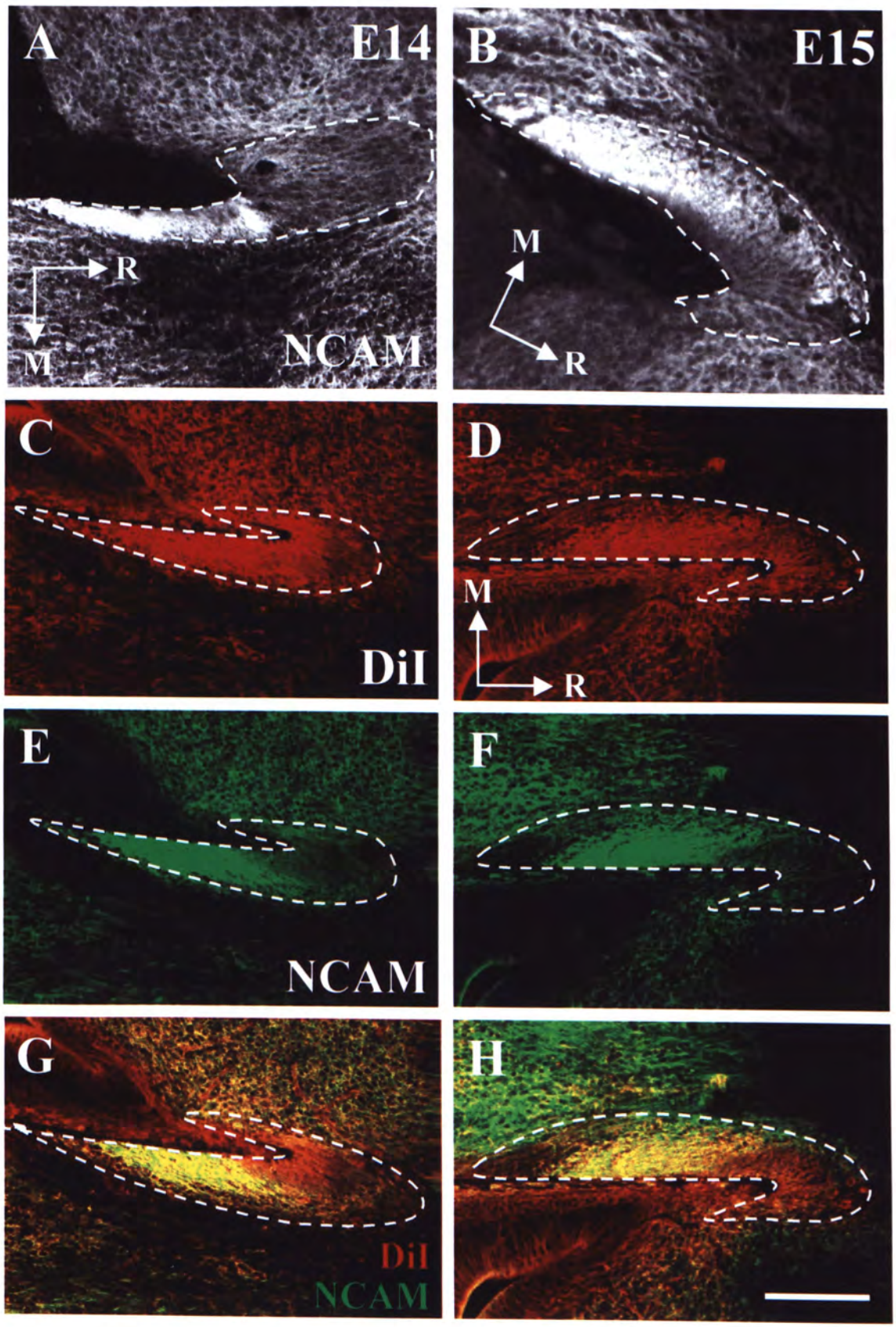
A
E14
R
M
NCAM
B
E15
M
R
C
DiI
D
M
R
E
NCAM
F
G
DiI
NCAM
H

Figure 7

Confocal photomicrographs showing transverse sections of the optic tract in C57 mouse embryos. The dash lines outline the retinal fibers in the optic tract. **A-C**: At E14, DiI filled fibers from the dorsal retina are found mostly in the caudal tail of the optic tract. **D-F**: The confined distribution of dorsal retinal fibers in the posterior region of the tract is disrupted after incubation with 5A5 anti-NCAM antibody. R, rostral; M, medial. Scale bar in **F** = 100 μm, applied to **A-E**.

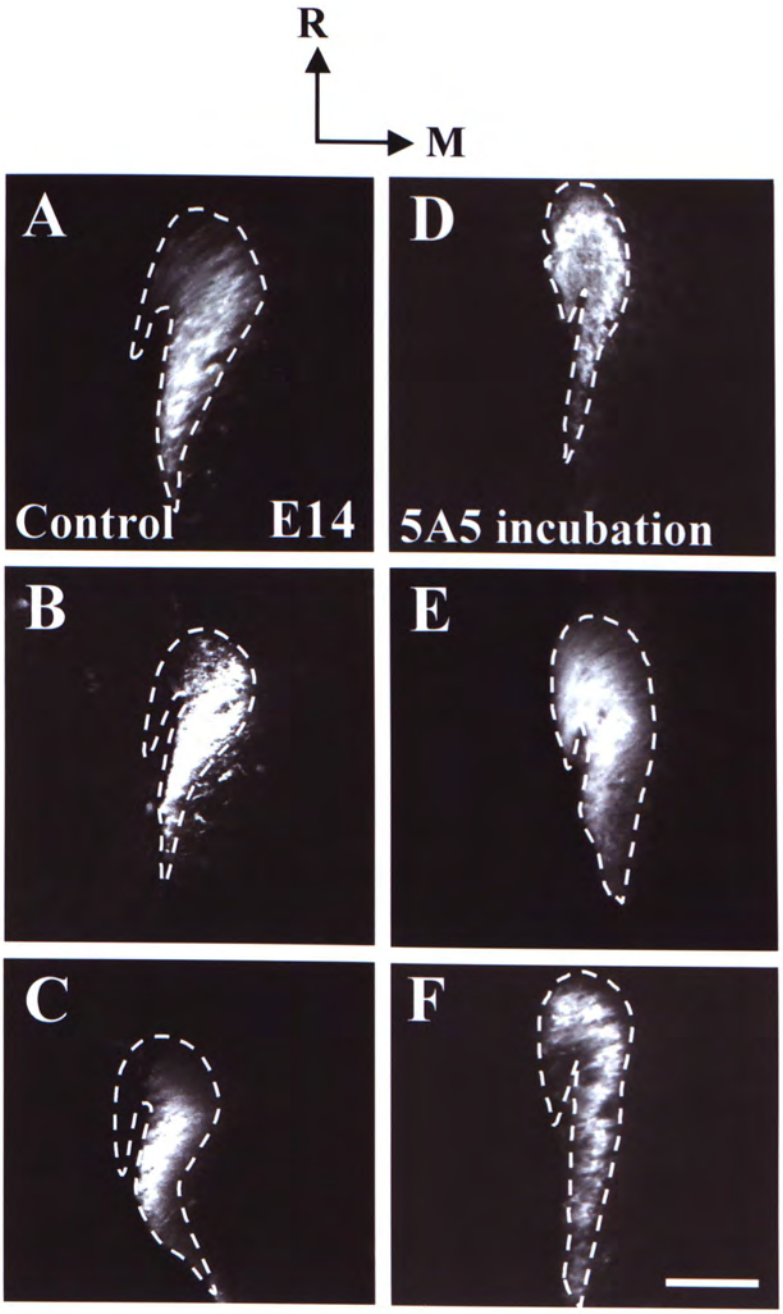
R
M
A
Control
E14
D
5A5 incubation
B
E
C
F

CHAPTER 6

GENERAL CONCLUSION

The studies in this thesis are mainly focused on the possible molecular mechanisms that are involved in the axon patterning in the mouse retinofugal pathway. In the first study, the role of chondroitin sulfate proteoglycans (CSPGs) in arranging the position of growth cones according to their time of arrival in the optic tract of mouse embryos has been investigated. Immunostaining for CS epitopes using CS-56 antibody was found to be restricted in the deep regions of the optic tract. Removal of CS chains using chondroitinase ABC abolishes the accumulation of growth cones at the subpial region of the optic tract. Chondroitinase treatment does not cause significant increase in growth cone collapses in explant cultures. Examination of the morphologies of retinal growth cones after enzymatic removal of CS demonstrates a significant increase in area, indicating that axons respond differently when CS chains are removed in the chiasm and reflect the changes by increasing the complexity of the growth cone morphology. However, the growth cones distribution across the depth of the fiber layer at the midline of the chiasm is not affected by the chondroitinase ABC treatment, despite the presence of chondroitin sulfate at this region. These results show that optic axons undergo regional changes in response to CSPGs, which are responsible for the reordering of chronotopic axon in the optic tract of mouse retinofugal pathway.

Study on the expressions of phosphacan and neurocans show that the two brain CSPGs have different spatial and temporal expression patterns in the developing mouse retinofugal pathway. At E13, the expressions of phosphacan and N-terminal

neurocan are probably involved in setting up the laminated pattern in the retina. Their staining patterns follow closely the distribution of SSEA-1 neuron as an inverted V-shaped configuration at the caudal half of the ventral diencephalon. At E14, phosphacan expression is particularly strong on the lateral regions of mid-chiasm, which suggests a possible role in channeling the axons to their targets precisely at the right time. At E15, C-terminal neurocan is detected in the superficial regions of the optic tract, when most axons are navigating toward the optic tract, with the youngest axons closest to the superficial region of the tract, suggesting a possible role in establishing the age-related order of retinal axons in the optic tract. The regulated spatiotemporal expressions of phosphacan and neurocan imply that they may play overlapping and/or complementary roles in axon guidance in the developing mouse retinofugal pathway.

In the next study, expression patterns of heparan sulfate proteoglycans (HSPGs) at the chiasm have been characterized. During E13 to E16, the expression of HSPGs is particularly strong at the midline, which suggests a role for HSPGs in regulating development of axon divergence at the midline. At E14, HS immunoreactivity is found in the deep parts of the fiber layer at the threshold of the optic tract, which is complementary to the location of growth cones in this region. These results bring out the possibility that the spatially restricted expression of HSPGs may regulate the rearrangement of age-related order in the optic tract.

In the study of the expression of sialylated form of neural cell adhesion molecule (PSA-NCAM), it is found to express abundantly in the developing retinofugal

pathway. An obvious down-regulation of PSA-NCAM immunoreactivity is observed when axons approach the midline of the chiasm and an up-regulation of this molecule is seen when axons enter the optic tract. While axons in the optic stalk are all immunopositive to PSA-NCAM, only axons from the dorsal retina that are located in the posterior region of the optic tract are immunoreactive to PSA-NCAM. These findings indicate that the changes in axon organization in the chiasm and the tract may be controlled by a regulated expression of PSA-NCAM or alternatively by a regulation of the amount of polysialic acid on the NCAM molecule.

REFERENCE

Acheson A, Sunshine JL, Rutishauser U. (1991) NCAM polysialic acid can regulate both cell-cell and cell-substrate interactions. *J Cell Biol. 114:143-53.*

Alberts B, Bray D, Lewis J, Raff M, Roberts K, Watson JD. (1994) Molecular biology of the cell. 3rd ed. *New York: Garland Publishing, 975-976, 1122-1124.*

Asher, RA, Morgenstern, DA, Fidler, PS, et al. (2000) Neurocan is upregulated in injured brain and in cytokine-treated astrocytes. *J Neurosci. 20: 2427-2438.*

Baker GE, Jeffery G. (1989) Distribution of uncrossed axons along the course of the optic nerve and chiasm of rodents. *J Comp Neurol. 289:455-61.*

Baker GE, Reese BE. (1993) Chiasmatic course of temporal retinal axons in the developing ferret. *J Comp Neurol. 330:95-104.*

Bandtlow CE, Zimmermann DR. (2000) Proteoglycans in the developing brain: new conceptual insights for old proteins. *Physiol Rev. 80:1267-90.*

Bastmeyer M, Schlosshauer B, Stuermer CA. (1990) The spatiotemporal distribution of N-CAM in the retinotectal pathway of adult goldfish detected by the monoclonal antibody D3. *Development. 108:299-311.*

Bernfield M, Götte M, Park PW, Reizes O, Fitzgerald ML, Lincecum J, Zako M. (1999) Functions of cell surface heparan sulfate proteoglycans. *Annu Rev Biochem. 68: 729-777.*

Bicknese AR, Sheppard AM, O'Leary DD, Pearlman AL. (1994) Thalamocortical axons extend along a chondroitin sulfate proteoglycan-enriched pathway coincident with the neocortical subplate and distinct from the efferent path. *J Neurosci. 14:3500-10.*

Bovolenta P, Mason C. (1987) Growth cone morphology varies with position in the developing mouse visual pathway from retina to first targets. *J Neurosci. 7:1447-60.*

Brickman YG, Ford MD, Small DH, Bartlett PF, Nurcombe V. (1995) Heparan sulfates mediate the binding of basic fibroblast growth factor to a specific receptor on neural precursor cells. *J Biol Chem. 270: 24941-24948.*

Brittis PA, Canning DR, Silver J. (1992) Chondroitin sulfate as a regulator of neuronal patterning in the retina. *Science. 255: 733-736.*

Brittis PA, Lemmon V, Rutishauser U, Silver J. (1995) Unique changes of ganglion cell growth cone behavior following cell adhesion molecule perturbations: a time-lapse study of the living retina. *Mol Cell Neurosci. 6:433-49.*

Brittis PA, Silver J, Walsh FS, Doherty P. (1996) Fibroblast growth factor receptor function is required for the orderly projection of ganglion cell axons in the developing mammalian retina. *Mol Cell Neurosci. 8: 120-128.*

Brown TA, Bouchard T, St. John T, Wayner E, Carter WG. (1991) Human keratinocytes express a new CD44 core protein (CD44E) as a heparan-sulfate intrinsic membrane proteoglycan with additional exons. *J Cell Biol. 113: 207-221.*

Burg MA, Halfter W, Cole GJ. (1995) Analysis of proteoglycan expression in developing chicken brain: characterization of a heparan sulfate proteoglycan that interacts with neural cell adhesion molecule. *J Neurosci Res. 41: 49-64.*

Canning DR, Hoke A, Malemud CJ, Silver J. (1996) A potent inhibitor of neurite outgrowth that predominates in the extracellular matrix of reactive astrocytes. *Int J Dev Neurosci. 14:153-75.*

Caudy M, Bentley D. (1986) Pioneer growth cone morphologies reveal proximal increases in substrate affinity within leg segments of grasshopper embryos. *J Neurosci. 6:364-79.*

Chan SO, Chung KY, Taylor JSH. (1999) Effects of prenatal monocular enucleation on the cellular specialization in the development of retinofugal pathway. *Eur J Neurosci. 11: 3225-3235.*

Chan SO, Chung KY. (1999) Changes in axon arrangement in the retinofugal

[correction of retinofungal] pathway of mouse embryos: confocal microscopy study using single- and double-dye label. *J Comp Neurol. 406:251-62.*

Chan SO, Guillery RW. (1994) Changes in fiber order in the optic nerve and tract of rat embryos. *J Comp Neurol. 344:20-32.*

Chan SO, Guillery RW. (1993) Developmental changes produced in the retinofugal pathways of rats and ferrets by early monocular enucleations: The effects of age and the differences between normal and albino animals. *J. Neurosci. 13: 5277-5293.*

Chan SO, Wong KF, Chung KY, Yung WH. (1998) Changes in morphology and behaviour of retinal growth cones before and after crossing the midline of the mouse chiasm: a confocal microscopy study. *Eur J Neurosci. 10: 2511-2522.*

Chung KY, Shum DK, Chan SO. (2000a) Expression of chondroitin sulfate proteoglycans in the chiasm of mouse embryos. *J Comp Neurol. 417:153-63.*

Chung KY, Taylor JS, Shum DK, Chan SO. (2000b) Axon routing at the optic chiasm after enzymatic removal of chondroitin sulfate in mouse embryos. *Development. 127:2673-83.*

Chung KY, Leung KM, Lin L, Chan SO. (2001) Heparan sulfate proteoglycan expression in the optic chiasm of mouse embryos. *J. Comp. Neurol. 436: 236-247.*

Chuong CM, McClain DA, Streit P, Edelman GM. (1982) Neural cell adhesion molecules in rodent brains isolated by monoclonal antibodies with cross-species reactivity. *Proc Natl Acad Sci U S A. 79:4234-8.*

Cole GJ, Glaser L. (1986) A heparin-binding domain from N-CAM is involved in neural cell-substratum adhesion. *J Cell Biol. 102: 403-412.*

Cole GJ, Loewy A, Glaser L. (1986) Neuronal cell-cell adhesion depends on interactions of N-CAM with heparin-like molecules. *Nature. 320: 445-447.*

Cole GJ, Schubert D, Glaser L. (1985) Cell-substratum adhesion in chick neural retina depends upon protein-heparan sulfate interactions. *J Cell Biol. 100:1192-9.*

Colello RJ, Guillery RW. (1990) The early development of retinal ganglion cells with uncrossed axons in the mouse: retinal position and axonal course. *Development. 108:515-23.*

Colello RJ, Guillery RW. (1992) Observations on the early development of the optic nerve and tract of the mouse. *J Comp Neurol. 317: 357-378.*

Colello SJ, Coleman L-A. (1997) Changing course of growing axons in the optic chiasm of the mouse. *J Comp Neurol. 379: 495-514.*

Colello SJ, Guillery RW. (1998) The changing pattern of fiber bundles that pass through the optic chiasm of mice. *Eur J Neurosci. 10: 3653-3663.*

Cooper ML, Pettigrew JD. (1979) The decussation of the retinothalamic pathway in the cat, with a note on the major meridians of the cat's eye. *J Comp Neurol. 187:285-311.*

Cucchiaro J, Guillery RW. (1984) The development of the retinogeniculate pathways in normal and albino ferrets. *Proc R Soc Lond B Biol Sci. 223:141-64.*

Cunningham BA, Hemperly JJ, Murray BA, Prediger EA, Brackenbury R, Edelman GM. (1987) Neural cell adhesion molecule: structure, immunoglobulin-like domains, cell surface modulation, and alternative RNA splicing. *Science. 236:799-806.*

David G, Bai XM, Van der Schueren B, Cassiman JJ, Van den Berghe H. (1992) Developmental changes in heparan sulfate expression: in situ detection with mABs. *J Cell Biol. 119: 961-975.*

De Iongh R, McAvoy JW. (1993) Spatio-temporal distribution of acidic and basic FGF indicates a role for FGF in rat lens morphogenesis. *Dev Dyn. 198: 190-202.*

Dodd J, Jessell TM. (1988) Axon guidance and the patterning of neuronal projections in vertebrates. *Science. 242:692-9.*

Dodd, J., Morton, S.B., Karagogeos, D., Yamamoto, M. , Jessell, T.M. (1988) Spatial segregation of axonal glycoprotein expression on subsets of embryonic spinal neurons. *Neuron. 1: 105-116.*

Doherty P, Walsh FS. (1994) Signal transduction events underlying neurite outgrowth stimulated by cell adhesion molecules. *Curr Opin Neurobiol. 4:49-55.*

Dou CL, Levine JM. (1994) Inhibition of neurite growth by NG2 chondroitin sulphate proteoglycan. *J Neurosci. 14:7616-7628.*

Dow KE, Riopelle RJ, Kisilevsky R. (1991) Domains of neuronal heparan sulphate proteoglycans involved in neurite growth on laminin. *Cell Tissue Res. 265: 345-351.*

Drager UC, Olsen JF. (1980) Origins of crossed and uncrossed retinal projections in pigmented and albino mice. *J Comp Neurol. 191:383-412.*

Dräger UC. (1985) Birth dates of retinal ganglion cells giving rise to the crossed and uncrossed optic projections in the mouse. *Proc R Soc Lond Biol. 224: 57-77.*

Dunlop SA, Tee LB, Beazley LD. (2000) Topographic order of retinofugal axons in a marsupial: implications for map formation in visual nuclei. *J Comp Neurol. 428:33-44.*

Edelman GM, Chuong CM. (1982) Embryonic to adult conversion of neural cell adhesion molecules in normal and staggerer mice. *Proc Natl Acad Sci U S A. 79:7036-40.*

Edelman GM. (1983) Cell adhesion molecules. *Science. 219:450-7.*

Faissner A, Clement A, Lochter A, Streit A, M,l C, Schachner M. (1994) Isolation of a neural chondroitin sulfate proteoglycan with neurite outgrowth promoting properties. *J Cell Biol. 126:783-799.*

Fernaud-Espinosa I, Nieto-Sampedro M, Bovolenta P. (1994) Differential effects of glycosaminoglycans on neurite outgrowth from hippocampal and thalamic neurons. *J Cell Sci. 107:1437-1448.*

Fichard A, Verna JM, Olivares J, Saxod R. (1991) Involvement of a chondroitin sulfate proteoglycan in the avoidance of chick epidermis by dorsal root ganglia fibers: a study using beta-D-xyloside. *Dev Biol. 148:1-9.*

Flaccus A, Janetzko A, Tekotte H, Margolis RK, Margolis RU, Grumet M. (1991) Immunocytochemical localization of chondroitin 4- and 6-sulfates in developing rat cerebellum. *J Neurochem. 56:1608-1615.*

Forscher P, Smith SJ. (1988) Actions of cytochalasins on the organization of actin filaments and microtubules in the neuronal growth cone. *J Cell Biol. 107: 1505-1516.*

Friedlander DR, Milev P, Karthikeyan L, Margolis RK, Margolis RU, Grumet M. (1994) The neuronal chondroitin sulfate proteoglycan neurocan binds to the neural cell adhesion molecules Ng-CAM/L1/NILE and N-CAM, and inhibits neuronal adhesion and neurite outgrowth. *J Cell Biol. 125:669-80.*

Gallagher JT, Turnbull JE. (1992) Heparan sulfate in the binding and activation of basic fibroblast growth factor. *Glycobiology. 2: 523-528.*

Garcia-Abreu J, Mendes FA, Onofre GR, De Freitas MS, Silva LCF, Neto VM, Cavalcante LA. (2000) Contribution of heparan sulfate to the non-permissive role of the midline glia to the growth of midbrain neurites. *Glia. 29: 260-272.*

Garwood, J, Schnadelbach, O, Clement, A, Schutte, K, Bach, A, Faissner, A. (1999) DSD-1-proteoglycan is the mouse homolog of phosphacan and displays opposing effects on neurite outgrowth dependent on neuronal lineage. *J Neurosci. 19:3888-3899.*

Godement P, Salaün J, Mason CA. (1990) Retinal axon pathfinding in the optic chiasm: divergence of crossed and uncrossed fibers. *Neuron. 5: 173-186.*

Godement P, Vanselow J, Thanos S, Bonhoeffer F. (1987) A study in developing visual systems with a new method of staining neurones and their processes in fixed tissue. *Development. 101: 697-713.*

Godement P, Wang LC, Mason CA. (1994) Retinal axon divergence in the optic chiasm: dynamics of growth cone behavior at the midline. *J Neurosci. 14: 7024-7039.*

Greenfield B, Wang W-C, Marquardt H, Piepkorn M, Wolff EA, Aruffo A, Bennett KL. (1999) Characterization of the heparin sulfate and chondroitin sulfate assembly sites in CD44. *J Biol Chem. 274: 2511-2517.*

Grumet M, Flaccus A, Margolis RU. (1993) Functional characterization of chondroitin sulfate proteoglycans of brain: interactions with neurons and neural cell adhesion molecules. *J Cell Biol. 120:815-824.*

Grumet M, Milev P, Sakurai T, Karthikeyan L, Bourdon M, Margolis RK, Margolis RU. (1994) Interactions with tenascin and differential effects on cell adhesion of neurocan and phosphacan, two major chondroitin sulfate proteoglycans of nervous tissue. *J Biol Chem. 269:12142-6.*

Guillemot F, Cepko CL. (1992) Retinal fate and ganglion cell differentiation are potentiated by acidic FGF in an in vitro assay of early retinal development. *Development. 114: 743-754.*

Guillery RW, Mason CA, Taylor JSH. (1995) Developmental determinants at the mammalian optic chiasm. *J. Neurosci. 15: 4727-4737.*

Guillery RW, Walsh C. (1987) Changing glial organization relates to changing fiber order in the developing optic nerve of ferrets. *J Comp Neurol. 265: 203-217.*

Halfter W, Schurer B, Yip J, Yip L, Tsen G, Lee JA, Cole GJ. (1997) Distribution and substrate properties of agrin, a heparan sulfate proteoglycan of developing axonal pathways. *J Comp Neurol. 383: 1-17.*

Halfter W. (1993) A heparan sulfate proteoglycan in developing avian axonal tracts. *J Neurosci. 13: 2863-2873.*

Hankin MH, Lagenaur CF. (1994) Cell adhesion molecules in the early developing mouse retina: retinal neurons show preferential outgrowth in vitro on L1 but not N-CAM. *J Neurobiol. 25:472-87.*

Hantaz-Ambroise D, Vigny M, Koenig J. (1987) Heparan sulfate proteoglycan and laminin mediate two different types of neurite outgrowth. *J Neurosci. 7: 2293-2304.*

Hardingham TE, Fosang AJ. (1992) Proteoglycans: many forms and many functions. *FASEB J. 6:861-70.*

Harman AM, Jeffery G. (1992) Distinctive pattern of organisation in the retinofugal pathway of a marsupial: I. Retina and optic nerve. *J Comp Neurol. 325:47-56.*

Haugen PK, McCarthy JB, Roche KF, Furcht LT, Letourneau PC. (1992) Central and peripheral neurite outgrowth differs in preference for heparin-binding versus integrin-binding sequences. *J Neurosci. 12: 2034-2042.*

Herndon ME, Lander AD. (1990) A diverse set of developmentally regulated proteoglycans is expressed in the rat central nervous system. *Neuron. 4: 949-961.*

Hoffman S, Edelman GM. (1983) Kinetics of homophilic binding by embryonic and adult forms of the neural cell adhesion molecule. *Proc Natl Acad Sci U S A. 80:5762-6.*

Hoffman S, Edelman GM. (1984) The mechanism of binding of neural cell adhesion molecules. *Adv Exp Med Biol. 181:147-60.*

Hoffman-Kim D, L,er AD, Jhaveri S. (1998) Patterns of chondroitin sulfate immunoreactivity in the developing tectum reflect regional differences in glycosaminoglycan biosynthesis. *J Neurosci. 18: 5881-5890.*

Ichijo H, Kawabata I. (2001) Roles of the telencephalic cells and their chondroitin sulfate proteoglycans in delimiting an anterior border of the retinal pathway. *J. Neurosci. 21: 9304-9314.*

Iijima N, Oohira A, Mori T, Kitabatake K, Kohsaka S. (1991) Core protein of chondroitin sulfate proteoglycan promotes neurite outgrowth from cultured neocortical neurons. *J Neurochem. 56:706-8.*

Inatani M, Honjo M, Otori Y, Oohira A, Kido N, Tano Y, Honda Y, Tanihara H. (2001) Inhibitory effects of neurocan and phosphacan on neurite outgrowth from retinal ganglion cells in culture. *Invest Ophthalmol Vis Sci. 42:1930-8.*

Inatani M, Tanihara H, Oohira A, Honjo M, Honda Y. (1999) Identification of a nervous tissue-specific chondroitin sulfate proteoglycan, neurocan, in developing rat retina. *Invest Ophthalmol Vis Sci. 40:2350-9.*

Inatani M, Tanihara H, Oohira A, Honjo M, Kido N, Honda Y. (2000) Spatiotemporal expression patterns of 6B4 proteoglycan/phosphacan in the developing rat retina. *Invest Ophthalmol Vis Sci. 41:1990-7.*

Iozzo RV. (1998) Matrix proteoglycans: from molecular design to cellular function. *Annu Rev Biochem. 67: 609-652.*

Irie A, Yates EA, Turnbull JE, Holt CE. (2002) Specific heparan sulfate structures involved in retinal axon targeting. *Development. 129:61-70.*

Isahara K, Yamamoto M. (1995) The interaction of vascular endothelial cells and dorsal root ganglion neurites is mediated by vitronectin and heparan sulfate proteoglycans. *Brain Res. 84: 164-178.*

Ivins JK, Litwack ED, Kumbasar A, Stipp CS, Lander AD. (1997) Cerebroglycan, a developmentally regulated cell-surface heparan sulfate proteoglycan, is expressed on developing axons and growth cones. *Dev Biol. 184: 320-332.*

Jeffery G. (1990) Distribution of uncrossed and crossed retinofugal axons in the cat optic nerve and their relationship to patterns of fasciculation. *Vis Neurosci. 5:99-104.*

Jessell TM. (1988) Adhesion molecules and the hierarchy of neural development. *Neuron. 1:3-13.*

Johnston RN, Wessells NK. (1980) Regulation of the elongating nerve fiber. *Curr Top Dev Biol. 16:165-206.*

Karthikeyan L, Flad M, Engel M, Meyer-Puttlitz B, Margolis RU, Margolis RK. (1994) Immunocytochemical and in situ hybridization studies of the heparan sulfate proteoglycan, glypican, in nervous tissue. *J Cell Sci. 107:3213-22.*

Katoh-Semba R, Matsuda M, Kato K, Oohira A. (1995) Chondroitin sulphate proteoglycans in the rat brain: candidates for axon barriers of sensory neurons and the possible modification by laminin of their actions. *Eur J Neurosci. 7:613-21.*

Katoh-Semba R, Oohira A. (1993) Core proteins of soluble chondroitin sulfate proteoglycans purified from rat brain block the cell cycle of PC12D cells. *J Physiol (Lond).*

Kinnunen A, Kinnunen T, Kaksonen M, Nolo R, Panula P, Rauvala H. (1998) N-syndecan and HB-GAM (heparin-binding growth-associated molecule) associate with early axonal tracts in the rat brain. *Eur J Neurosci. 10: 635-648.*

Kinnunen A, Niemi M, Kinnunen T, Kaksonen M, Nolo R, Rauvala H. (1999) Heparan sulphate and HB-GAM (heparin-binding growth-associated molecule) in the development of the thalamocortical pathway of rat brain. *Eur J Neurosci. 11:491-502.*

Klagsbrun M, Baird A. (1991) A dual receptor system is required for basic fibroblast growth factor activity. *Cell. 67: 229-231.*

Lafont F, Rouget M, Triller A, Prochiantz A, Rousselet A. (1992) In vitro control of neuronal polarity by glycosaminoglycans. *Development. 114:17-29.*

Lander AD. (1993) Proteoglycans in the nervous system. *Curr Opin Neurobiol. 3:716-723.*

Landolt RM, Vaughan L, Winterhalter KH, Zimmermann DR. (1995) Versican is selectively expressed in embryonic tissues that act as barriers to neural crest cell migration and axon outgrowth. *Development. 121:2303-2312.*

Lin X, Buff EM, Perrimon N, Michelson AM. (1999) Heparan sulfate proteoglycans are essential for FGF receptor signaling during Drosophila embryonic development. *Development. 126: 3715-3723.*

Lockerbie RO. (1987) The neuronal growth cone: a review of its locomotory, navigational and target recognition capabilities. *Neuroscience. 20:719-29.*

Lustig M, Erskine L, Mason CA, Grumet M, Sakurai T. (2001) Nr-CAM expression in the developing mouse nervous system: ventral midline structures, specific fiber tracts, and neuropilar regions. *J Comp Neurol. 434:13-28.*

Maeda N, Hamanaka H, Oohira A, Noda M. (1995) Purification, characterization and developmental expression of a brain-specific chondroitin sulfate proteoglycan, 6B4 proteoglycan/phosphacan. *Neuroscience. 67:23-35.*

Maeda N, Noda M. (1996) 6B4 proteoglycan/phosphacan is a repulsive substratum but promotes morphological differentiation of cortical neurons. *Development. 122:647-58.*

Marcus RC, Mason CA. (1995) The first retinal axon growth in the mouse optic chiasm: axon patterning and the cellular environment. *J Neurosci. 15: 6389-6402.*

Margolis RK, Margolis RU. (1993) Nervous tissue proteoglycans. *Experientia. 49:429-446.*

Margolis RU, Margolis RK. (1994) Aggrecan-versican-neurocan family proteoglycans. *Methods Enzymol. 245:105-26.*

Margolis RU, Margolis RK. (1997) Chondroitin sulfate proteoglycans as mediators of axon growth and pathfinding. *Cell Tissue Res. 290:343-8.*

Mason CA, Sretavan DW. (1997) Glia, neurons and axon pathfinding during optic chiasm development. *Curr Opin Neurobiol. 7: 647-653.*

Mason CA, Wang LC. (1997) Growth cone form is behavior-specific and consequently, position-specific along the retinal axon pathway. *J. Neurosci. 17: 1086-1100.*

Maurel P, Meyer-Puttlitz B, Flad M, Margolis RU, Margolis RK. (1995)

Nucleotide sequence and molecular variants of rat receptor-type protein tyrosine phosphatase-zeta/beta. *DNA Seq. 5:323-8.*

Maurel P, Rauch U, Flad M, Margolis RK, Margolis RU. (1994) Phosphacan, a chondroitin sulfate proteoglycan of brain that interacts with neurons and neural cell-adhesion molecules, is an extracellular variant of a receptor-type protein tyrosine phosphatase. *Proc Natl Acad Sci U S A. 91:2512-6.*

McCabe KL, Gunther EC, Reh TA. (1999) The development of the pattern of retinal ganglion cells in the chick retina: mechanisms that control differentiation. *Development. 126: 5713-5724.*

McFarlane S, Zuber ME, Holt CE. (1998) A role for the fibroblast growth factor receptor in cell fate decisions in the developing vertebrate retina. *Development. 125: 3967-3975.*

Metin C, Godement P, Imbert M. (1988) The primary visual cortex in the mouse: receptive field properties and functional organization. *Exp Brain Res. 69:594-612*

Meyer-Puttlitz B, Junker E, Margolis RU, Margolis RK. (1996) Chondroitin sulfate proteoglycans in the developing central nervous system. II. Immunocytochemical localization of neurocan and phosphacan. *J Comp Neurol. 366:44-54.*

Meyer-Puttlitz, B, Milev, P, Junker, E, Zimmer, I, Margolis, RU, Margolis, RK. (1995) Chondroitin sulfate and chondroitin/keratan sulfate proteoglycans of nervous tissue: developmental changes of neurocan and phosphacan. *J Neurochem. 65:2327-2337.*

Milev P, Friedl,er DR, Sakurai T, Karthikeyan L, Flad M, Margolis RK, Grumet M, Margolis RU. (1994) Interactions of the chondroitin sulfate proteoglycan phosphacan, the extracellular domain of a receptor-type protein tyrosine phosphatase, with neurons, glia, and neural cell adhesion molecules. *J Cell Biol. 127:1703-15.*

Miller B, Sheppard AM, Bicknese AR, Pearlman AL. (1995) Chondroitin sulfate proteoglycans in the developing cerebral cortex: the distribution of neurocan

distinguishes forming afferent and efferent axonal pathways. *J Comp Neurol. 355:615-28.*

Monnier PP, Beck SG, Bolz J, Henke-Fahle S. (2001) The polysialic acid moiety of the neural cell adhesion molecule is involved in intraretinal guidance of retinal ganglion cell axons. *Dev Biol. 229:1-14.*

Naito J. (1986) Course of retinogeniculate projection fibers in the cat optic nerve. *J Comp Neurol. 251:376-87.*

Naito J. (1994) Retinogeniculate projection fibers in the monkey optic chiasm: a demonstration of the fiber arrangement by means of wheat germ agglutinin conjugated to horseradish peroxidase. *J Comp Neurol. 346:559-71.*

Niederost BP, Zimmermann DR, Schwab ME, Bandtlow CE. (1999) Bovine CNS myelin contains neurite growth-inhibitory activity associated with chondroitin sulfate proteoglycans. *J Neurosci. 19:8979-89.*

Nordlander RH. (1987) Axonal growth cones in the developing amphibian spinal cord. *J Comp Neurol. 263:485-96.*

Nurcombe V, Ford MD, Wildschut JA, Bartlett PF. (1993) Developmental regulation of neural response to FGF-1 and FGF-2 by heparan sulfate proteoglycan. *Science. 260: 103-106.*

Oakley RA, Tosney KW. (1991) Peanut agglutinin and chondroitin-6-sulfate are molecular markers for tissues that act as barriers to axon advance in the avian embryo. *Dev Biol. 147: 187-206.*

Oohira A, Matsui F, Watanabe E, Kushima Y, Maeda N. (1994) Developmentally regulated expression of a brain specific species of chondroitin sulfate proteoglycan, neurocan, identified with a monoclonal antibody IG2 in the rat cerebrum. *Neuroscience. 60:145-57.*

Oohira, A, Matsui, F, Katoh-Semba, R. (1991) Inhibitory effects of brain chondroitin sulfate proteoglycans on neurite outgrowth from PC12D cells. *J Neurosci.*

11:822.

Ornitz DM. (2000) FGFs, heparan sulfate and FGFRs: complex interactions essential development. *Bioessays. 22: 108-112.*

Park CM, Hollenberg MJ. (1989) Basic fibroblast growth factor induces retinal regeneration in vivo. *Dev Biol. 134: 201-205.*

Peach RJ, Hollenbaugh D, Stamenkovic I, Aruffo A. (1993) Identification of hyaluronic acid binding sites in the extracellular domain of CD44. *J Cell Biol. 122: 257-264.*

Perris R, Krotoski D, Lallier T, Domingo C, Sorrell JM, Bronner-Fraser M. (1991) Spatial and temporal changes in the distribution of proteoglycans during avian neural crest development. *Development. 111: 583-599.*

Piepkorn M, Hovingh P, Bennett KL, Aruffo A, Linker A. (1997) Chondroitin sulphate composition and structure in alternatively spliced CD44 fusion proteins. *Biochem J. 327: 499-506.*

Pindzola RR, Doller C, Silver J. (1993) Putative inhibitory extracellular matrix molecules at the dorsal root entry zone of the spinal cord during development and after root and sciatic nerve lesions. *Dev Biol. 156:34-48.*

Pittack C, Grunwald GB, Reh TA. (1997) Fibroblast growth factors are necessary for neural retina but not pigmented epithelium differentiation in chick embryos. *Development. 124: 805-816.*

Pittack C, Jones M, Reh TA. (1991) Basic fibroblast growth factor induces retinal pigment epithelium to generate neural retina in vitro. *Development. 113: 577-588.*

Provis JM, Watson CR. (1981) The distribution of ipsilaterally and contralaterally projecting ganglion cells in the retina of the pigmented rabbit. *Exp Brain Res. 44:82-92.*

Rapraeger AC, Krufka A, Olwin BB. (1991) Requirement of heparan sulfate for

bFGF-mediated fibroblast growth and myoblast differentiation. *Science. 252: 1705-1708.*

Rauch U, Gao P, Janetzko A, Flaccus A, Hilgenberg L, Tekotte H, Margolis RK, Margolis RU. (1991) Isolation and characterization of developmentally regulated chondroitin sulfate and chondroitin/keratan sulfate proteoglycans of brain identified with monoclonal antibodies. *J Biol Chem. 266:14785-801.*

Rauch U, Karthikeyan L, Maurel P, Margolis RU, Margolis RK. (1992) Cloning and primary structure of neurocan, a developmentally regulated, aggregating chondroitin sulfate proteoglycan of brain. *J Biol Chem. 267:19536-47.*

Raulo E, Chernousov MA, Carey DJ, Nolo R, Rauvala H. (1994) Isolation of a neuronal cell surface receptor of heparin binding growth-associated molecule (HB-GAM). Identification as N-syndecan (syndecan-3). *J Biol Chem. 269: 12999-13004.*

Rauvala H, Vanhala A, Castren E, Nolo R, Raulo E, Merenmies J, Panula P. (1994) Expression of HB-GAM (heparin-binding growth-associated molecules) in the pathways of developing axonal processes in vivo and neurite outgrowth in vitro induced by HB-GAM. *Brain Res. 79: 157-176.*

Reese BE, Baker GE. (1992) Changes in fiber organization within the chiasmatic region of mammals. *Vis Neurosci. 9:527-33.*

Reese BE, Baker GE. (1993) The re-establishment of the representation of the dorso-ventral retinal axis in the chiasmatic region of the ferret. *Vis Neurosci. 10:957-68.*

Reese BE, Johnson PT, Hocking DR, Bolles AB. (1997) Chronotopic fiber reordering and the distribution of cell adhesion and extracellular matrix molecules in the optic pathway of fetal ferrets. *J Comp Neurol. 380: 355-372.*

Reese BE, Maynard TM, Hocking DR. (1994) Glial domains and axonal reordering in the chiasmatic region of the developing ferret. *J Comp Neurol. 349: 303-324.*

Ring C, Lemmon V, Halfter W. (1995) Two chondroitin sulfate proteoglycans differentially expressed in the developing chick visual system. *Dev Biol. 168:11-27.*

Rothbard JB, Brackenbury R, Cunningham BA, Edelman GM. (1982) Differences in the carbohydrate structures of neural cell-adhesion molecules from adult and embryonic chicken brains. *J Biol Chem. 257:11064-9.*

Rougon G, Deagostini-Bazin H, Hirn M, Goridis C. (1982) Tissue- and developmental stage-specific forms of a neural cell surface antigen linked to differences in glycosylation of a common polypeptide. *EMBO J. 1:1239-44.*

Rutishauser U, Acheson A, Hall AK, Mann DM, Sunshine J. (1988) The neural cell adhesion molecule (NCAM) as a regulator of cell-cell interactions. *Science. 240:53-7.*

Rutishauser U, Hoffman S, Edelman GM. (1982) Binding properties of a cell adhesion molecule from neural tissue. *Proc Natl Acad Sci U S A. 79:685-9.*

Rutishauser U, Landmesser L. (1991) Polysialic acid on the surface of axons regulates patterns of normal and activity-dependent innervation. *Trends Neurosci. 14:528-32.*

Rutishauser U, Watanabe M, Silver J, Troy FA, Vimr ER. (1985) Specific alteration of NCAM-mediated cell adhesion by an endoneuraminidase. *J Cell Biol. 101: 1842-1849.*

Rutishauser U. (1993) Adhesion molecules of the nervous system. *Curr Opin Neurobiol. 3:709-15.*

Santoni MJ, Barthels D, Barbas JA, Hirsch MR, Steinmetz M, Goridis C, Wille W. (1987) Analysis of cDNA clones that code for the transmembrane forms of the mouse neural cell adhesion molecule (NCAM) and are generated by alternative RNA splicing. *Nucleic Acids Res. 15:8621-41.*

Schlessinger J, Lax I, Lemmon M. (1995) Regulation of growth factor activation by proteoglycans: what is the role of the low affinity receptors? *Cell. 83:357-60.*

Schubert D, LaCorbiere M. (1985) Isolation of an adhesion-mediating protein from chick neural retina adherons. *J Cell Biol. 101:1071-7.*

Schultz, M, Raju, T, Ralston, G, Bennett, MR. (1990) A retinal ganglion cell neurotrophic factor purified from the superior colliculus. *J Neurochem. 55:832-841.*

Sheppard AM, Hamilton SK, Pearlman AL. (1991) Changes in the distribution of extracellular matrix components accompany early morphogenetic events of mammalian cortical development. *J Neurosci. 11:3928-3942.*

Silver J, Poston M, Rutishauser U. (1987) Axon pathway boundaries in the developing brain. I. Cellular and molecular determinants that separate the optic and olfactory projections. *J Neurosci. 7:2264-72.*

Silver J, Rutishauser U. (1984) Guidance of optic axons in vivo by a preformed adhesive pathway on neuroepithelial endfeet. *Developmental Biology. 106: 485-499.*

Silver J, Sidman RL. (1980) A mechanism for the guidance and topographic patterning of retinal ganglion cell axons. *J Comp Neurol. 189: 101-111.*

Silver J. (1984) Studies on the factors that govern directionality of axonal growth in the embryonic optic nerve and at the chiasm of mice. *J Comp Neurol. 223:238-51.*

Small DH, Mok SS, Williamson TG, Nurcombe V. (1996) Role of proteoglycans in neural development regeneration, and the aging brain. *J Neurochem. 67: 889-899.*

Snow DM, Lemmon V, Carrino DA, Caplan DA, Silver J (1990) Sulfated proteoglycans in astroglial barriers inhibit neurite outgrowth in vitro. *Exp Neurol. 109:111-130.*

Snow DM, Letourneau PC. (1992) Neurite outgrowth on a step gradient of chondroitin sulfate proteoglycan (CS-PG). *J Neurobiol. 23: 322-336.*

Snow DM, Watanabe M, Letourneau PC, Silver J. (1991) A chondroitin sulfate proteoglycan may influence the direction of retinal ganglion cell outgrowth.

Development. 113: 1473-1485.

Solter D, Knowles BB. (1978) Monoclonal antibody defining a stage-specific mouse embryonic antigen (SSEA-1). *Proc Natl Acad Sci USA. 75: 5565-5569.*

Sretavan DW, Feng L, Puré E, Reichardt LF. (1994) Embryonic neurons of the developing optic chiasm express L1 and CD44, cell surface molecules with opposing effects on retinal axon growth. *Neuron. 12: 957-975.*

Sretavan DW. (1990) Specific routing of retinal ganglion cell axons at the mammalian optic chiasm during embryonic development. *J Neurosci. 10:1995-2007.*

Sretavan DW, Feng L, Puré E, Reichardt LF. (1994) Embryonic neurons of the developing optic chiasm express L1 and CD 44, cell surface molecules with opposing effects on retinal axon growth. *Neuron. 12: 957-975.*

Storms SD, Kim AC, Tran BH, Cole GJ, Murray BA. (1996) NCAM-mediated adhesion of transfected cells to agrin. *Cell Adhes Commun. 3: 497-509.*

Storms SD, Rutishauser U. (1998) A role for polysialic acid in neural cell adhesion molecule heterophilic binding to proteoglycans. *J Biol Chem. 273:27124-9.*

Tang J, Rutishauser U, Landmesser L. (1994) Polysialic acid regulates growth cone behavior during sorting of motor axons in the plexus region. *Neuron. 13:405-14.*

Taylor JS, Guillery RW. (1994) Early development of the optic chiasm in the gray short-tailed opossum, Monodelphis domestica. *J Comp Neurol. 350:109-21.*

Taylor JSH, Guillery RW. (1995) Effect of a very early monocular enucleation upon the development of the uncrossed retinofugal pathway in ferrets. *J Comp Neurol. 357: 331-340.*

Teel AL, Yost HJ. (1996) Embryonic expression patterns of Xenopus syndecans. *Mech Dev. 59: 115-127.*

Thanos S, Bonhoeffer F, Rutishauser U. (1984) Fiber-fiber interaction and tectal

cues influence the development of the chicken retinotectal projection. *Proc Natl Acad Sci U S A. 81:1906-10.*

Thanos S, Mey J, Wild M. (1993) Treatment of the adult retina with microglia-suppressing factors retards axotomy-induced neuronal degradation and enhances axonal regeneration in vivo and in vitro. *J Neurosci. 13:455-66.*

Torrealba F, Guillery RW, Eysel U, Polley EH, Mason CA. (1982) Studies of retinal representations within the cat's optic tract. *J Comp Neurol. 211:377-96.*

Tosney KW, Landmesser LT. (1985) Growth cone morphology and trajectory in the lumbosacral region of the chick embryo. *J Neurosci. 5:2345-58.*

Treloar HB, Nurcombe V, Key B. (1996) Expression of extracellular matrix molecules in the embryonic rat olfactory pathway. *J Neurobiol. 31: 41-55.*

Verna JM, Fichard A, Saxod R. (1989) Influence of glycosaminoglycans on neurite morphology and outgrowth patterns in vitro. *Int J Dev Neurosci. 7: 389-399.*

Vlodavsky I, Folkman J, Sullivan R, Fridman R, Ishai-Michaeli R, Sasse J, Klagsbrun M. (1987) Endothelial cell-derived basic fibroblast growth factor: synthesis and deposition into subendothelial extracellular matrix. *Proc Natl Acad Sci U S A. 84:2292-6.*

Walker A, Turnbull JE, Gallagher JT. (1994) Specific heparan sulfate saccharines mediate the activity of basic fibroblast growth factor. *J Biol Chem. 269: 931-935.*

Walsh C, Guillery RW. (1985) Age-related fiber order in the optic tract of the ferret. *J Neurosci. 5:3061-9.*

Walz A, McFarlane S, Brickman YG, Nurcombe V, Bartlett PF, Holt CE. (1997) Essential role of heparan sulfates in axon navigation and targeting in the developing visual system. *Development. 124: 2421-2430.*

Wang LC, Dani J, Godement P, Marcus RC, Mason CA. (1995) Crossed and uncrossed retinal axons respond differently to cells of the optic chiasm midline in

vitro. *Neuron. 15:1349-64.*

Watanabe E, Matsui F, Keino H, Ono K, Kushima Y, Noda M, Oohira A. (1996) A membrane-bound heparan sulfate proteoglycan that is transiently expressed on growing axons in the rat brain. *J Neurosci Res. 44: 84-96.*

Wizenmann A, Thanos S, von Boxberg Y, Bonhoeffer F. (1993) Differential reaction of crossing and non-crossing rat retinal axons on cell membrane preparations from the chiasm midline: an in vitro study. *Development. 117:725-35.*

Wulf E, Deboben A, Bautz FA, Faulstich H, Wielaud TH. (1979) Fluorescent phallotoxin, a tool for the visualization of cellular actin. *Proc Natl Acad Sci USA. 76: 4498-4502.*

Yamagata T, Saito H, Habuchi O, Suzuki S. (1968) Purification and properties of bacterial chondroitinases and chondrosulfatase. *J Bio Chem. 243: 1523-1535.*

Yayon A, Klagsbrun M, Esko JD, Leder P, Ornitz DM. (1991) Cell surface, heparin-like molecules are required for binding of basic fibroblast growth factor to its high affinity receptor. *Cell. 64: 841-848.*

Yin X, Watanabe M, Rutishauser U. (1995) Effect of polysialic acid on the behavior of retinal ganglion cell axons during growth into the optic tract and tectum. *Development. 121:3439-46.*